CREWES

Research Report 2017
Volume 29

In this volume…

Report Summaries

On the memory stick…

Complete Reports
Student Theses

UNIVERSITY OF CALGARY
FACULTY OF SCIENCE
Department of Geoscience

Notice of Intent to Publish

Please note that the authors of the research in this 29th Volume of the Abstract Book intend to publish or otherwise publically disseminate their full research papers in the coming calendar year. According to the contracts between the University of Calgary (CREWES) and each Sponsor, the University will make available to the Sponsor a copy of the proposed publication resulting from the CREWES Project prior to submission for publication. In the event that the Sponsor determines that Research Results within the proposed publication contain Sponsor Confidential Information, the Sponsor shall have thirty (30) days to notify the University in writing and the University shall remove Sponsor Confidential information prior to publication. This 30 day period shall be considered to have started at the end of this meeting (December 1, 2017). These full research reports are distributed on memory sticks at the CREWES annual meeting and are available on the CREWES website to all Sponsors and their employees.

CREWES Project faculty, staff and students, October 2017

Left to Right:

Front Row: Kevin Hall, Adriana Gordon, Hussain Aldhaw, Hani Alzahrani, Laura Baird, Dennis Ellison, Tyler Spackman, Matt Eaid, Andrew Mills

Second Row: Heather Hardeman, Nadine Igonin, Winnie Ajiduah, Ron Weir, Saul Guevara, Emma Lv, Sergio Romahn, Bernie Law, Marie Macquet, Claude Ribordy, Helen Isaac, Tim Cary, Scott Keating

Third Row: Daniel Trad, Jorge Monsegny, Arthur Lee

Back Row: Junxiao Li, Wenyong Pan, Larry Lines, Kris Innanen, Lei Yang, Jian Sun, Raul Cova, Yu Geng, Zhan Niu, Dave Henley, Huaizhen Chen, Marcelo Guarido, Ellen Liu, Malcolm Bertram, Don Lawton, Ali Fathalian, Hassan Khaniani, Shahpoor Moradi, Andy Iverson, Xiucheng Wei

CREWES in 2017

I am delighted to welcome you to the 2017 CREWES Annual Sponsors' Meeting. The time and energy you as sponsor representatives have put in to keeping our group working and progressing exploration and monitoring geophysics is very much on our minds at this time of year—thank you for this, and for your continuing support.

Once again I am in awe of what the students have accomplished this year, and I am greatly looking forward to being able to help show this off to you in Banff. The degree of critical thinking, imagination, care and technical skill required to create what these young scientists have created in 2017, cannot be overstated. In areas of imaging, processing, standard and full waveform inversion, and acquisition, new algorithms, new insights, and new knowledge seems to simply flow from the abstracts in this book.

Our continuing collaborations with the Containment and Monitoring Institute (CaMI), headed up by Don Lawton, have provided a set of unique opportunities for CREWES students, faculty and staff to take part in field work as you can see by perusing this year's report. Further collaborations, for instance with SINTEF in Norway, have brought additional funding to support CaMI site field work and our ongoing development of reservoir-ready multi-parameter full waveform inversion.

Changes continue to happen for our group. Through active engagement with research priorities and priority-setting on campus, a great deal of financial support from the Canada First Research Excellence Fund (CFREF) has begun to appear, multiplying our ability to produce research results of interest (we believe) to our industrial sponsors. For instance, three postdoctoral fellowships have been funded for CREWES researchers Drs. Raul Cova, Marcelo Guarido, and (soon to be Dr.) Junxiao Li. These young researchers will be able to take on key leadership roles within the group, and I believe great things will result. We greatly enjoyed being visited by Dr. Huixing Zhang, who has now returned to China after visiting CREWES for a year, during which time she developed and refined simulation of waves in patchy-saturated media. We are also extremely pleased to have as a new collaborator Dr. Rachel Lauer, a geophysicist with tremendous field experience and a fluid modeller. She is co-supervising one of our grad students who is making forays into seismic characterization of potential geothermal reservoirs.

Those are some highlights of a very highlight intensive year. I hope you will be as struck as I am to see the big steps forward taken by CREWES researchers in the creation of technology and knowledge this year. Once again, welcome to our year-end Annual Meeting, and thanks for your ongoing support.

Calgary, Alberta
November, 2017

Kristopher Innanen
CREWES Director

Table of Contents

* Presenter

2017 CREWES Sponsors

Acceleware

CGG

Chevron Corporation

Devon Energy Corporation

Halliburton

INOVA Geophysical

Nexen Energy ULC

Petronas Carigali SDN BHD

Repsol Oil & Gas Canada Inc.

RIPED, PetroChina

TGS

Natural Sciences and Engineering Research Council of Canada (NSERC) - Collaborative Research and Development Grant

NSERC CRSNG

Additional funding provided by:

CANADA FIRST RESEARCH EXCELLENCE FUND

MITACS

CREWES Personnel

LEADERSHIP

Kristopher A. Innanen, Director
Associate Professor, Department of Geoscience, University of Calgary

B.Sc. Physics and Earth Science, 1996, York University
M.Sc. Physics, 1998, York University
Ph.D. Geophysics, 2003, University of British Columbia

- Work Experience: University of Houston

Don C. Lawton, Associate Director
Professor, Department of Geoscience, University of Calgary

B.Sc. (Hons. Class I) Geology, 1973, University of Auckland
Ph.D. Geophysics, 1979, University of Auckland

- Work Experience: New Zealand Steel Mining Ltd., Amoco Minerals (N.Z.) Ltd., Carbon Management Canada

Daniel Trad, Associate Director
Associate Professor, Department of Geoscience, University of Calgary

Licenciatura in Geophysics, 1994, Universidad Nacional de San Juan, Argentina
Ph.D. Geophysics, 2001, University of British Columbia

- Work Experience: Electromagnetic Methods (Argentina and Brazil), Seismic Research and development (Veritas, CGG, Techco, in Calgary and France).

Gary F. Margrave, Emeritus Director
Emeritus Professor, Faculty Professor, Department of Geoscience, University of Calgary

B.Sc. Physics, 1975, University of Utah
M.Sc. Physics, 1977, University of Utah
Ph.D. Geophysics, 1981, University of Alberta

- Work Experience: Chevron Canada Resources, Chevron Geoscience Company, Devon Canada

Laura A. Baird, Program Manager

BA, History, 1992, University of Calgary

- Work Experience: Alberta Cancer Board, Department of Geoscience at the University of Calgary

Kevin W. Hall, Technical Manager

B.Sc. Geophysics, 1992, University of Calgary
M.Sc. Geophysics, 1996, University of Calgary

- Work Experience: Lithoprobe Seismic Processing Facility at the University of Calgary

ADJUNCT DIRECTOR

Laurence R. Lines
Professor and Interim Head, Department of Geoscience, University of Calgary

B.Sc. Physics, 1971, University of Alberta
M.Sc. Geophysics, 1973, University of Alberta
Ph.D. Geophysics, 1976, University of B.C.

- Work Experience: Amoco Production Research, Tulsa University, Memorial University of Newfoundland

RESEARCH STAFF, POST DOCS and VISITING SCHOLARS

Kevin L. Bertram

Electronics Technician Certificate, 2005, Southern Alberta Institute of Technology

- Work Experience: Aram Systems Ltd.

Malcolm B. Bertram

B.Sc. Geology, Auckland, New Zealand

- Work Experience: GSI (Western Australia), Western Geophysics (Western Australia), Auckland University, University of Calgary.

Huaizhen Chen

B.Sc. Geophysics, 2010, China University of Petroleum
Ph.D. Geophysics, 2015, China University of Petroleum

Raúl Cova

B.Sc. Geophysical Engineering, 2004. Simon Bolivar University, Venezuela.
Ph.D. Geophysics, 2017, University of Calgary
Graduate Diploma in Petroleum Studies, 2011. IFP School. Venezuela

- Work experience: PDVSA Intevep. Venezuela, Shell Canada

Yu Geng

B.Sc. Information Engineering, 2005, Xi'an Jiaotong University
Ph.D. Information and Communication System, 2014, Xi'an Jiaotong University

- Work Experience: MILAB, IGPP, Department of Earth and Planetary Sciences, University of California, Santa Cruz

Marcelo Guarido de Andrade

B.Sc. Physics, 2006, University of São Paulo, Brazil
M.Sc. Geophysics, 2008, University of São Paulo, Brazil
Ph.D. Geophysics, 2017, University of Calgary

- Work Experience: Schlumberger (Houston), PGS (Rio de Janeiro, Brazil), Orthogonal Geophysics, Husky Energy

David C. Henley

B.Sc. Physics, 1967, Colorado State University
M.Sc. Physics, 1968, University of Michigan

- Work Experience: Shell Oil Co., Shell Canada Ltd.

Helen Isaac

B.Sc. Mathematics, 1973, Imperial College, London
M.Sc. Geophysics, 1974, Imperial College, London
Ph.D. Geophysics, 1996, University of Calgary

- Work Experience: Phillips Petroleum Company, Hudson's Bay Oil and Gas, Canterra Energy, Husky, Fold-Fault Research Project at the University of Calgary

Hassan Khaniani

B.Sc. Petroleum Exploration Engineering, 2002, Petroleum University of Technology (PUT)-Iran
M.Sc. Petroleum Exploration Engineering, 2006, University of Calgary / PUT
Ph.D. Geophysics, 2015, University of Calgary

- Work Experience: National Iranian Oil Co. (NIOC), Nexen, Suncor Energy, Reservoir Waveform Solution Ltd. (RWS)

Junxiao Li

B.Sc. Science of Information and Computing (Geophysics), 2009, China University of Petroleum (Beijing)
Bachelor of Arts. English, 2009, China University of Petroleum (Beijing)
M.Sc. Geophysics, 2012, China University of Petroleum (Beijing)
Ph.D. Geophysics, 2017, University of Calgary

Marie Macquet

B.Sc. Earth Science, 2009, University of Nantes (France)
M.Sc. Planetology, 2011, University of Nantes (France)
Ph.D. Geophysics, 2014, Isterre, University of Grenoble (France)

Shahpoor Moradi

B.Sc. Applied Physics, 2000, University of Razi, Iran
M.Sc. Theoretical Physics, 2002, University of Razi, Iran
Ph.D. Theoretical Physics, 2006, University of Razi, Iran
Ph.D. Geophysics, 2017, University of Calgary

GRADUATE STUDENTS

Winnie Ajiduah

B.Sc. Physics, University of Benin, Nigeria
M.Sc. Geophysics, University of Port Harcourt, Nigeria

- Work Experience: Shell Petroleum Development Company of Nigeria

Khaled Al Dulaijan

B.Sc. Geosciences, 2003, University of Tulsa, Oklahoma
M.Sc. Geophysics, 2008, University of Calgary

- Work Experience: Saudi Aramco

Hussain Aldhaw

B.Sc. Geosciences, 2012, University of Tulsa, Oklahoma

- Work Experience: Saudi Aramco

Hani Alzahrani

B.Sc. Geophysics, 2010, University of Oklahoma
M.Sc. Geophysics, 2014 King Abdullah University of Science and Technology (KAUST), Saudi Arabia

- Work Experience: Saudi Aramco

Tim Cary

BA in Physics University of Oxford 2012
BSc in Geophysics with distinction, University of Calgary 2016

- Work experience: Imperial Oil, Nexen Energy UCL

Matt Eaid

BSc. (First Class Honours) Geophysics, University of Calgary, 2015

- Work experience: Shell Canada Ltd.

Dennis Ellison

BSc Geophysics, 2013, University of Calgary.

- Work experience: Thrust Belt Imaging, Devon Energy Corporation

Ali Fathalian

B.Sc. Applied Physics, 2001, University of Razi, Iran
M.Sc. Condensed Matter Physics, 2003, University of Razi, Iran
Ph.D. Condensed Matter Physics, 2007, University of Razi, Iran

Adriana Gordon

B.Sc. Geophysics 2015, Simon Bolivar University, Venezuela

Saul Guevara

B.Eng. Civil Engineering, 1984, National University of Colombia
M.Sc. Geophysics, 2001, University of Calgary

- Work Experience: Ecopetrol ICP

Heather Hardeman

B.Sc. Mathematics (summa cum laude), 2012, University of Montevallo, AL, USA.
M.A. Mathematics, 2014, Wake Forest University, NC, USA.

- Work Experience: Fotech Solutions

Nadine Igonin

B.Sc. Geophysics (first class honours), 2016, University of Calgary

- Work Experience: Microseismic Industry Consortium at the University of Calgary

Andy Iverson

B.Sc. Geophysics (First Class Honours), 2012, University of Calgary

- Work Experience: Apache Canada Ltd, Nexen Energy ULC, Velvet Energy Ltd.

Scott Keating

B.Sc. Honours Physics 2014, University of Alberta

Bernie Law

B.Sc. Geological Engineering (Geophysics), 1982, University of Saskatchewan

- Work Experience: Key Seismic Solutions Ltd.

Arthur Lee

B.Sc. in Electrical Engineering (minor in Computer Engineering), 1988, University of Calgary

- Work Experience: Hampson-Russell GeoSoftware CGG Calgary

Ellen Liu

BSc. Chemical Engineering, 2014, University of Alberta

- Work Experience: ConocoPhillips Canada

Siming (Emma) Lv

B.Sc. Geophysics, 2015, China University of Petroleum (East China)

Andrew Mills

BSc Geophysics, 2014, University of Calgary

- Work experience: Nexen Energy

Jorge Monsegny

B.Sc. Computer Science, 2003, National University of Colombia
M.Sc. Mathematics, 2007, National University of Colombia

- Work Experience: Santander Industrial University, Ecopetrol ICP, National University of Colombia

Evan Mutual

B.Sc. Geophysics, 2015, University of Calgary

- Work experience: Qeye Labs

Zhan Niu

B.Sc., Geophysics, 2017, University of Calgary, (Honor degree with minor in geology)

Wenyong Pan

B.Sc. Computer and Software Engineering, 2009, China University of Geosciences (Beijing)
M.Sc. Geophysics, 2012, China University of Geosciences (Beijing)
Ph.D. Geophysics, 2017, University of Calgary

Sergio Jorge Romahn Reynoso

B. Eng. Geophysics, 2004, National University of Mexico
M.Sc. Exploration Geophysics, 2012, University of Leeds. U.K.

- Work Experience: PEMEX

Tyler Spackman

BSc Geophysics 2014, University of Calgary

- Work Experience: Tourmaline Oil Corp., Husky Energy, Shell Canada, Repsol Oil & Gas Canada Inc.

Jian Sun

B.Sc. Geophysics, 2009, Shandong University of Science and Technology, China
M.Sc. Geophysics, 2012, Shandong University of Science and Technology, China

Ron Weir

B.Sc. Geophysics, 1978, University of Alberta

- Work Experience: Harvest Operations Corp/KNOC

Lei Yang

B.Sc. Exploration Geophysics, 2015, China University of Petroleum, China

ASSOCIATED FACULTY and SCIENTISTS

Andreas Cordsen
Technical Advisor, CREWES, University of Calgary

M.Sc. Geology, 1975, Queen's University, Kingston
M.Sc. Geophysics, 1980, Dalhousie University, Halifax

- Work Experience: BEB, Esso Resources, Norcen Energy, GEDCO, Schlumberger, CHAD Data Ltd.

Patrick F. Daley

B.Sc. Mathematics, 1974, University of Alberta
M.Sc. Physics 1976, University of Alberta
Ph.D. Geophysics, 1979, University of Alberta

- Work Experience: Independent contractor associated with research centres of major oil companies, CREWES

Sam Gray
Technical Advisor, CREWES, University of Calgary

B.S. Math, 1970, Georgetown University
Ph.D., Math, 1978, University of Denver

- Work experience: U.S. Naval Research Lab, General Motors Institute, Amoco, BP, Veritas, CGG

Michael P. Lamoureux
Professor, Department of Mathematics and Statistics, University of Calgary
Adjunct Professor, Department of Geoscience, University of Calgary

B.Sc. Mathematics, 1982, University of Alberta
M.Sc. Mathematics, 1983, Stanford University
Ph.D. Mathematics, 1988, University of California, Berkeley

- Work Experience: Farallon Computing, NSERC Canada

Roy O. Lindseth MC., FRSC
Technical Advisor, CREWES, University of Calgary

Doctor of Laws, Honoris Causa, 1978, University of Calgary

- Work Experience: Chevron; NSERC, Teknica Corporation; TCPL

Faranak Mahmoudian
Technical Advisor, CREWES, University of Calgary

B.Sc., Applied Physics, 2000, K. N. Toosi University of Technology, Iran
M.Sc., Geophysics, 2006, University of Calgary
Ph.D., Geophysics, 2013, University of Calgary

- Work Experience: Shell Canada, Earth Signal Processing

Claude Ribordy
Technical Advisor, CREWES, University of Calgary

Dipl. Physics, 1960, Eidgenossische Technische Hochschule ETH, Zurich
Ph. D. Nuclear Physics, University of Fribourg

- Work Experience: Aquitaine Canada, Petro-Canada, BP, Hampson-Russell Software Ltd., CGG

Brian H. Russell
Adjunct Professor, Department of Geoscience, University of Calgary

B.Sc. Physics, 1972, University of Saskatchewan
Honours Certificate in Geophysics, 1975, University of Saskatchewan
M.Sc. Geophysics, 1978, University of Durham
Ph.D. Geophysics, 2004, University of Calgary

- Work Experience: Chevron Geoscience Company, Teknica Resource Development, Veritas Software Ltd., Hampson-Russell Software Ltd., CGG GeoSoftware

Robert R. Stewart
Cullen Chair in Exploration Geophysics, University of Houston
Adjunct Professor, Department of Geoscience, University of Calgary

B.Sc. Physics and Mathematics, 1978, University of Toronto
Ph.D. Geophysics, 1983, Massachusetts Institute of Technology

- Work Experience: Veritas Software Ltd., Gennix Technology Corp., University of Calgary

Xiucheng Wei
Technical Advisor, CREWES, University of Calgary

B.Sc. Geophysics, 1982, China University of Petroleum
M.Sc. Geophysics, 1992, China University of Petroleum
Ph.D. Geophysics, 1995, China University of Petroleum

- Work Experience: China National Petroleum Company (CNPC), China University of Petroleum (CUP), British Geological Survey (BGS), China Petroleum & Chemical Corporation (Sinopec), International Research Coordinator with the Faculty of Science at the University of Calgary

Joe Wong

B.Sc. Physics/Mathematics, 1971, Queen's University
M.Sc. Applied Geophysics, 1973, University of Toronto
Ph.D. Applied Geophysics, 1979, University of Toronto

- Work Experience: Ontario Ministry of the Environment, University of Toronto, JODEX Applied Geoscience Limited, CREWES

Matt Yedlin
Associate Professor, Department of Electrical and Computer Engineering, University of British Columbia

B.Sc. Honors Physics, 1971, University of Alberta
M.Sc. Physiology, 1973, University of Toronto
Ph.D. Geophysics, 1978, University of British Columbia

- Work Experience: Conoco

Student Theses

The following theses are included with the CREWES 2017 Research Report:

M.Sc.	Khalid Almuteri	Evaluating the Potential of Reflection-Based Waveform Inversion
Ph.D.	Raul Cova	Near-surface S-wave traveltime corrections and inversion: a raypath-consistent and interferometric approach
Ph.D.	Saul Guevara	PS-wave processing in complex land settings: statics correction, wave-mode separation and migration
Ph.D.	Marcelo Guarido de Andrade	Convergence of a full waveform inversion scheme based on PSPI migration and forward modeling-free approximation: procedure and validation
M.Sc.	Bobby Gunning	Multicomponent seismic analysis from an oil sands field, Alberta, Canada
M.Sc.	Michelle Montano	Seismic attenuation measurements from multicomponent vertical seismic profile data
Ph.D.	Shahpoor Moradi	Scattering of Seismic Waves from Arbitrary Viscoelastic-Isotropic and Anisotropic Structures with Applications to Data Modelling, FWI Sensitivities and Linearized AVO-AVAz Analysis
Ph.D.	Davood Nowroozi	Integration of the seismic data with rock physics and reservoir modeling in the FRS project

Ph.D.	Wenyong Pan	Waveform Inversion for Estimating Subsurface Properties: Phase-encoding Strategies, Optimization Methods, Interparameter Tradeoffs Quantification and Reduction
M.Sc.	Eric Rops	Predicting heavy oil and bitumen viscosity from well logs and calculated seismic properties
M.Sc.	Hong (Kiki) Xu	Determination of Reservoir Characteristics Using Geostatistical Analysis

NOTES

Full-Waveform seismic AVAZ responses from orthorhombic models

Sitamai Winnie Ajiduah* and Gary Frank Margrave

ABSTRACT

Fractures are one of the crucial features in the exploration and exploitation for unconventional shale reservoir. In this study, we investigate a set of parallel vertical fractures embedded in a VTI background. Seismic waves propagating through this type of model will exhibit orthorhombic anisotropy. We used staggered-grid finite difference method to estimate the seismic responses from the interface containing the orthorhombic symmetry. We calculated AVAZ responses of the compressional waves and its mode conversions from the fractured layer and compared the results between HTI symmetry and orthorhombic symmetry.

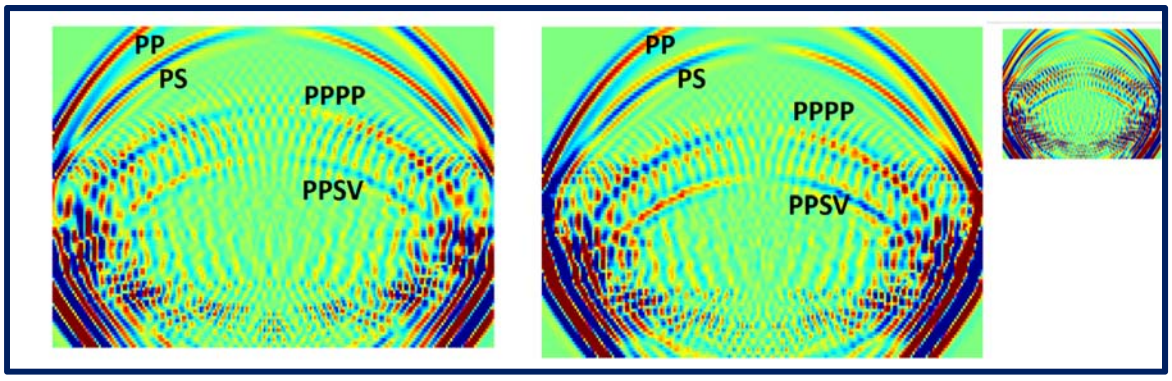

a). x-component snapshots from (i) HTI and (ii) Orthorhombic (iii) differences

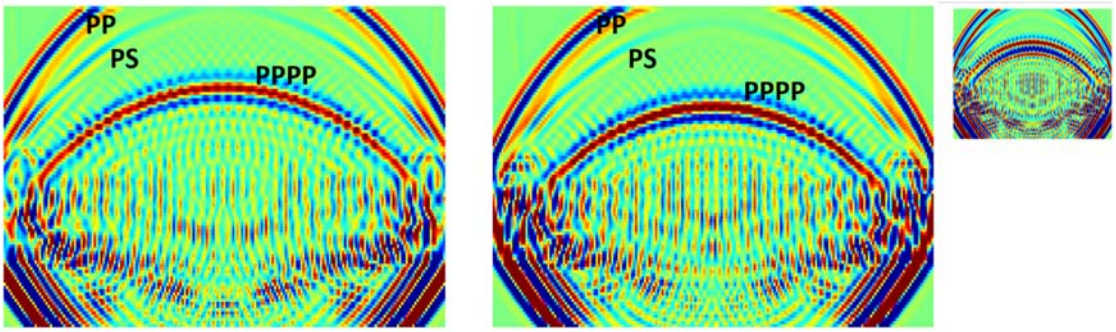

b). z-component snapshots from (i) HTI and (ii) Orthorhombic (iii) differences

FIG. 1. 3-D elastic finite-difference modelling of seismic response from an HTI symmetry and an Orthorhombic symmetry showing snapshots of the x-components and z-components of the displacement in a vertical plane coinciding with the source position at 0.8 s.

AVA & AVAZ of 3D pre-stack seismic data in Altamont-Bluebell field

Khaled Al Dulaijan and Gary F. Margrave

ABSTRACT

In this paper, the Altamont-Bluebell 3D pre-stack seismic data is analyzed using AVA to identify sweet spots and using AVAZ to identify azimuthal seismic anisotropy zones and correlate them to sweet spots. In AVA analysis, the reflection coefficient is a function of incident angle and the three elastic parameters or P-wave velocity, S-wave velocity, and density. Therefore, those parameters are inverted for. In AVAZ analysis, four additional quantities (the symmetry angle and the three TI symmetry parameters) need to be found by inversion of the azimuth/angle-dependent reflection coefficient. Since the reflection coefficient in the AVAZ case is a higher-order function of seven parameters, we may require include information from larger incident angles as compared to AVA analysis. This will be discussed here. The geology of the field, and seismic data acquisition were described earlier in Al Dulaijan (2017). Our focus will be on the main two targets. The first target is the most prolific oil interval within the overpressured Wasatch. This interval is about 500' thick, and called Wasatch 180. Most horizontal wells are drilled within this target. The second target is the shallower and thicker gas reservoir within the Upper Green River (UGR) formation.

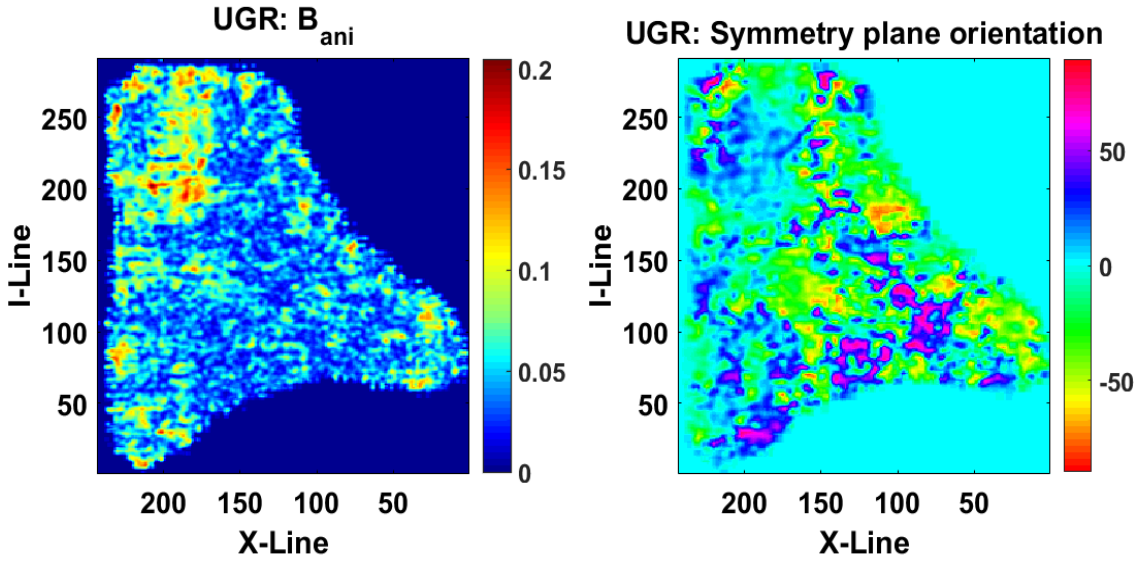

FIG. 1. AVAZ inversion for Upper Green River: Bani horizon (left), symmetry plane orientation horizon (middle), and symmetry plane orientation circular histogram (right).

VSP analysis for azimuthal anisotropy: AVAZ, VVAZ, & S-wave splitting in Altamont-Bluebell field

Khaled Al Dulaijan, Gary F. Margrave and Joe Wong

ABSTRACT

Within the Altamont-Bluebell survey, multiple VSP datasets were acquired. The first dataset was a conventional zero-offset VSP. The second dataset was six shots of offset VSPs. The objective of those shots was to estimate VTI Thomsen parameters to aid with 3D processing of seismic data, and also to create a HTI model for fracture characterization of the reservoirs. However, these offset VSPs were limited in terms of depth, offset, and azimuthal coverage, and walkaway VSPs would have been a better choice for such an objective, but certainly more expensive. The third data set was a 4-component VSP. Its objective is S-wave splitting analysis for fracture characterization of the reservoirs.

In this paper, we began with the raw field data, applied processing, including some twists in order to use surface seismic methods of AVAZ and VVAZ on VSP data, which resulted in final products of azimuthal anisotropy intensity and orientation parameters. Offset VSPs were processed through the VSP-CDP transform, then AVAZ analysis was applied. A VVAZ workflow is developed here for offset, walkaround, or walkaway VSPs using a method for surface seismic, and interval anisotropy properties are calculated for each receiver. For AVAZ and VVAZ, deeper levels including the deeper target of Wasatch-180 are more reliable because of better coverage. S-wave analysis is carried out using Alford (1986) 4-C rotation to separate fast and slow modes. This method assumes that the symmetry axis is vertically invariant. To overcome this assumption, a layer stripping technique was applied using Winterstien and Meadows (1991).

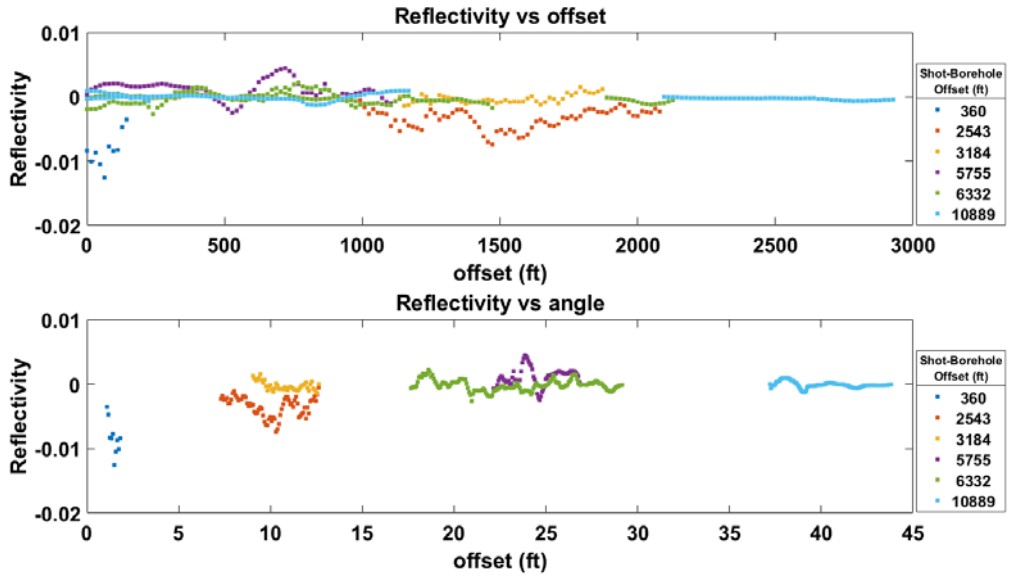

FIG. 1. Reflectivity vs offset (top), and reflectivity vs angle of incidence (bottom).

Field acquisition in 2017

Kevin L. Bertram, Kevin W. Hall, Malcolm B. Bertram, Donald C. Lawton and Kristopher Innanen

ABSTRACT

CREWES continues to be one of the few research consortiums that has access to industry acquisition equipment. CREWES also has the collective knowledge to use this equipment to design and carry out acquisition experiments at any time of year. This provides the opportunity to take ideas from the office to the field. This is also used to educate staff and students on the procedures and realities of real world data acquisition.

Acquisition that was carried out by CREWES in 2017 include: a) a multi receiver 3D 3C seismic survey at FRS with vibe and thumper sources in May; b) GPS experiments at Priddis in June; c) another multi receiver 3D 3C seismic survey at FRS with just the vibe as a source in July; d) the geophysics undergraduate field school in August; e) a final multi receiver 3D 3C seismic survey at the FRS in October.

FIG. 1. CREWES in the field.

Moving forward with physical modeling

Kevin L. Bertram, Kristopher Innanen and Joe Wong

ABSTRACT

For many years now CREWES has used a physical modeling facility to acquire scaled-down repeatable 2D and 3D marine seismic data. This system is capable of producing seismic industry standard SEGY files that can easily be used by processing software. This is an invaluable tool for conducting experiments in house with various interface modules.

Piezo pin transducers are used for both sources and receivers. Currently the system can run with a single source and receiver or a single source and eight receivers. There is a desire to increase the number of active transducers in a survey to reduce the acquisition time. New transducers have been developed that produce S-waves, but these are larger in size and are contact transducers that require physical contact with the model. CREWES is interested in using this technology to conducting further experiments.

Currently the software is text based and requires some changes in the source code to perform different surveys. There is a need to create a GUI interface for simplicity's sake to make using the system more accessible to members of CREWES.

There is also an interest in creating newer more complicated models. The idea of using 3D printing technology is being looked at. This will require testing with new materials for contrast results of interfaces.

FIG. 1. The physical modeling system.

Procedure for determining geothermal viability

Timothy Cary, R. Lauer and K. Innanen

ABSTRACT

The initial research to determine a procedure for evaluating the viability of a site and optimization of placement for geothermal energy installation (ground source heat pump, Fig. 1.), based on rock and soil properties, is outlined. The current routine begins with a joint p-wave and s-wave velocity inversion utilizing refraction and surface wave seismic data. There is the potential to include resistivity data to further constrain the inversion as part of the joint inversion scheme, whereby, the difference between two inverted porosity values calculated from the p and s-wave velocities and the resistivity are integrated into the minimization of the objective function. The resulting porosity inversion would have further use in the ground water flow modeling exercise to characterize heat transfer and flow.

The temperature distribution of the subsurface remains consistent throughout the year, the global average temperature gradient is $30℃/km$. Variations in this gradient are due to ground water flow direction and the minerology of the local rock and soil. Of these two, ground water flow has the largest influence. Hydrothermal modeling will serve to replicate the fluid flow around the site. Well logs, core logs, and hydraulic head data will be required for calibrating such models. The velocity and porosity inversions will provide mineralogical information, via rock physics templating, to further calibrate the fluid flow modeling.

The refraction seismic and surface wave seismic data can be extracted from the same survey, performed using a vibroseis, increasing efficiency. The ERT data set can also be gathered along the same survey line. The inversion is then performed holding the structure constant for both models – resistivity and velocity.

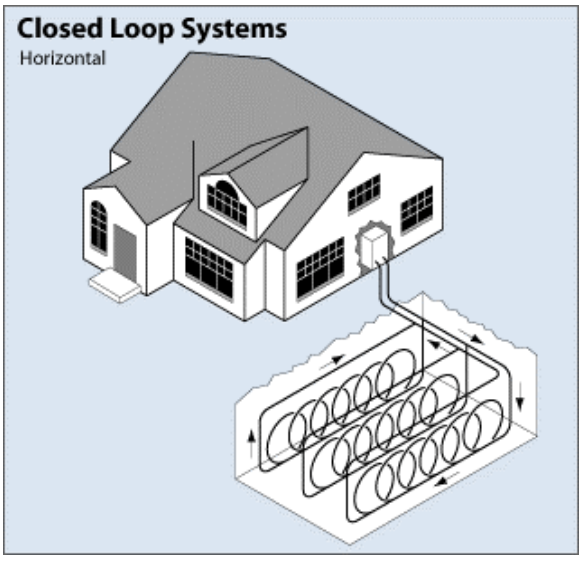

FIG. 1. Example of a horizontal layout for a closed loop geothermal heat pump (image taken from https://energy.gov/energysaver/geothermal-heat-pumps).

Estimation of fracture weaknesses and integrated attenuation factors from azimuthal seismic data

Huaizhen Chen* and Kristopher Innanen

ABSTRACT

Seismic wave propagation in fractured reservoirs exhibits anisotropy and attenuation that are related to fracture properties (e.g. fracture density) and fluid parameters (e.g., fluid moduli and viscosity). Based on the linear slip theory, we derive stiffness parameters for fractured and attenuative rocks, and present the integrated inverse quality factors involving both host rock intrinsic attenuation and fracture-induced attenuation. Using the simplified stiffness parameters, we derive a linearized reflection coefficient in terms of fracture weaknesses and integrated inverse quality factors. A two-step inversion approach is proposed, which involves an iterative damped least-squares algorithm to predict P- and S-wave moduli using angle gathers at the azimuthal angle approximately equal to fracture orientation azimuth, and a Bayesian inversion method to estimate fracture weaknesses and integrated inverse quality factors from seismic amplitude differences among the data at different azimuthal angles. Tests on synthetic data confirm the proposed approach makes a stable inversion for fracture weaknesses and integrated inverse quality factors in the presence of moderate data noise. The proposed approach is further confirmed on a fractured carbonate real data set, within which we observe that reasonable parameters (P- and S-wave moduli, fracture weaknesses and integrated inverse quality factors) are determined. We conclude that the proposed inversion approach can provide reliable parameters for prediction of natural fractures and discrimination of fluid type.

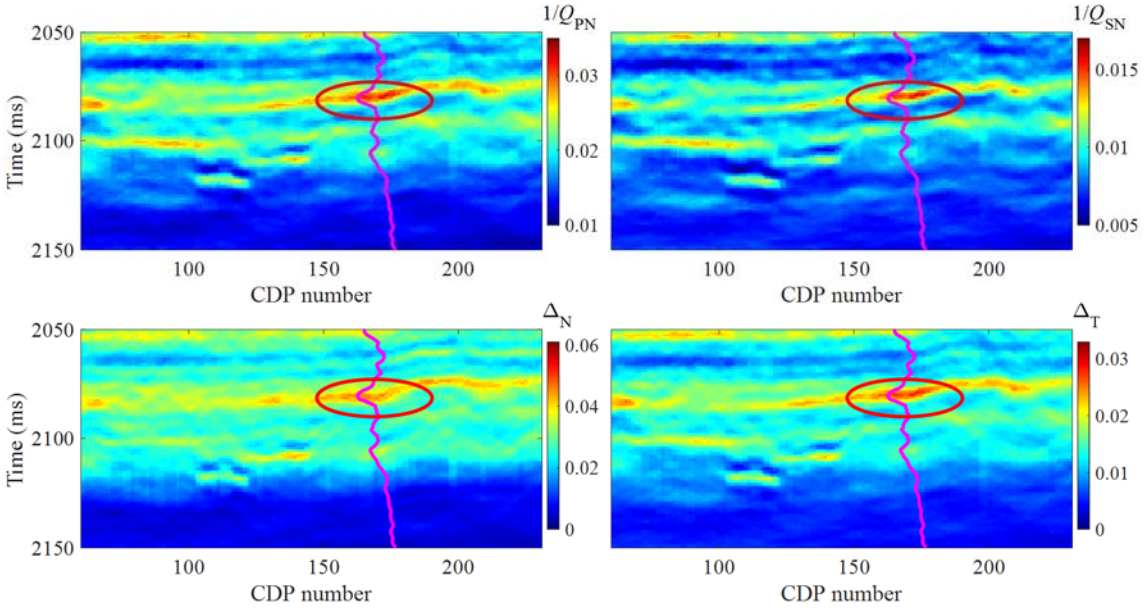

FIG. 1. Inversion results of integrated attenuation factors and fracture weaknesses.

Exact solution of reflection coefficient in reservoirs with tilted fractures

Huaizhen Chen and Kristopher Innanen

ABSTRACT

We first present detailed expressions of polarization vectors of P- and SV-waves for a transversely isotropic medium with a tilted symmetry axis (TTI) as a function of stiffness parameters of a transversely isotropic medium with a vertical symmetry axis (VTI), and then we propose the equation to calculate the exact solution of PP-wave reflection coefficient in TTI media. In order to relate the stiffness matrix of TTI media to fracture properties (e.g. fracture density and filling's moduli), we use the stiffness matrix of HTI media given by the linear slip theory to obtain the stiffness matrix of VTI media using the Bond rotation, which provides us to calculate stiffness parameters for TTI media given different fracture properties and tilted angles. We also study how to compute the transmission angle in TTI media using the extended Snell's law. We finally model PP-wave reflection coefficient variations with the incidence angle and the azimuthal angle given different values of fracture density and tilted angle. We conclude that in the case of TI media with a high tilted angle, the tilted angle mainly affects the value of the reflection coefficient, while the fracture density affects the variation of reflection coefficient with the azimuthal angle.

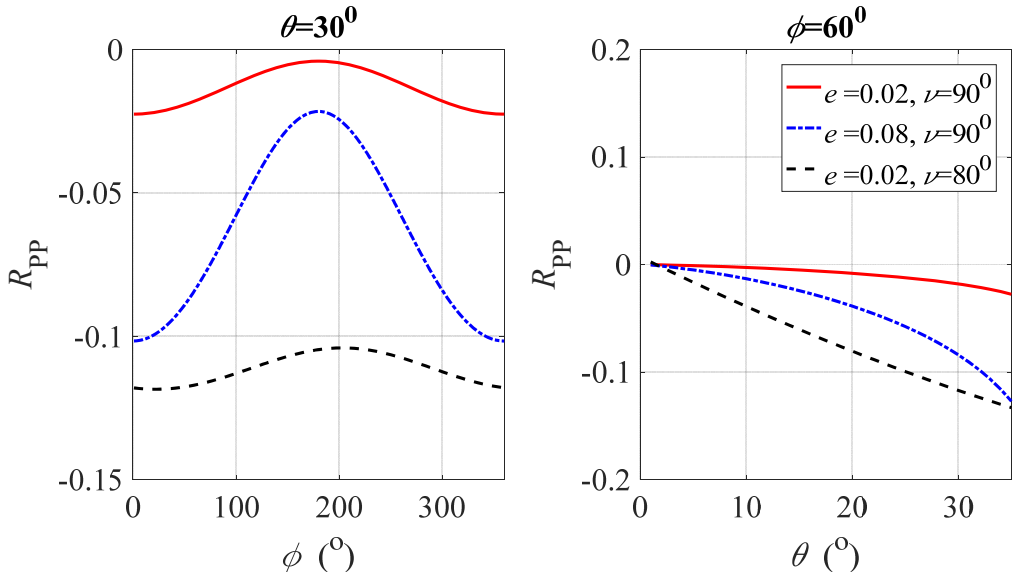

FIG. 1. Reflection coefficient variations with the incident angle θ and the azimuthal angle ϕ in the case of different values of fracture density and tilted angle. The quantities e and ν are the fracture density and the tilted angle, respectively.

Linearized reflection coefficient and reflectivity modeling in fractured and attenuative reservoirs

Huaizhen Chen and Kristopher Innanen

ABSTRACT

Based on the complex linear slip theory, we derive complex stiffness parameters in terms of fracture weaknesses and induced attenuation factor under the assumption of the host rock being elastic and isotropic. Incorporating with the attenuative crack model, we present an explicit expression of the induced attenuation factor, and study how fracture density and water saturation affect the variation of the induced factor. Using perturbations in the complex stiffness parameters, we derive a complex linearized reflection coefficient involving the induced attenuation factor and fracture weaknesses. The accuracy of the derived reflection coefficient is confirmed by comparing the result calculated using the extended reflectivity method and that computed using the derived equation. We finally use the derived linearized reflection coefficient to obtain the seismic reflection response for the case of fractured reservoirs with different values of fracture density and water saturation. We conclude that the attenuation factor is applicable to distinguish between oil-bearing and water-bearing reservoirs, and seismic response difference induced by fracture density and water saturation increases with the incidence angle.

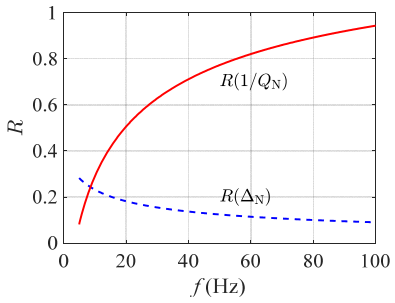

FIG. 1. Absolute value of relative difference between water and oil saturated rocks for the normal fracture weakness and the attenuation factor.

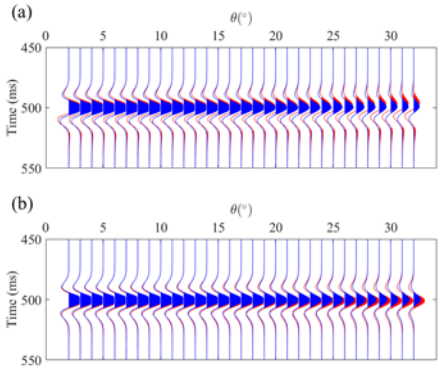

FIG. 2. Seismic profiles generated for oil-bearing fractured and attenuative rocks. (a) effect of water saturation; (b) effect of fracture density.

Computing velocity models for S-wave static corrections using tau-differences in the rayparameter domain

Raúl Cova, David Henley and Kris Innanen

ABSTRACT

A near-surface velocity model is one of the typical products generated when computing static corrections, particularly in the processing of PP data. Critically-refracted waves are the input usually needed for this process. In addition, for the converted PS mode, S-wave near-surface corrections must be applied at the receiver locations. In this case, however, critically-refracted S-waves are difficult to identify when using P-wave energy sources. Here we use the τ-p representation of the converted-wave data to capture intercept-time differences between receiver locations. These τ differences are then used in the inversion of a near-surface S-wave velocity model. Our processing work-flow provides not only a set of raypath-dependent S-wave static corrections but also a velocity model that is based on those corrections. Our computed near-surface S-wave velocity model can be used for building migration velocity models or to initialize elastic full waveform inversions. Our tests on synthetic and field data provided superior results to those obtained by using a surface-consistent solution.

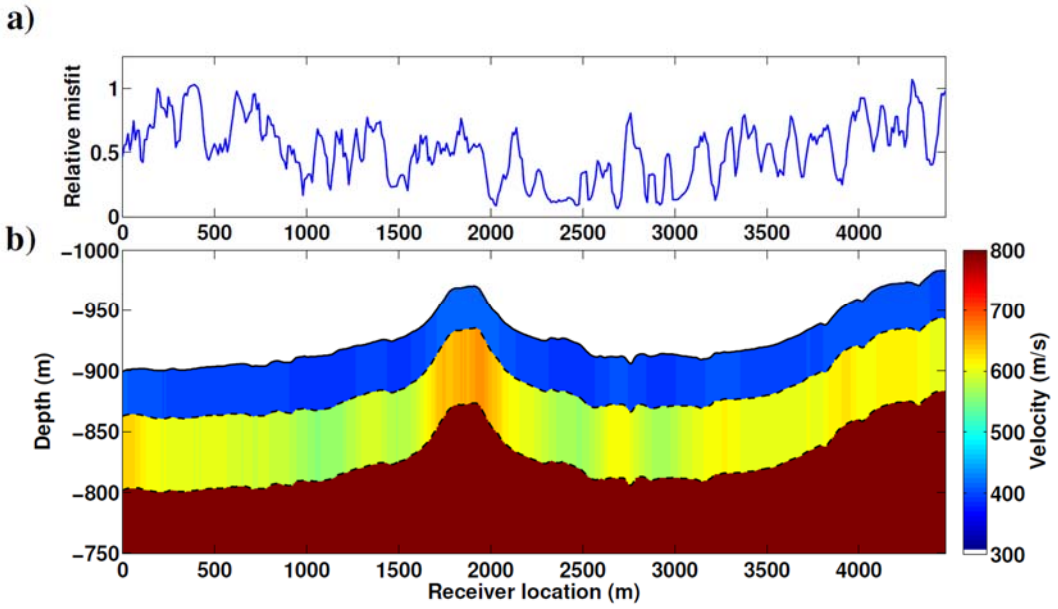

FIG. 1. (a) Relative inversion misfit (ratio between the average misfit and the average measured Δτ) per receiver location. (b) Inverted near-surface S-wave velocity model, used to compute raypath-dependent near-surface and elevation corrections for the converted-wave data of the Hussar dataset.

Toward robust multicomponent FWI on land data: handling topography and data conditioning

Raúl Cova*, Bernie K. Law and Kris Innanen

ABSTRACT

Successful full-waveform inversion (FWI) studies using multicomponent marine data have been often reported in the literature. However, FWI applications to multicomponent land data remain limited. Among the challenges for a successful FWI in this setting we can find source repeatability, receiver coupling, rough topography, near-surface heterogeneities and strong elastic and attenuation effects. Due to the difficulty of including all these effects during the inversion process, it is a common practice to minimize their imprint on the data by conditioning the data before the inversion. Here we present a framework to study the effect of this conditioning on the FWI output. We first address the convenience of using a finite difference algorithm to include the topography during the forward modelling and its implications on the modelling of surface-waves. We compared this with the output of a spectral element method (SEM) algorithm. The latter one showed a more accurate modelling of the surface-wave dispersion profile expected from the data. Also, less backscattered energy resulting from the discretization of the model was obtained. A benchmark dataset was also created to understand the effect of the data conditioning processes on the FWI output. Well log data available along the Hussar 2D-3C seismic line was used to build V_p, V_s and density models. A near-surface V_p model derived from first arrivals tomography was used to include velocity changes in the near-surface. Then, surface-consistent residual static corrections, amplitude corrections, and deconvolution operators, for the vertical and horizontal components, were derived from the real data and their inverse applied to the synthetic data. The goal was to obtain a synthetic dataset that would include some of the effects that are observed in the real multicomponent land data. This dataset will be used for understanding to what extent the conditioning of the data affects the inversion output and what strategies can be used to minimize their imprint in the inversion process.

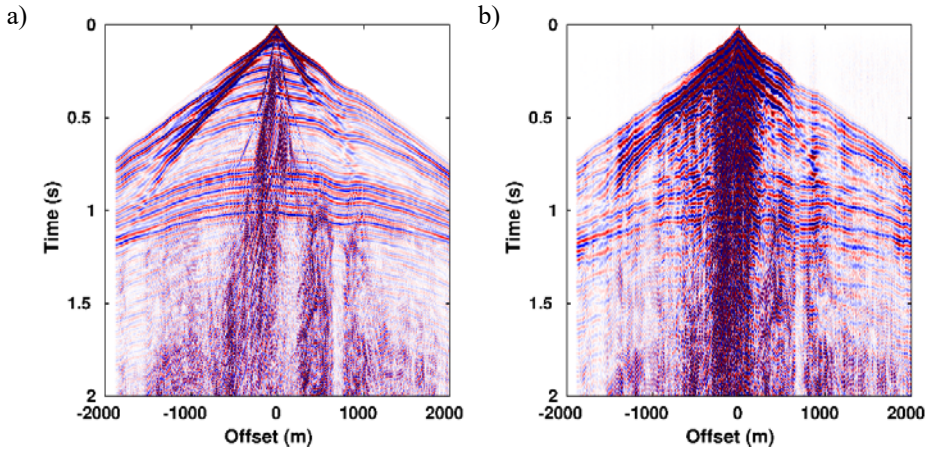

FIG. 1. a) Synthetic gather computed from the velocity and density models derived from well log data and including the topography. b) Synthetic data after applying the inverse of the surface-consistent residual static corrections, amplitude corrections and deconvolution operators derived from the real data.

Efficiency in multiple prediction, leveraging the CMP gather

Matt Eaid and Kris Innanen

ABSTRACT

Geophysics has seen a shift from mapping large-scale obvious features, to the mapping of subtle features, and accurate inversions for subsurface parameters. The presence of large amplitude multiples in the data makes both a challenging task, motivating the need for more robust methods of internal multiple prediction. The most successful method of internal multiple prediction is the fully data-driven algorithm based on the inverse scattering series, which has proven very successful on synthetic data, and is currently being adapted to work on land and marine data. However, one of the main hurdles obstructing its successful application is its computational expense. Typically, computationally expensive 2D algorithms must be applied when the underlying geology contains any structure, in order to produce an accurate prediction. By leveraging properties of the CMP gather we show that the 1.5D algorithm may be applied in the presence of moderate dip, greatly improving efficiency, while maintaining a high level of accuracy.

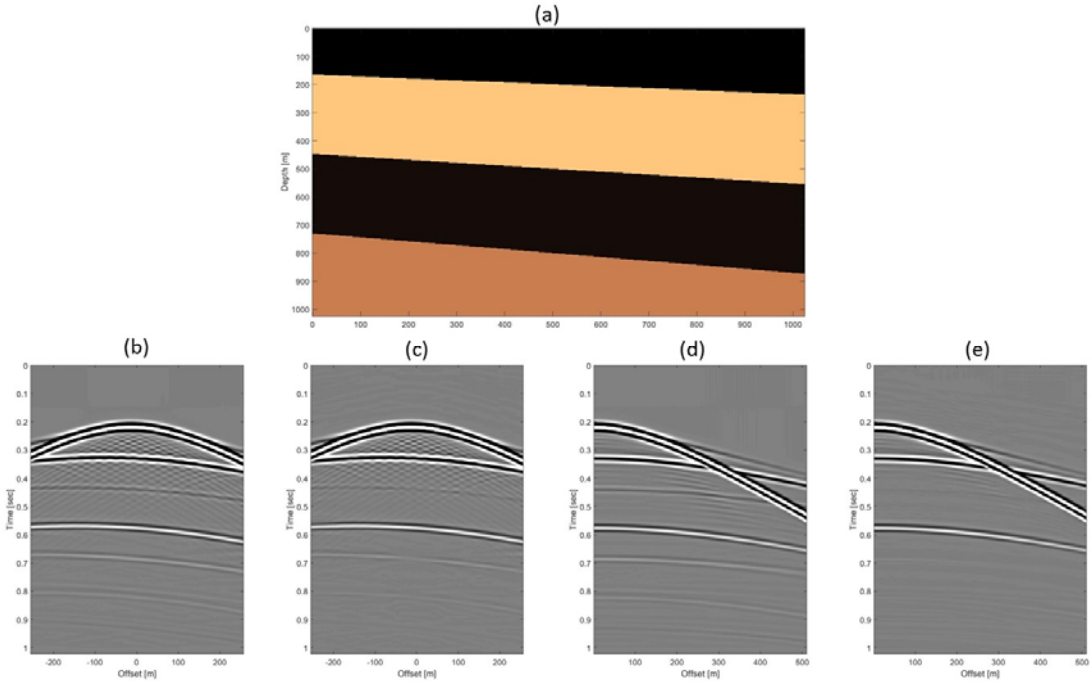

FIG. 1. Velocity model (a) with layers dipping at 2, 4, and 6 degrees respectively. (a) Split spread shot record from velocity model, (b) resulting 1.5D internal multiple prediction, (c) CMP gather extracted from center of velocity model, (d) Resulting 1.5D internal multiple prediction. Results show much better attenuation of multiples when the input to the prediction a CMP.

Three dimensional elastic wave modeling with shaped DAS fibres

Matt Eaid* and Kris Innanen

ABSTRACT

The interest in Distributed Acoustic Sensing (DAS) fibres, for improved geophysical acquisition, has seen substantial growth over the last half decade. The ability to drive down acquisition costs, improve repeatability, and expand the application of seismic acquisition are all attractive properties of DAS technologies. While applications of straight DAS fibres have proven successful, their well-known broadside insensitivity greatly limits their application. Research efforts have recently shifted to creating fibres in more complicated shapes, such as helices, to better characterize, and recover the wavefield. These technologies show promise in negating the effects of broadside insensitivity, however, the interpretation of seismic signals recorded on helically-wound fibres is not well understood. In order to learn more about how the signal captured by shaped fibres relates to the signal captured by conventional geophones, it is imperative to develop full 3D elastic modeling tools to investigate the response of fibres of arbitrary shape, in the presence of elastic wavefields. We begin with a discussion of the geometrical model of fibres of arbitrary shape, and how they measure the seismic wavefield. We then discuss the velocity-stress method of 3D elastic wave propagation, and how it may be extended to apply to DAS fibres. Finally, we conclude with some examples of elastic wave modeling using DAS fibres, and discuss how this technology will expand.

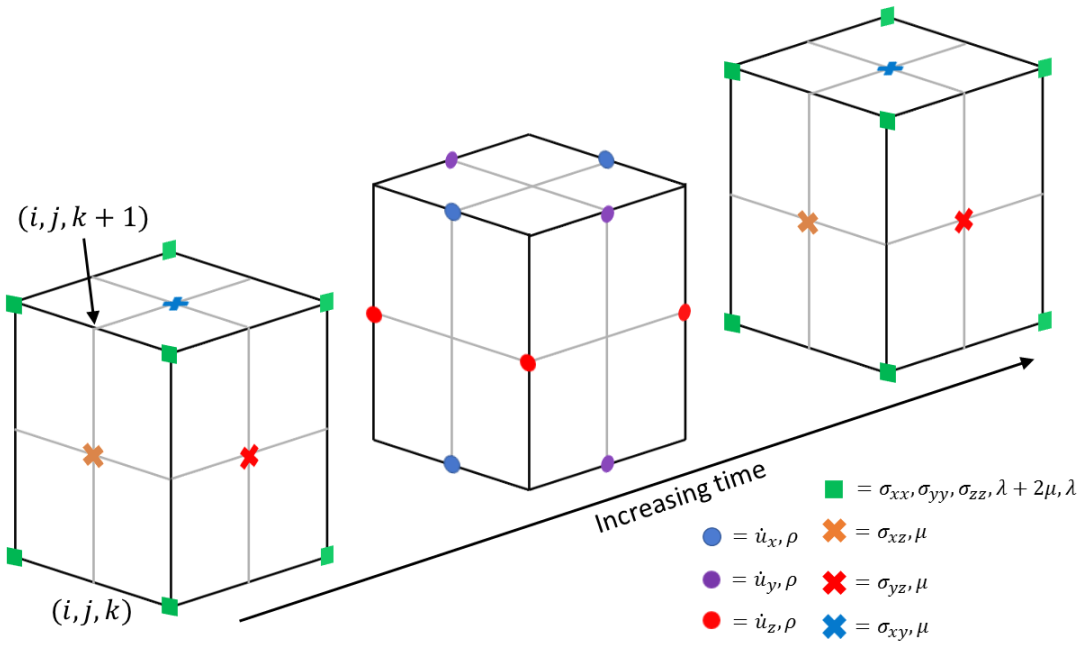

FIG. 1. Staggered grids required for 3D velocity-stress finite difference propagation of an elastic wavefield.

Eliminating time statics from depth imaging

Dennis K. Ellison and Greg Cameron

ABSTRACT

When seismic data are used to image the subsurface, assumptions (Figure 1a) and calculations are made about the near-surface to overcome the uncertainty of the velocities of the low velocity layer.

Refraction and reflection statics are calculated because often the lack of detailed near-surface information leads to inaccuracies. A normal moveout (NMO) velocity field is picked and applied to stack the data in preparation for the reflection statics calculations. NMO is a correction based on the assumption that the moveout can be approximated by a hyperbola (Figure 1c). However, the accuracy of this assumption is valid when the moveout on data is near-hyperbolic and symmetric, and deviates when the moveout is more complicated due to complex geology (Figure 1d). Scenarios of non-hyperbolic non-symmetric moveout are when high velocities are near the surface and when there are variations in the seismic weathering thickness and velocities (Figure 1b).

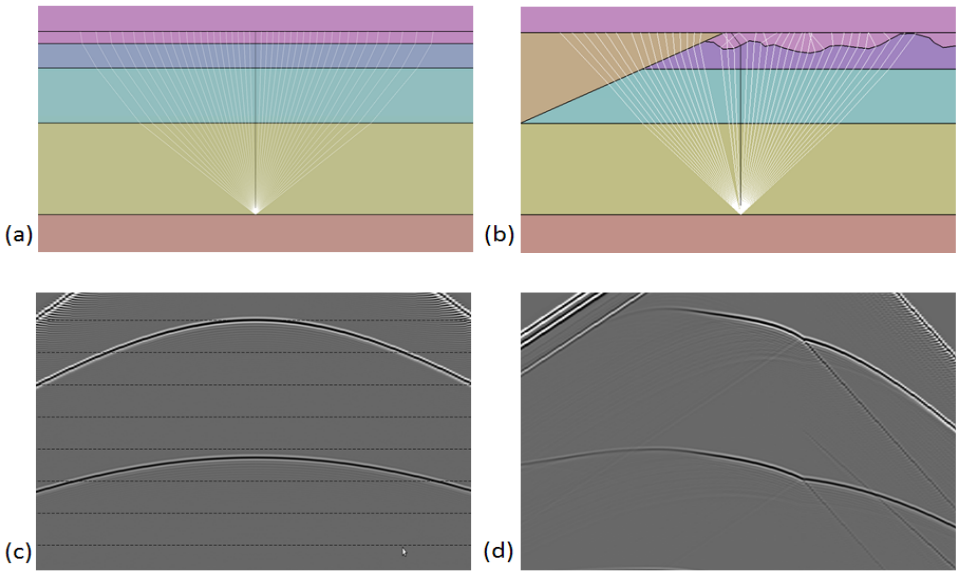

FIG. 1. Ray fan showing (a) near-vertical rays at the near-surface when velocities are slower in the near surface and when seismic weathering is flat and geology is horizontally homogeneous, (b) non-vertical rays in the near-surface when velocities are faster than the layer below and when seismic weathering is complicated. (c) The expected hyperbolic moveout for flat geology, (d) moveout that deviates from the hyperbolic assumption given a complex geology.

Raytracing in depth migration has overcome many of the issues with the assumptions in time migration. Foothills datasets and other geologically complex environments compel us to look for ways to overcome these assumptions as they are violated. By merging the near-surface tomographic with the depth velocity model and calculating a model-based moveout correction for reflection statics depth imaging can be enhanced.

Approximation constant-Q reverse time migration in the time domain: Unsplit-field PML formulation

Ali Fathalian and Kris Innanen

ABSTRACT

We investigate the simulation of wave propagation in attenuation medium within approximating constant-Q. Such wave propagation can be modelled with a finite difference scheme by introducing a series of standard linear solid (SLS) mechanisms, and it can be carried out within a computationally tractable region by making use of perfectly-matched layer (PML) boundary conditions. To consider the effects of the number of relaxation mechanisms (L), we compare numerical and analytical solution of the wave equation for a homogeneous and complex medium. In strong attenuation (Q = 20), when the wave reaches greater depth, the error of numerical solutions using single SLS mechanism increase and the viscoacoustic RTM images using a single SLS mechanisms are not so accurate in the deeper layers. Although the results of single SLS relaxation mechanism are still useful for practical application, the three SLS relaxation mechanisms are quite accurate for both weak and strong attenuation.

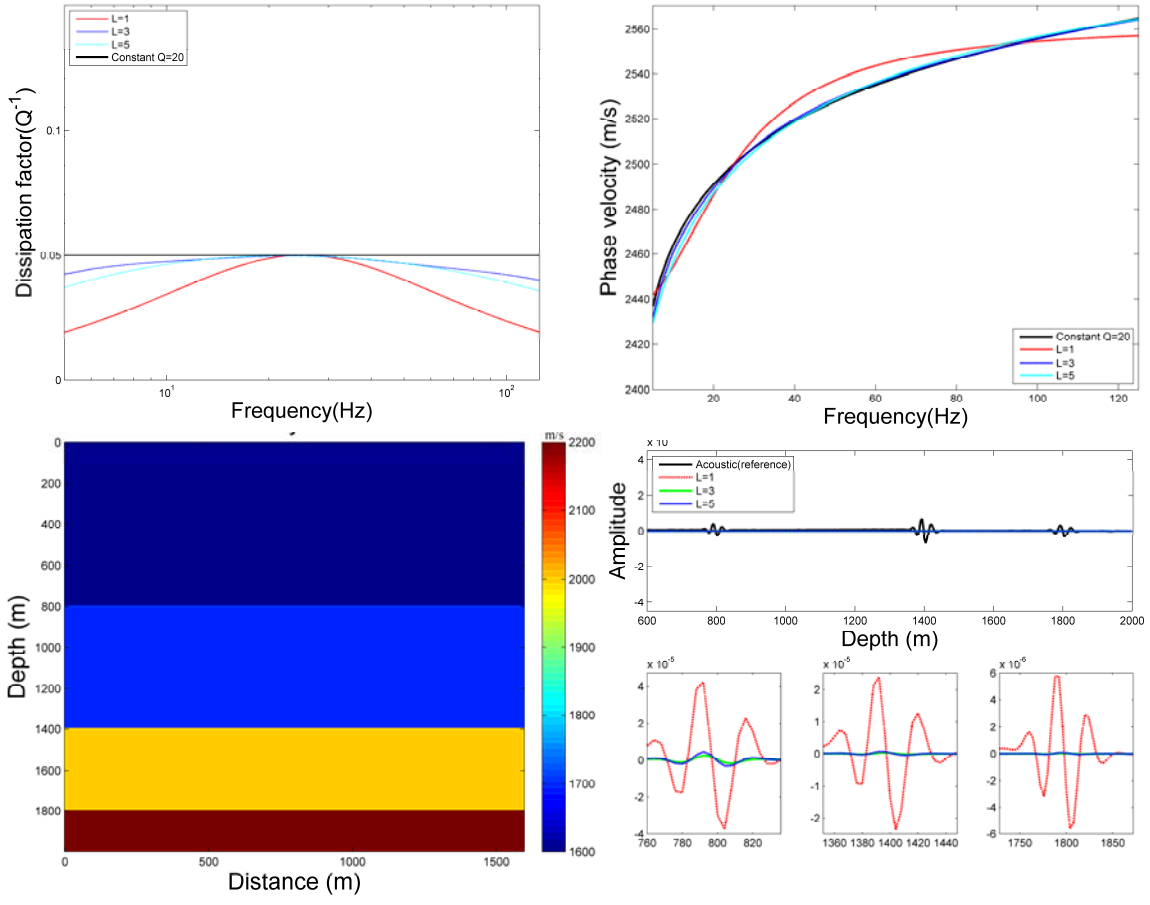

FIG. 5. The dissipation factor (a) , phase velocity (b), the layered velocity model (c) , and depth slices from RTM images showing the effect of attenuation and comparison of acoustic and viscoacoustic cases with different relaxation mechanisms (d) of constant Q = 20.

Viscoacoustic VTI and TTI wave equations and their application for anisotropic reverse time migration: Constant-Q approximation

Ali Fathalian* and Kris Innanen

ABSTRACT

We investigated the simulation of viscoacoustic wave propagation and reverse time migration (RTM) in transversely isotropic (TI) media, vertical TI (VTI) and tilted TI (TTI), within approximating constant-Q. Reverse time migration (RTM) is based on two-way wave equation and has advantages over than other imaging methods. Such wave propagation can be modeled with a finite difference scheme by introducing a series of standard linear solid (SLS) mechanisms, and it can be carried out within a computationally tractable region by making use of perfectly-matched layer (PML) boundary conditions. The viscoacoustic wave equation for VTI and TTI mediums have been derived using the wave equation in anisotropic media by setting shear wave velocity as zero. Using the TI approximation and ignoring all spatial derivatives of the anisotropic symmetry axis direction leads to instabilities in some area of the model with the rapid variations in the symmetry axis direction. A solution to this problem is proposed that involves using a selective anisotropic parameter equating in the model to reduce the difference of Thompson parameters in areas of rapid changes in the symmetry axes. To eliminate the high-frequency instability problem, we applied the regularization operator and built a stable viscoacoustic wave propagator in TI media. After correcting for the effects of anisotropy and viscosity, the anisotropy RTM image in attenuation media with high resolution is obtained and compared with the isotropic RTM image.

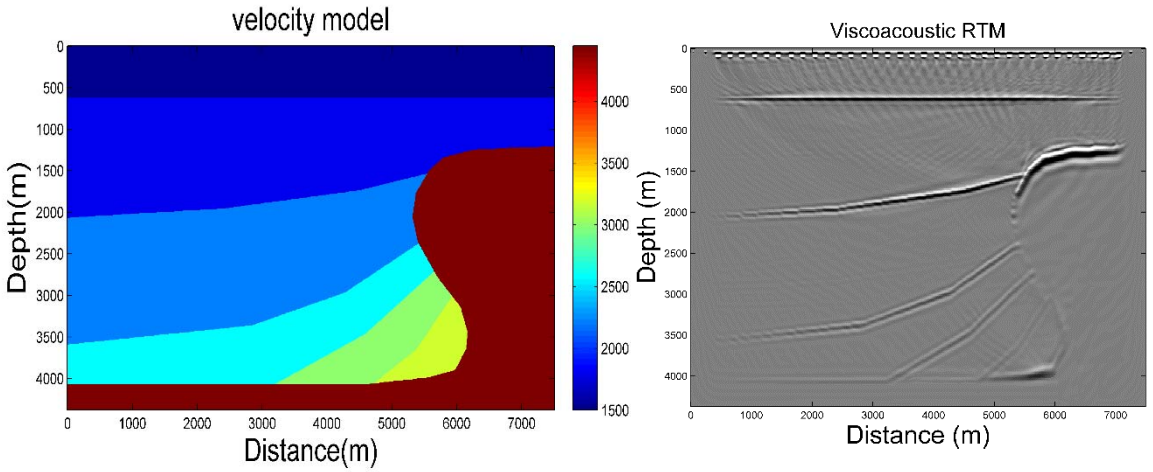

FIG. 5. Transversely isotropic velocity model with specially varying symmetry axis direction (a) and TTI migration result (b).

Nonlinear multiparameter full waveform inversion based on truncated Newton method

Yu Geng, Kris Innanen and Wenyong Pan

ABSTRACT

Full waveform inversion (FWI) is a powerful tool to reconstruct subsurface parameters. This highly nonlinear inverse problem is normally solved iteratively to minimize a misfit function, which is usually defined as the distance between the observed and predicted data, by gradient-based method or Newton type method. Incorporating more nonlinearity within each update in FWI, especially for multiparameter reconstruction, may have very important consequences for convergence rates and discrimination of different parameter classes. In this study, we focus on acoustic media with variable density, and the goal is to simultaneously update velocity and density, other parameterization is also discussed. We start from the physical interpretation of both the gradient and the Hessian of the misfit function, and derive one approach from the Newton method, to include the additional term of the Hessian, which contains the second-order partial derivative of the wavefield and related to the second-order scattering, into the gradient, to construct a new descent direction. A matrix-free scheme is used to efficiently calculate the product of the Hessian and a vector.

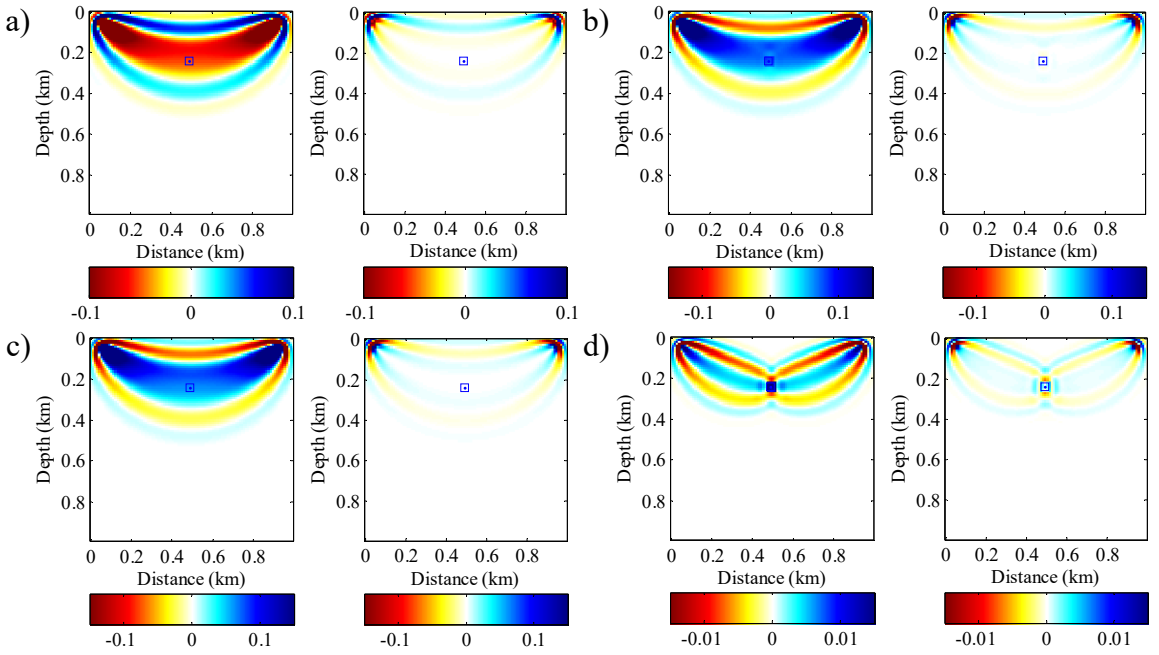

FIG. 1. Gradient and Hessian-vectors for velocity (left column) and density (right column) in a linearly changing media with one small velocity perturbation (indicated with blue box) inside the first Fresnel zone. a), gradient, b), full Hessian-vector, c), Gauss-Newton Hessian-vector and d), Hessian-vector with the first term in Hessian.

Subspace method for multiparameter FWI

Yu Geng, Kris Innanen and Wenyong Pan

ABSTRACT

Full waveform inversion aims to find the high-resolution subsurface model parameters. It is usually treaded as a nonlinear least square problem, and the minimum of the related misfit function is found by updating the model parameters. Simple gradient methods could mix different parameter types in the case of inversion with multi-parameter classes, which could lead to a poor convergence and strong dependence on the scaling of the different parameter types. Searching the step length in a subspace domain instead of treating the gradients of different parameters as the same could help solving this problem. The subspace used can be defined in a span of different sets of data or different parameter classes, which is a small amount of vectors compared to the whole model space. Using the subspace method, the basis vectors are needed to be defined first, and a local minima is found in the spanned space to invert the perturbations. We are investigating this method to get a better update of density.

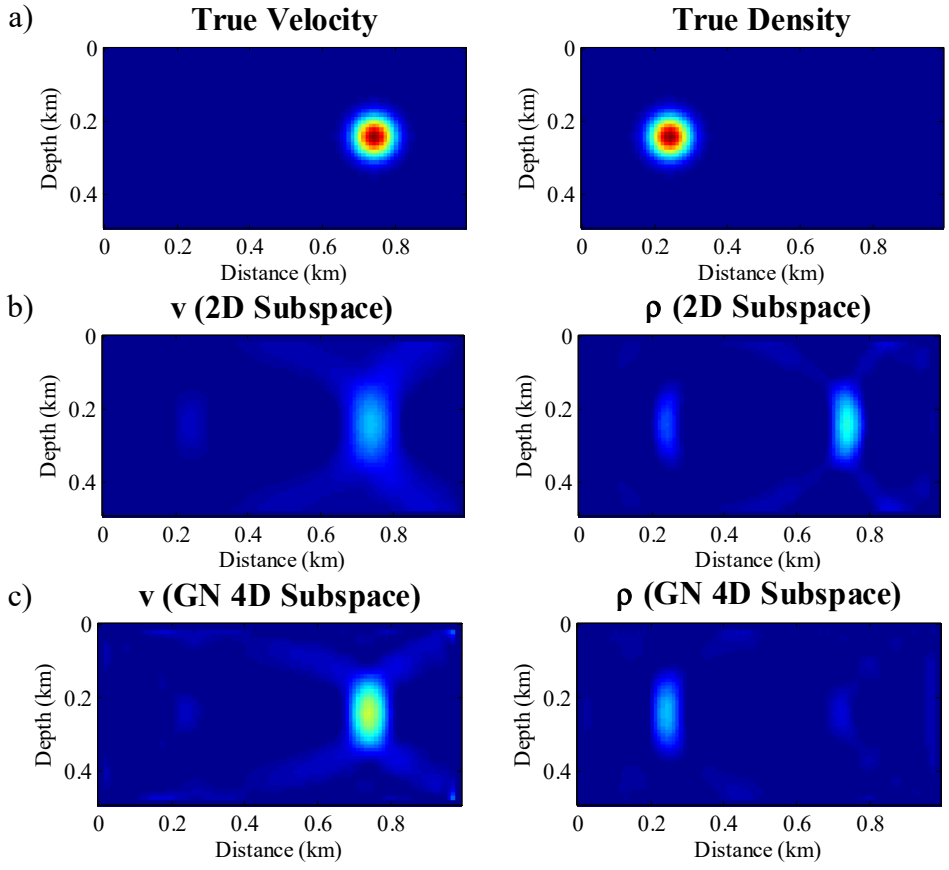

FIG. 1. True velocity model a), inversion using 2D subspace method b) and Gauss-Newton method combined with 4D subspace method c).

Zero offset VSP processing of fibre optic cable (DAS) and geophone array at the CaMI Field Research Station

Adriana Gordon* and Don C. Lawton

ABSTRACT

Two Vertical Seismic Profiles (VSP) were acquired in May and July of 2017 at the Containment and Monitoring Institute Field Research Station (FRS) in Newell County, Alberta. These surveys were recorded using two different receiver types; a 24-level 3C geophones array and an integrated fibre optic cable (DAS and DTS). A zero-offset processing flow was completed for two shot points and an 80 m offset shot for both the fibre optic cable and geophone array. Before processing, a calibration step was necessary to estimate the exact depth for each trace in the fibre optic data set. There was an accurate result between the cross-correlation of the first and last geophone trace, a difference between 0 to 3 m or 0 to 12 traces was calculated from the calibration. After the processing flow was completed, a good match was obtained between the corridor stack of both the down-going and up-going segments of the fibre loop, as expected. A time difference of approximately 20 ms between the DAS and geophone data was also noticeable which might be caused to the difference between the signal recorded by the geophones and the fibre optic cable. A few tests for converting the DAS signals to particle velocity were evaluated and a similar calibration difference between the first and last geophone was obtained.

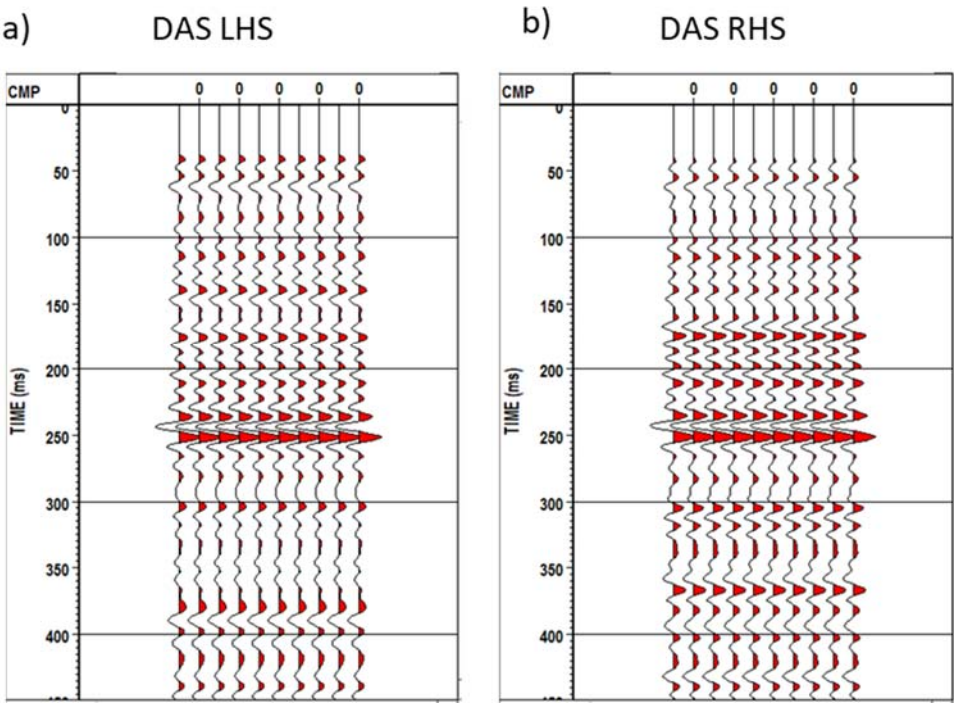

FIG. 1. Outside corridor stack comparison of two segments of the fibre optic loop for a zero-offset shot gather acquired in July 2017 (source point 132, line 21). a) Corridor stack of left hand side (LHS) of fibre loop. b) Corridor stack of right hand side (RHS) of fibre loop.

Comparing the RTM and PSPI migrations to estimate the gradient using the fast waveform inversion

Marcelo Guarido, Sergio J. Romahn, Laurence R. Lines, Robert J. Ferguson and Kristopher A. H. Innanen

ABSTRACT

The gradient that optimize the model update in the full waveform routine is mainly obtained by a reverse-time migration of the residuals. However, if we can interpret the whole routine as a combination of seismic processing tools, we believe it is possible to obtain the gradient using any kind of depth migration. In this paper, we are comparing the use of RTM and PSPI migration to estimate the gradient, using the post-stack forward modeling-free approximations of the FWI, the FastWI. The inverted models using RTM and PSPI migrations have similar resolution in a simple velocity model, with the advantage of the PSPI been cheaper, but the RTM may lead to more continuous and high-resolution models on more complex geologies.

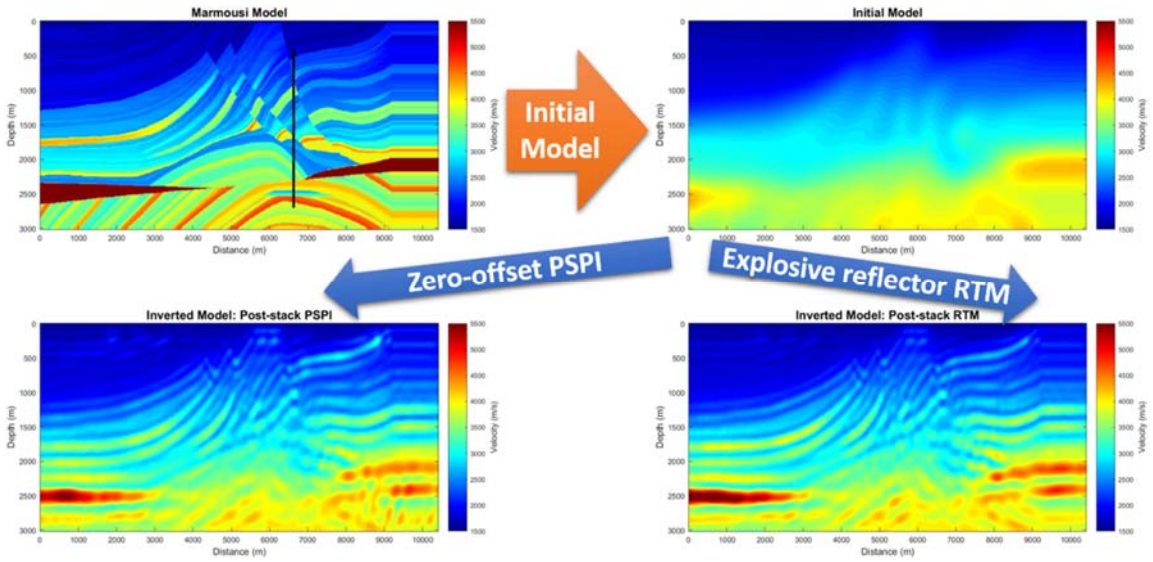

FIG. 1. Comparing the FastWI by using a zero-offset PSPI migration and an explosive reflector RTM.

Fast waveform inversion strategies applied to Hussar

Marcelo Guarido*, Raul Cova, Sergio J. Romahn, Laurence R. Lines, Robert J. Ferguson and Kristopher A. H. Innanen

ABSTRACT

The Fast Waveform Inversion (FastWI) is a linear solution of the Full Waveform Inversion. It is fast, as it is applied on post-stack data, and does not require any forward modeling. The gradient is calibrated by available sonic logs. We tested the inversion to apply an acoustic inversion on the vertical component of the processed Hussar data. The inversion is driven and compared with three sonic logs acquired over the 2D line. The inverted P-wave velocities show consistency in the well location and with the stacked section, with the clear limitations of the acoustic inversion on elastic data.

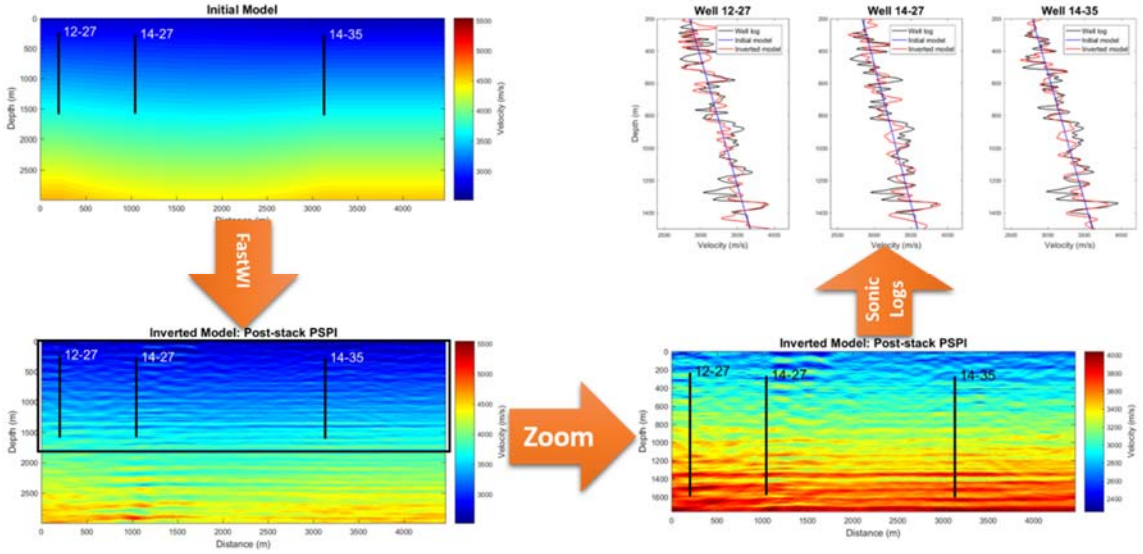

FIG. 1. FastWI applied to Hussar leads to a velocity model that matches the wells and are consistent in between them.

Forward modeling-free full waveform inversion with well calibration

Marcelo Guarido, Laurence Lines and Robert Ferguson

ABSTRACT

Full waveform inversion (FWI) has the goal to find the Earth's model parameters that minimize the difference of acquired and synthetic shots. It is a powerful tool to automatize some complex processes. However, when we talk about seismic data, we are talking about huge datasets, and the FWI shows to be very hard to be applied in large scale, as it requires a large number of synthetic data and migrations at each iteration. In this work, we are proposing an approximation for the FWI that is forward modeling-free, requiring only the migration of the acquired data, which can be pre or post stack, and the optimization driven by a sonic log calibration. We tested the approximation for acoustic inversion in a synthetic 2D Marmousi survey. It is stable and leads to detailed inverted models with reduced computational costs.

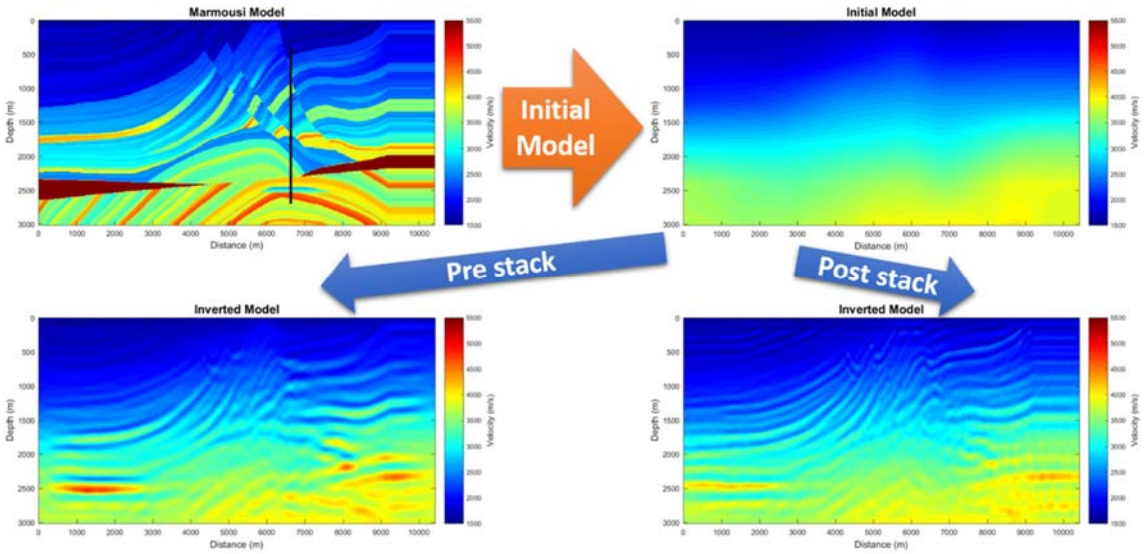

FIG. 1. Forward modeling-free FWI with well calibration can be done using pre and post stack depth migration.

Attenuation of P and S waves in the near surface using uphole data

Saul E. Guevara and Gary F. Margrave

ABSTRACT

Attenuation of seismic waves in the near surface can be significant, and uphole surveyscan contribute to its characterization. Possible methods to find the parameter Q using uphole data are analyzed in this work. The 60 m depth uphole is illustrated in Fig. 1. The sources generate a radiation pattern, illustrated for the 50 m depth example in Fig.2, together with the horizontal component (S-wave). The estimated attenuation for the 5 m depth shot using the dominant freuency method is illustrated in Fig. 3.

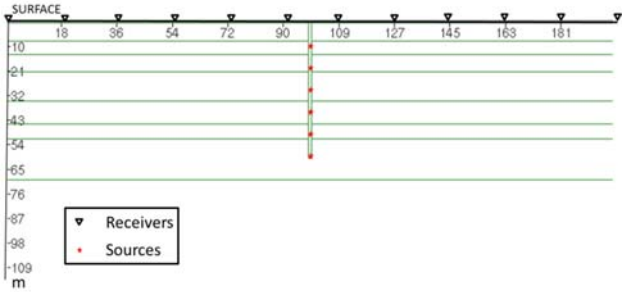

FIG. 1. Uphole design: the sources of energy are inside the borehole and the sensors are on the surface. Energy sources are explosives separated by 5 m from each other, like the distance between receivers. These sources generate P and S-waves in a radiation pattern.

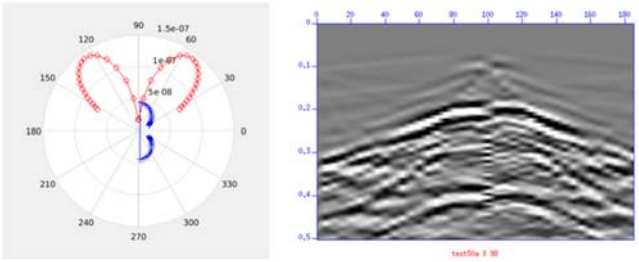

FIG. 2. The radiation pattern for the shot at 50 m depth is shown to the left, and the corresponding synthetic S-wave (horizontal component) obtained with an elastic FD code, is shown to the right. This model does not include attenuation.

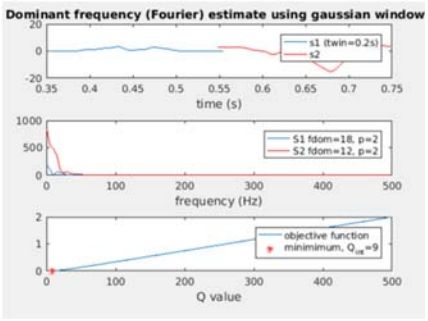

FIG. 3. Example of the application of the Dominant Frequency attenuation method, for the 5 m depth source, and the receivers at 10 m and 90 m offset. A Q value of 9 was estimated.

Since they have the same source, the uncertainty is reduced, however it is affected by factors such as interfering events caused by the near surface, and the free surface affect. This effect was filtered before the attenuation calculation.

Comparing data from different sources has many uncertainties. Even data from the same source is challenging, since besides attenuation the signal is affected by factors such as the radiation pattern, and different wave-paths. Since each shot spans a wide area, attenuation tomography could be an appropriate approach.

On S-waves generated by conventional sources: a numerical experiment

Saul E. Guevara and Gary F. Margrave

ABSTRACT

Field experiments and theoretical studies have shown that S-waves can be generated by conventional sources of energy, such as vibrators or explosives. However they are rarely identified in conventional surface seismic data. A synthetic model experiment illustrates these events as well as the possibility of generating an image using PreSTM applied to SS reflections. The relation with real data is also considered.

Fig. 1 illustrates the geological model and Fig. 2 shows the horizontal component record of a synthetic shot, obtained with a 2-D elastic FD algorithm. Fig. 3 shows the PreSTM section for SS waves, using the Kirchhoff algorithm.

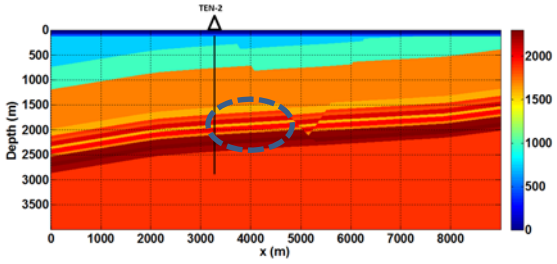

FIG. 1. Geological model used to generate the synthetic data.

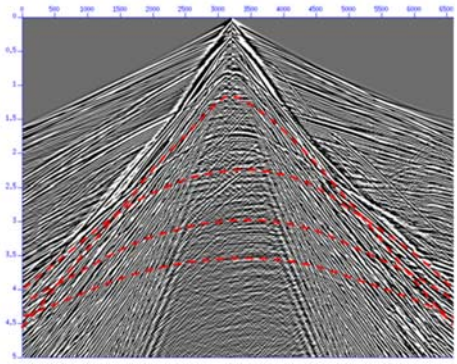

FIG. 2. A shot gather, horizontal component. The dashed red lines correspond to the calculated arrival time of SS waves, according to the geological model.

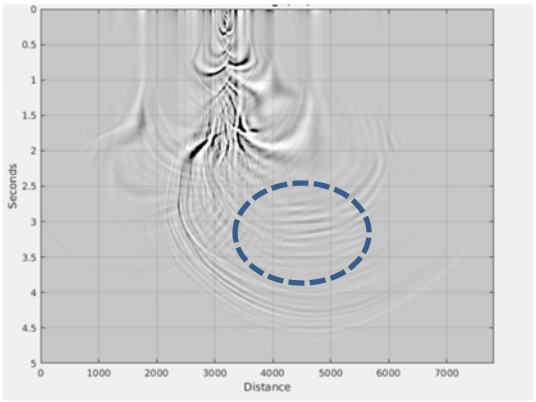

FIG. 3. PreSTM of the shot gather in Fig. 2. The events inside the dashed blue circle correspond to the expected arrival time from SS reflections from the interfaces in the blue dashed circle of Fig.1. Notice the artifacts at earlier times, which can be caused by SS and other reflections (e.g. PS) and by surface waves.

CREWES Matlab® toolbox SEG-Y Input/Output update

Kevin W. Hall and Gary F. Margrave

ABSTRACT

The ability to read and write SEG-Y files into Matlab® using the CREWES toolbox has been evolving for a long time. Along the way, at least six separate attempts to code SEG-Y input/output (I/O) have been written by many people. None of this code was able to effectively deal with trace headers, custom trace headers, or with very large SEG-Y files. In addition, outputs were incompatible so that, for example, trace headers read from disk by one set of CREWES code could not be written to an output SEG-Y file using an unrelated set of CREWES code. This lead to user frustration. A major re-write has been undertaken that combines ideas from legacy code in an object-oriented way that can handle very large datasets, trace headers and custom trace headers. Coding has also begun to support SEG-Y revision 2 which was released in January of 2017. Legacy code in the CREWES toolbox is being removed from the toolbox or being re-written as wrappers that call the new code for backwards compatibility. This report provides an overview of the current state of the new code with examples of how to use it.

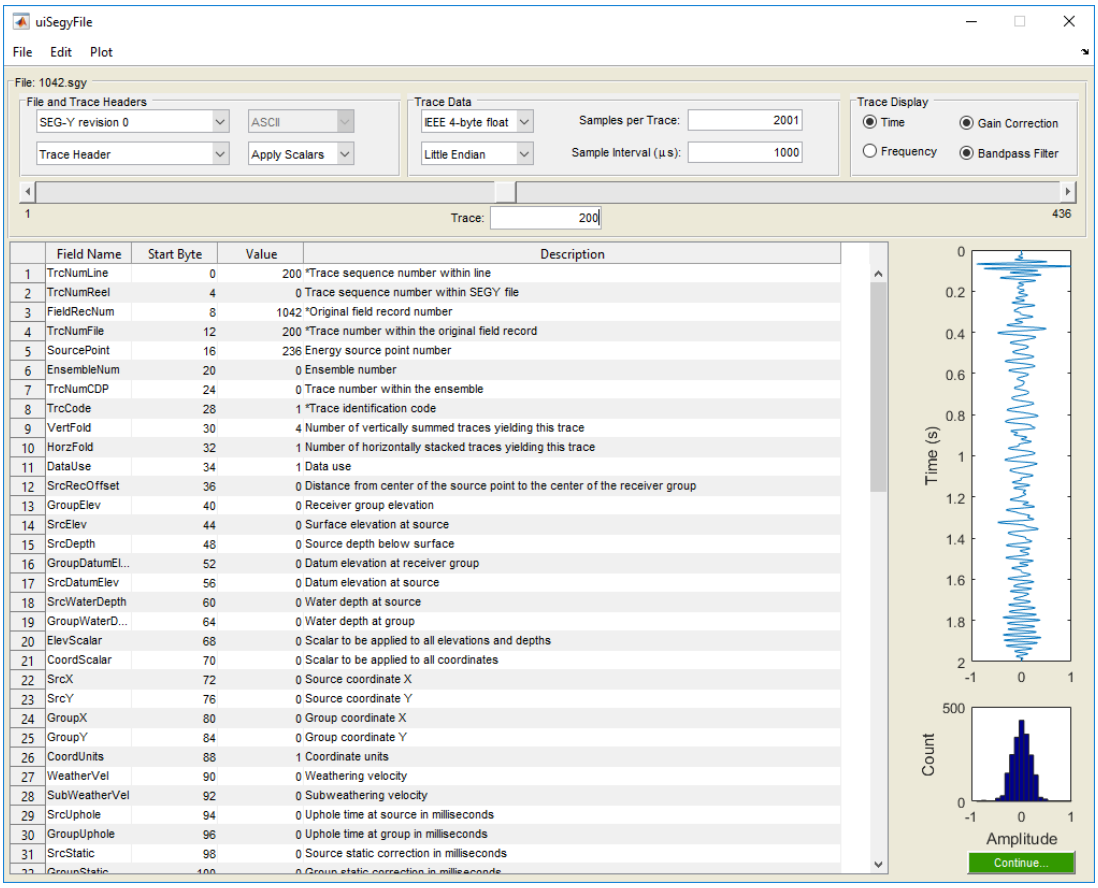

FIG. 1. Trace header and trace data displayed with gain correction and bandpass filter in *uiSegyFile()*.

Everything you never wanted to know about IBM and IEEE floating point numbers

Kevin W. Hall

ABSTRACT

CREWES Matlab® toolbox SEG-Y Input/Output functions have long been able to read four-byte IBM floating-point trace data, but have not unable to write IBM floats to disk. In addition, the code has not been able to differentiate between IBM and IEEE trace data in the case where a SEG-Y file was created using IEEE floats, but the SEG-Y binary file header data sample format code was set to one (IBM floating point). This was left to the user.

New Matlab® functions *num2ibm()* and *ibm2num()* have been written, tested, and are now available in the toolbox for writing IBM floats. The *guessFormatCode()* method has been written, tested and added to the *SegyTrace* class. This method reads a non-zero trace from an input file and attempts to determine if the trace data are IBM or IEEE.

Although 4-byte IBM floats can store larger and smaller numbers than IEEE floats, very large and very small numbers should be stored as 8-byte IEEE floating-point using SEG-Y Revision 2, as seismic processing software may not be able read IBM numbers that are out of the IEEE range.

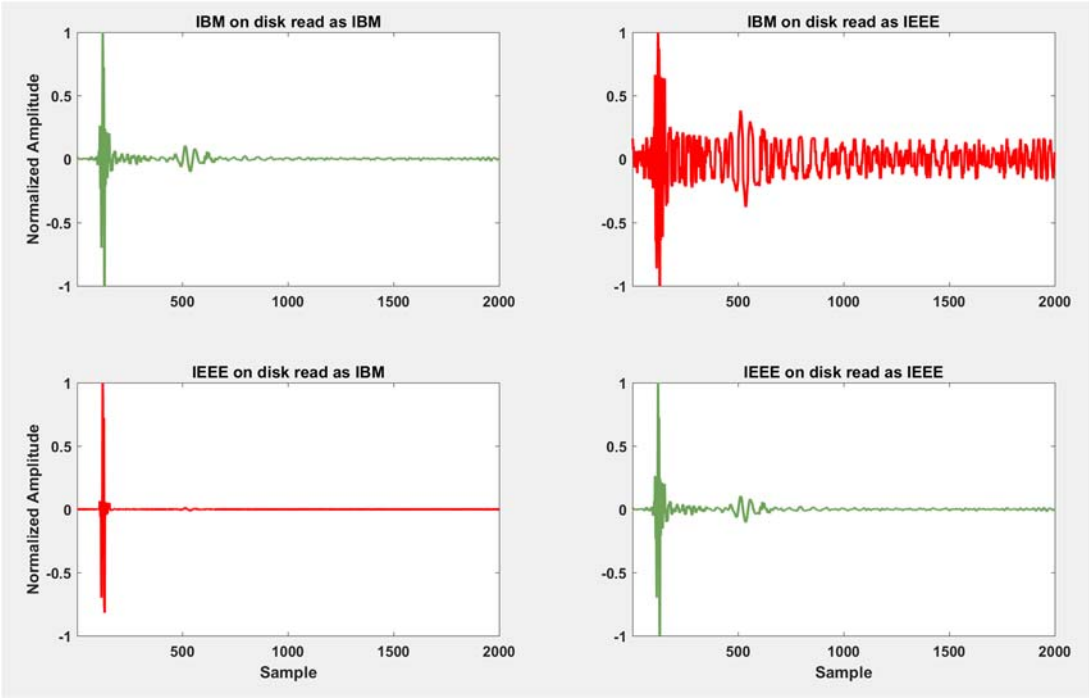

FIG. 1. Correlated Vibroseis data acquired with a 10-250 Hz sweep stored as IBM (top) and IEEE (bottom) floating point, that has been read into memory as IBM (left) and IEEE (right). Trace amplitudes have been normalized for comparison, but no other processing has been applied. Correct answers are shown in green.

Source distance and source effort on DAS data

Kevin W. Hall*, Don C. Lawton, Tom Daley, Barry Freifeld and Paul Cook

ABSTRACT

Vibroseis and weight-drop sources were recorded on looped vertical seismic profile and surface fibre optic lines using distributed acoustic sensing (DAS) at the Containment and Monitoring Institute (CaMI) Field Research Site (FRS) in Newell County, Alberta. This report examines the effects of source distance and source effort on DAS data.

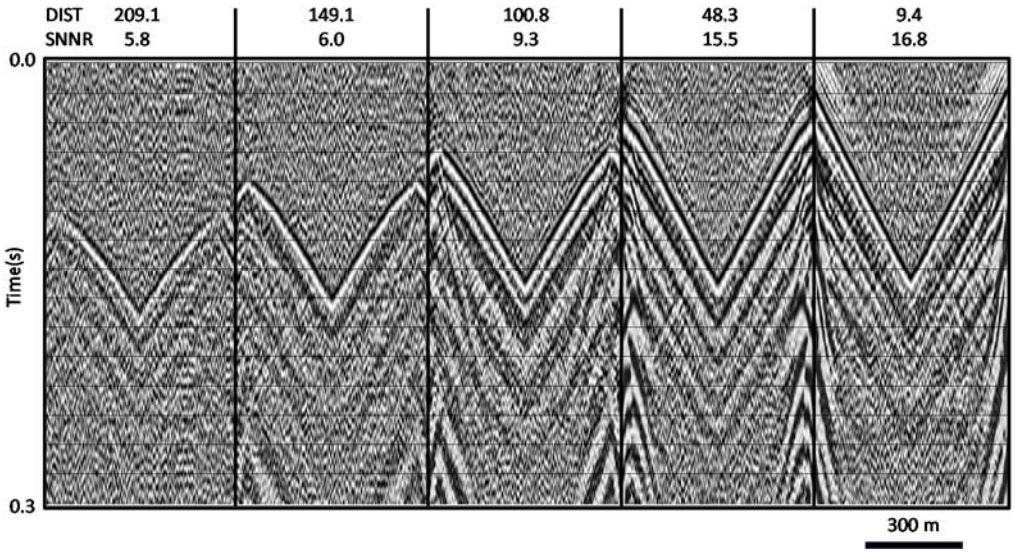

FIG. 1. Source line 21, VP 152 (left), 146, 121, 136, 132 (right) single sweeps recorded on straight fibre in geophysics observation well with a 10 ms AGC for display. Source distance from well decreases from 209 m (left) to 9 m (right).

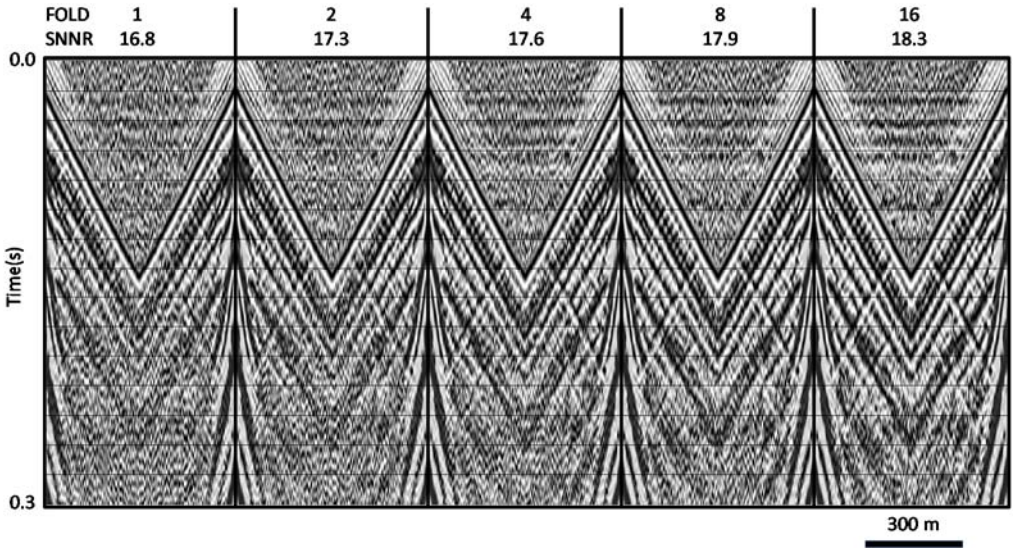

FIG. 2. Source line 21, VP 132 recorded on straight fibre in geophysics observation well with a 10 ms AGC for display. Vertical fold increases from one (left) to 16 (right).

Accuracy of numerical solutions to the elastic wave equation in multiple dimensions

Heather K. Hardeman and Michael P. Lamoureux

ABSTRACT

In this paper, we will solve for the exact solutions for reflection coefficients of the elastic wave equation in 1D, 2D, and 3D. The velocities in which we are most interested have a transition zone, or a portion of the velocity which is non-constant. As such, we will discuss what occurs at the start and end of the transition zone. In particular, we will find that certain continuity conditions are required. We will also discuss the case when the plane wave is orthogonal to the transition zone as well as the non-normal incidence case in 2D and 3D. This work is a extension of a paper by Hardeman and Lamoureux written in 2016. Finally, using the general solution for the reflection coefficients we find in the 1D and 2D cases, we will compare the results of the exact solution to numerical solutions of the elastic wave equation in 1D and 2D.

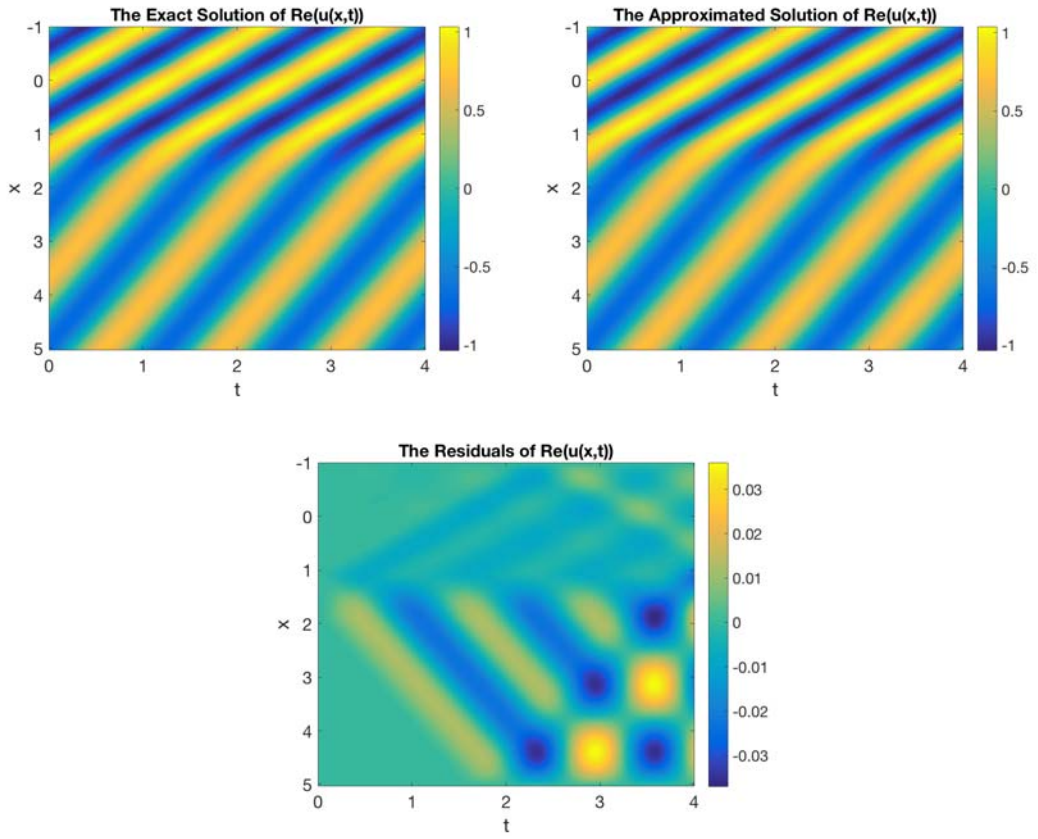

FIG. 1. (Top left) The real part of the exact solution. (Top right) The real part of the approximated solution. (Bottom) The residuals from the real part of the exact solution and the approximated solution.

Scale-invariant image recognition using convolutional neural networks and wavelet analysis

Heather K. Hardeman, Michael P. Lamoureux, Matt McDonald

ABSTRACT

We begin with a discussion of machine learning and its applications to seismic interpretation. We provide a brief overview of convolutional neural networks as well as tree-structured wavelet transforms. We introduce a new wavelet transform called the inverted tree-structured wavelet transform which renders scale-invariance for image recognition. Also, we explain our method for processing data in real-time. Then we introduce a training set extracted from real data. We test the trained convolutional neural network on a portion of the training set to determine accuracy. Afterwards, we employ this trained convolutional neural network to identify events in microseismic data.

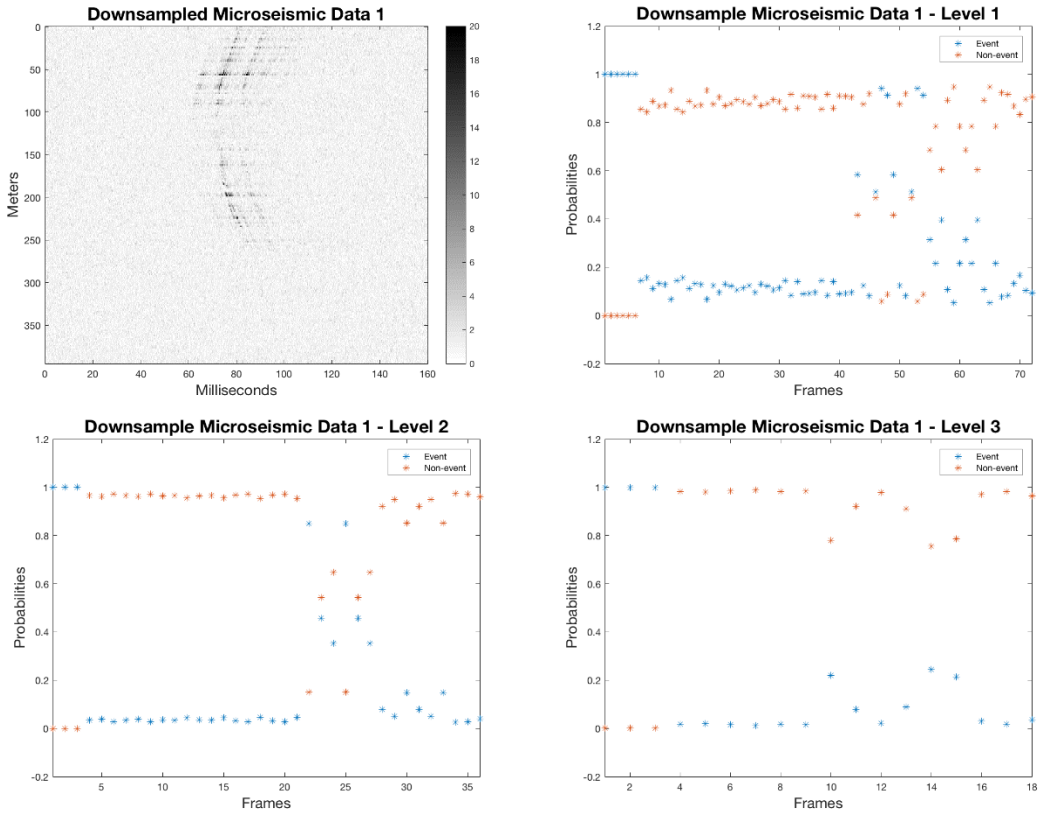

FIG. 1. (Top left) The downsampled microseismic data acquired using distributed acoustic sensing and fibre-optics. (Top right) The probabilities of an event in Level 1 of the inverted wavelet tree. (Bottom left) The probabilities of an event in Level 2 of the inverted wavelet tree. (Bottom right) The probabilities of an event in Level 3 of the inverted wavelet tree.

Vertical seismic profiling using distributed acoustic sensing

Heather K. Hardeman*, Tom Daley, Barry Freifeld, Michael P. Lamoureux, Don Lawton and Matt McDonald

ABSTRACT

We explain the methods behind distributed acoustic sensing (DAS) using fibre optic cables. We consider the application of DAS in the acquisition of vertical seismic profile (VSP) data. After conversion from optical backscatter to a strain measurement in terms of time and space, we apply common processing techniques to the VSP data acquired from the Containment and Monitoring (CaMI) site in Newell County, AB using Fotech Solutions DAS technology.

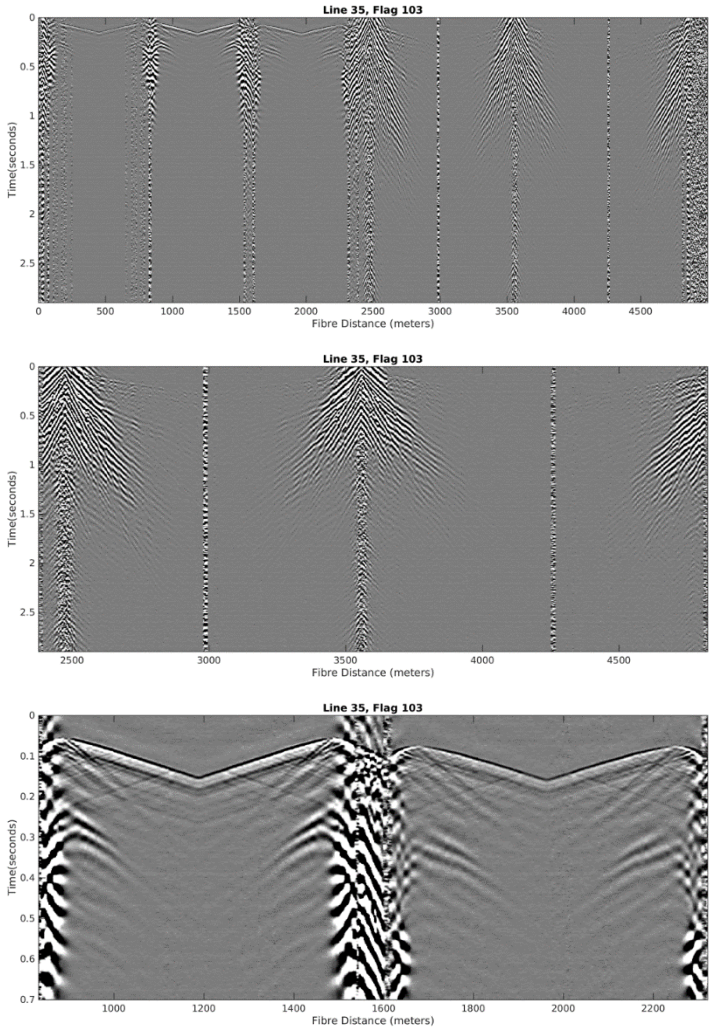

FIG. 1. Vertical seismic profiling data acquired at the CAMI site in Brooks, AB when the vibroseis truck was at source locations 103. (Top) VSP of Well 1, Well 2 and the trench. (Middle) VSP of the trench. (Bottom) VSP of Well 1 and Well 2.

A shift in time: time-lapse detection using interferometry

David C. Henley

ABSTRACT

Most seismic time-lapse studies attempt to detect a reflection amplitude anomaly as the residual of the subtraction of a 'baseline' seismic image from a 'time-lapse' image obtained using the same acquisition parameters and seismic processing stream as the baseline survey. The amplitude anomaly corresponds to a change in the reflectivity of the boundary between the formation of interest, where fluids are being injected or extracted, and either overlying or underlying formations, where no changes occur. Often, this amplitude anomaly is rather subtle. In this case, a secondary effect may prove to be more detectable; the changed seismic transit time through the affected layer may cause a detectable time delay (or advance) of all reflection events from layers beneath the target formation. We demonstrate here a method for detecting very small time shifts, of less than one sample interval, between portions of seismic images recorded and processed with identical parameters. We first demonstrate the feasibility of detecting small shifts using a simple model; then we adapt the near-surface correction technique, raypath interferometry, to detect the differences for both a synthetic model and a field time-lapse experiment performed over the period of 2005 to 2007 at Violet Grove, Alberta.

Figure 1 below shows a time-lapse CMP stack difference image, in which the amplitude anomalies observed are due almost entirely to actual reflection time differences between the stack images, rather than amplitude differences per se.

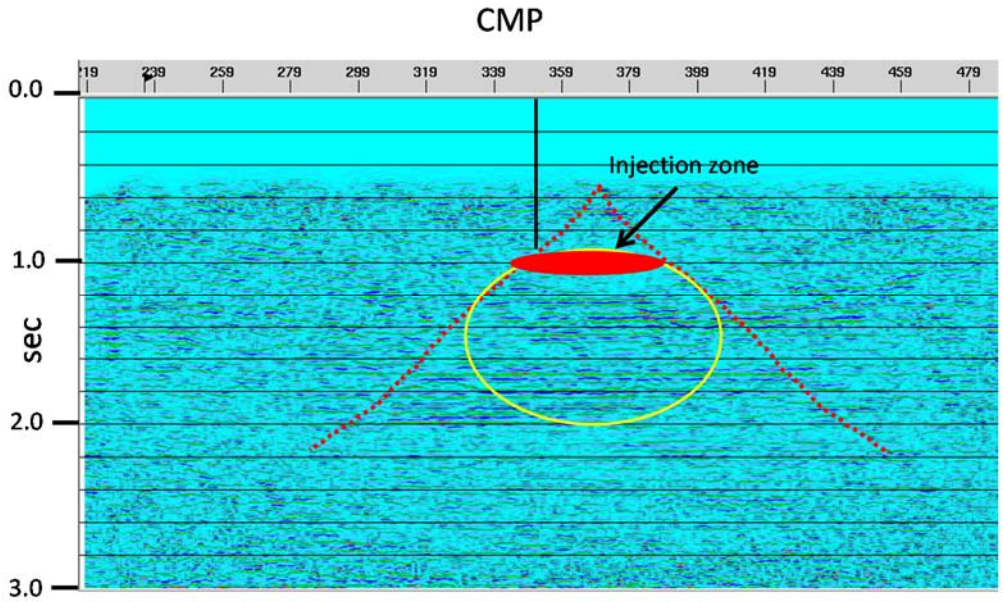

FIG. 1. Time-sag anomaly for the Violet Grove 2005-2007 time-lapse experiment as detected using raypath interferometry. Time shift is ~1.6ms. Red cone illustrates approximate shadow zone for a *plausible* injection zone. Based on this *interpreted* image, it is possible that the actual injection anomaly extended further to the right of the borehole than to the left, since the actual injection zone was never clearly delineated by a seismic amplitude anomaly.

A tale of two transforms: 3D raypath interferometry

David C. Henley*

ABSTRACT

The heart of the near-surface correction technique known as raypath interferometry is the transform (and its inverse) used to move standard field seismic data from the conventional X/T domain to a raypath-oriented domain, and back to the X/T domain. We have extensively tested two different transforms for this purpose; the Radial Trace Transform, a simple point-to-point mapping, and the Tau-P Transform, an integral transform. We show here that, while either transform can be used on 2D seismic data, for the 3D case, geometrical considerations favour the Tau-P Transform, since the current Radial Trace algorithm does not properly handle seismic survey geometry. The Tau-P Transform exhibits a different problem, however, the massive storage required for transforms whose parameters have been chosen to properly preserve the lateral resolution of the input data. In this report, we illustrate these issues using the 1995 Blackfoot 3D 3C data set and show images of the successful application of raypath interferometry to both the PP (vertical) and PS (radial) components of this data set.

Figure 1 illustrates the considerable storage problem posed by the Tau-P transform at required resolution. Figure 2 demonstrates the successful application of 3D raypath interferometry to the Blackfoot PP data set.

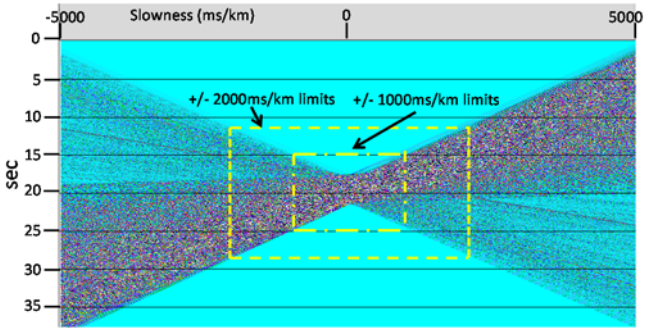

FIG. 1. Tau-P transform for a single common-azimuth gather showing the size of the transform for three different resolution limits. This illustrates the file size problem with the Tau-P domain.

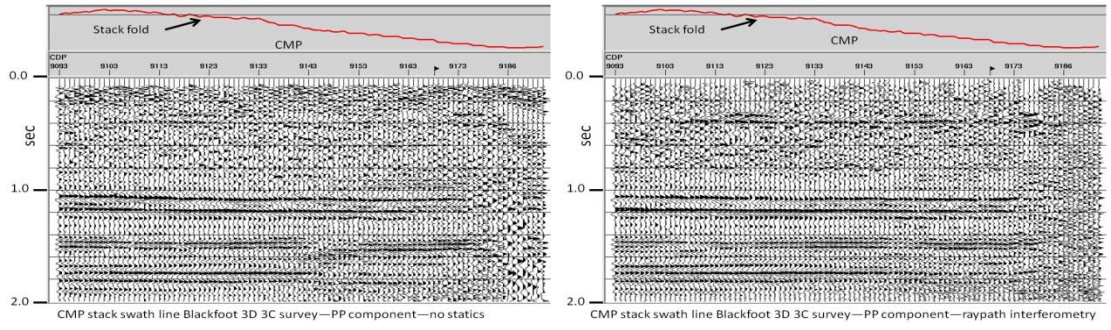

FIG. 2 inline-direction 2D slice of 3D CMP stack cube from Blackfoot 3D 3C survey ***before*** (left) and ***after*** (right) application of 3D raypath interferometry using the 2D Tau-P Transform.

Applications of FWI to the microseismic source problem

Nadine Igonin* and Kristopher H. Innanen

ABSTRACT

Both the microseismic source location problem and velocity model inversion problem can be approached using full waveform inversion (FWI). This is the second of a pair of companion reports that moves towards a modified FWI scheme that iteratively solves for both source distribution uncertainty and velocity model uncertainty in the acoustic environment. A time-domain acoustic FWI implementation in Python is used to create numeric examples of the gradients for both parameters, as well as to take a first look at the cross-talk.

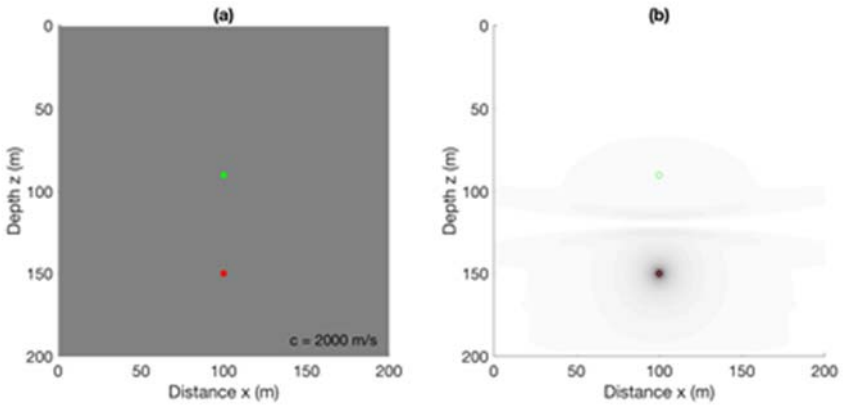

FIG. 3. Model and gradient with a large vertical discrepancy. (a) Homogeneous velocity model, with true position in green and starting position in red; (b) gradient, with darker colours being negative.

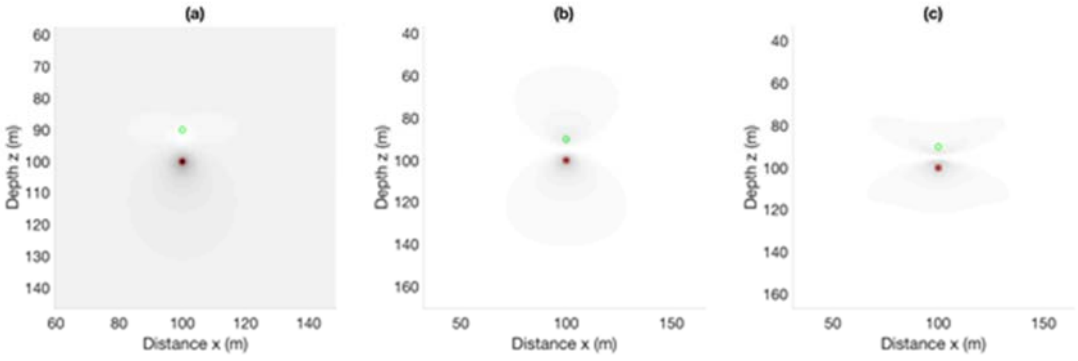

FIG. 4. Gradient as a function of frequency: (a) 5 Hz, (b) 20 Hz, (c) 40 Hz.

Toward full waveform inversion for source location and velocity model: gradient and Hessian

Nadine Igonin and Kristopher H. Innanen

ABSTRACT

Full waveform inversion (FWI) is used to reconstruct physical parameters of the sub-surface. This is the first of a pair of companion reports that moves towards a modified FWI scheme that iteratively solves for both source distribution uncertainty and velocity model uncertainty in the acoustic environment. This report focuses on the derivation of the sensitivities for source and velocity model uncertainty in both time and frequency do-main. Additionally, to begin exploring the cross-talk between these two parameters, the Hessian is derived in the frequency domain. The paper concludes with an analytic example demonstrating the behaviour of this formulation and a discussion on the implications of these results.

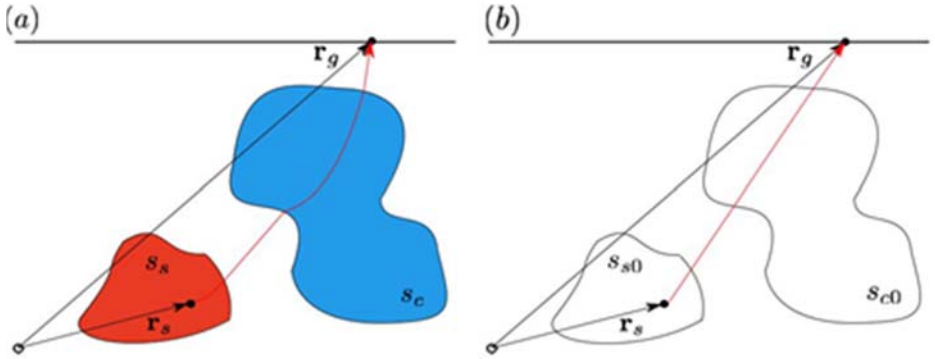

FIG. 1. Schematic illustration of coordinate system and key variables. (a) Red region shows source distribution, while blue region shows the true velocity model distribution. Red line indicates ray path from source to receiver; (b) The same model space where the dashed regions are the background source and velocity distributions.

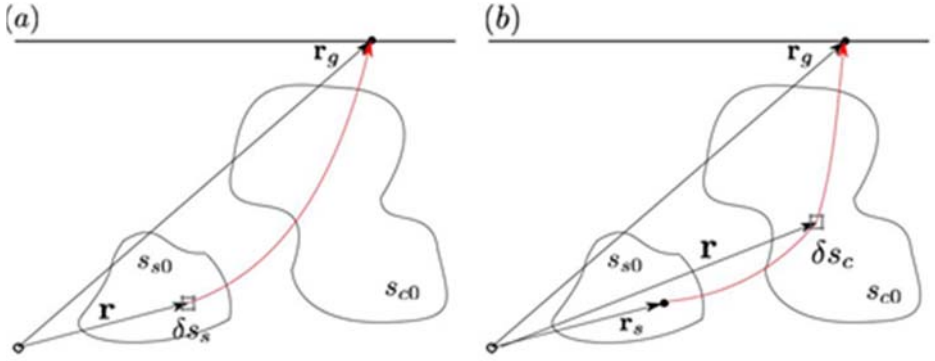

FIG. 2. Schematic illustration of model space with elements ss (a) and sc (b).

Design of DAS fibres for elastic wave mode discrimination

Kris Innanen* and Matthew Eaid

ABSTRACT

In 2016 a "Fibre Geometry and Sensing Model" was introduced in order to facilitate characterization of DAS fibres and their shapes as they respond to various types of elastic wave. The directionality of an arbitrary fibre and its capacity to enable multicomponent DAS sensing were both considered. The model grew considerably in 2017 and now contains the beginnings of a framework to analyze the characteristic response of a given fibre shape to a range of different elastic modes, P- and S-waves at a range of 3D obliquities, and Rayleigh waves for instance. The model can be set up to experience these waves in a simple dynamic form, "lighting up" in regions where the fibre response is above a given threshold. These responses are planned to be the basis for designing fibres which can optimally enhance certain wave modes (e.g., body waves) and suppress others (e.g., surface waves).

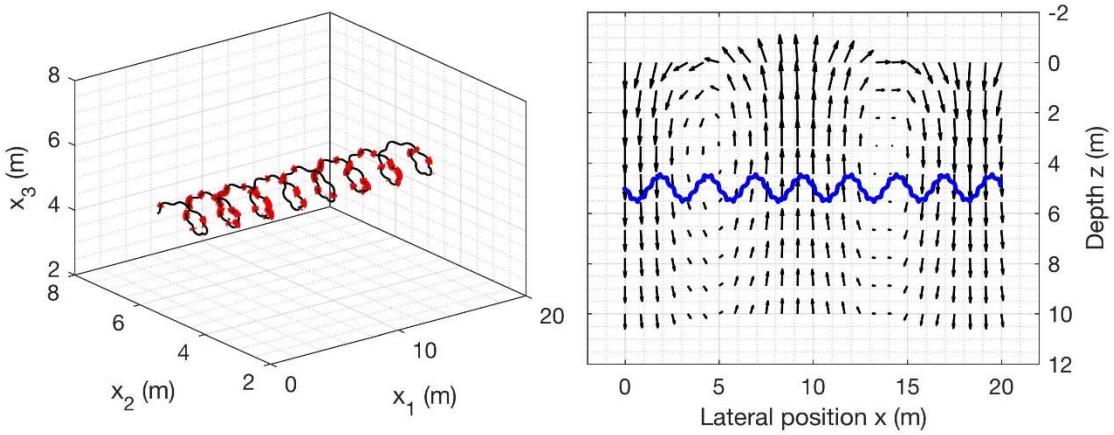

FIG. 1. Response of a 2-helix fibre to a plane harmonic 2D Rayleigh wave, at one instant during its propagation. Left panel: fibre shape is illuminated in red if its instantaneous response to the surface waveform is above a certain threshold. Right panel: the 2-helix fibre observed from along the y-axis.

Seismic reflection and transmission within in an extended scatterer

Kris Innanen

ABSTRACT

A range of methods for making FWI stable in its construction of long wavelength model components in deep regions of the model (relative to maximum offset) have been introduced over the last several years, as discussed and presented by Geng, Almuteri and Innanen in CREWES. Many of these either quantitatively or qualitatively invoke multiple scattering. Using multiple scattering formalisms to model wave fields is not straightforward when the model error or perturbation is large, however. In this paper a Matlab code that quickly models the Nth order truncated Born series approximation of a 1D wave field is written and used to flesh out some of the ways the series goes about creating events like direct arrivals and coda contributions. The main conclusion is a reminder not to say things like "the series did not converge by Nth order", but only things like "the series only converged to a maximum frequency f_N by Nth order".

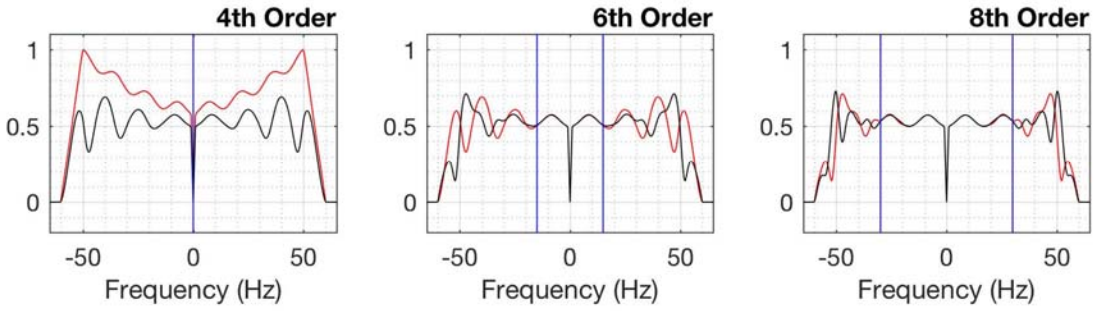

FIG. 1. The pathology of a Born series as it converges. The key is to analyze the process in the Fourier rather than the time domain. Here you see that convergence occurs over an increasing band of frequencies starting at 0Hz. In black is the current iteration of the field approximation, and in red is the previous term. In this example by the 8^{th} term the series has converged out to roughly 30Hz.

Seismic reflections for space-, time- and mixed boundaries

Kris Innanen

ABSTRACT

It has been pointed out that if a homogeneous medium that is supporting a propagating wave were to suddenly undergo a change in medium properties, the propagating wave would immediately partition into reflected and transmitted components—exactly as if it had impinged on a spatial boundary. Bacot et al. in 2016 in fact published laboratory examples of this, referring to the change causing the reflection as a "time mirror". Here we model this phenomenon numerically, speculate on a practical usage of it in monitoring reservoirs undergoing significant pressure changes, and offer a modest extension of the theoretical description. In the extension we point out that the time-mirror reflections are essentially "normal incidence", and then, motivated by the explorationists' tendency to think about obliquely incident waves, we ask the question of how we could force a wave to impinge on a time-boundary at an angle. The answer requires the introduction of boundaries with both space- and time features. Upon setting up such a problem basic rules for reflection angles and transmission angles are straightforwardly derivable by appeal to Huygens' principle.

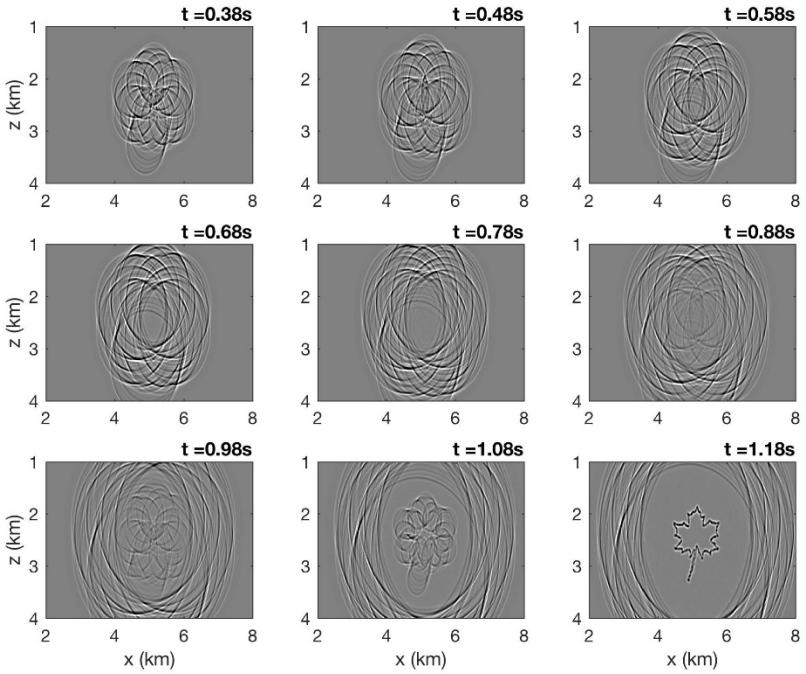

FIG. 1. Bacot images, Canadian style. A maple leaf lands on a pool of water and waves propagate outward. At 0.75s the velocity of the waves change, exciting new forward and backward propagating modes. At 1.18s the backward propagating field re-focuses on the original source distribution.

Towards optimal detection and characterization of microseismic sources with shaped DAS fibre

Kris Innanen, Faranak Mahmoudian and Matthew Eaid

ABSTRACT

A significant possible application of fibre-optic DAS sensing, assuming it becomes robustly sensitive to a range of different strain components, is for the characterization of microseismic sources. In this paper we adjust the growing DAS geometrical model such that it can be brought to bear on the problem of sensing various moment tensors. The model is so designed that appraisal (i.e., for a source at the following position with the following focal mechanism, can the moment tensor be resolved?) is straightforward. It is hoped that this line of inquiry will dovetail with the microseismic FWI work reported this year.

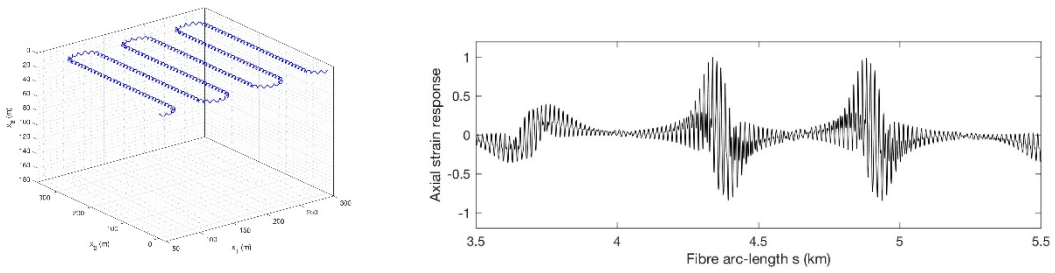

FIG. 1. Surface S-shaped HWC-DAS array (left panel); modeled response to a moment tensor source at depth (right panel). We frame the question of whether the structures we see in the right panel help us determine the moment tensor.

A summary of surface seismic reflection data acquired at the Field Research Station near Brooks, Alberta

J. Helen Isaac and Don C. Lawton

ABSTRACT

We have been acquiring surface seismic reflection data at the Field Research Station near Brooks, Alberta, since 2014. The data include 3D3C, 2D3C and 2D1C surveys. All the seismic data had similar processing, designed to attenuate noise and enhance reflectivity, and were post-stack migrated. The 3D3C data acquired in 2014 exhibits the best imaging of the subsurface on both PP and PS sections. Offset gathers show that offsets of 200-400 m are best for imaging the Basal Belly River, which is the CO_2 injection sandstone, with PP surface seismic data. Preliminary investigations of distributed acoustic sensor data suggest that these data hold promise for real-time monitoring of the subsurface.

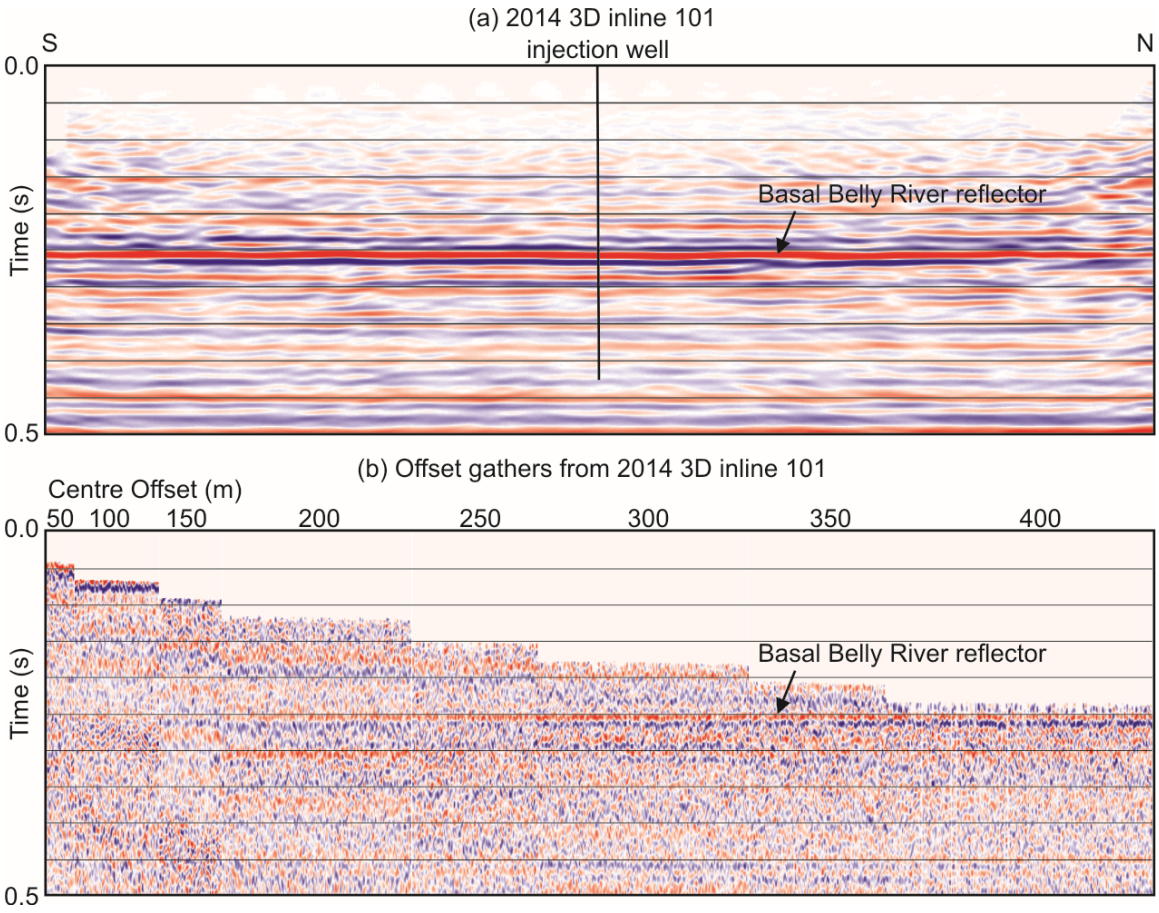

FIG 1. The best-imaged surface seismic data are the 2014 3D3C. (a) This inline runs through the injection well and is in the centre of the survey. (b) The Basal Belly River is imaged best with source-receiver offsets of 200-400 m.

1.5D tau-p internal multiple prediction in Seismic Unix

Andrew Iverson, Kris Innanen and Daniel Trad

ABSTRACT

The inverse scattering series developed by Weglein et al is utilized for the prediction of internal multiples. The algorithm is implemented in 1.5 dimensions in the tau-p domain. While the method has shown promise in its ability to predict multiples there are still challenges to overcome to become a standard in processing. The issue addressed here is the computational expense of the method, which is shown to be decreased using Seismic Unix and parallel processing. The computational time for the chosen model is reduced by a factor of approximately 120 in comparison to the MATLAB implementation. It is also shown how artifacts from the prediction in 1.5D tau-p can be minimized through a time domain tau-p transform and a spatial cosine taper.

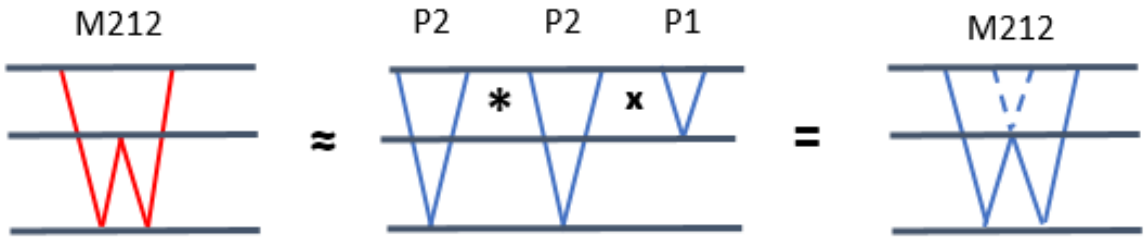

FIG. 1. Schematic displaying how a multiple can be replicated with a combination of primaries through a convolution (*) and correlation (x)

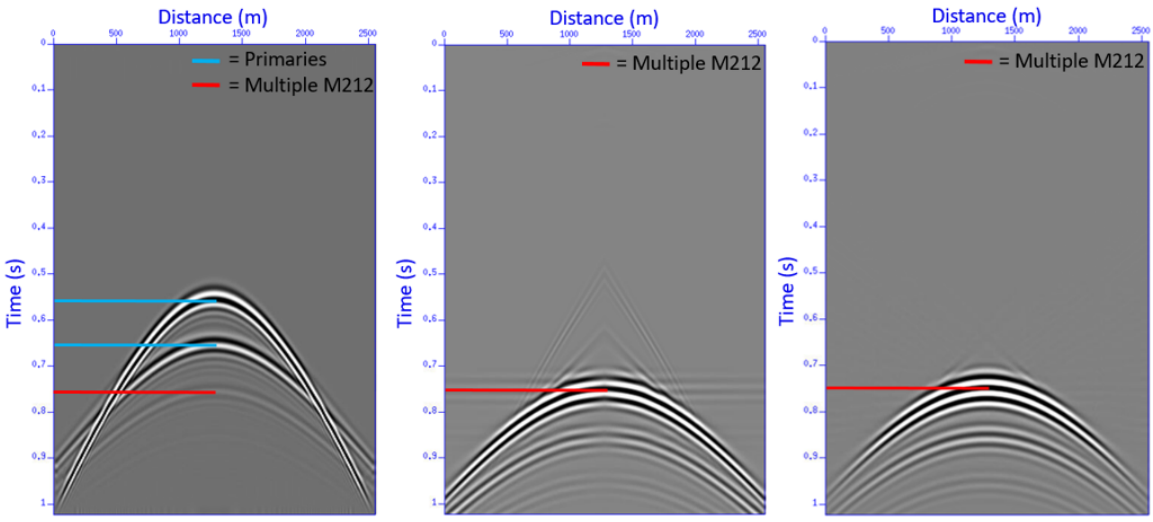

FIG. 2. (Left) Synthetic seismic shot record (Middle) 1.5D tau-p internal multiple prediction in Seismic Unix (Right) Prediction using an aggressive cosine taper and time domain tau-p transform.

Internal multiple prediction in the time and offset domains

Andrew Iverson*, Kris Innanen and Daniel Trad

ABSTRACT

Varying strategies have been implemented to predict and attenuate internal multiples (Xio et al., 2003). One data driven method to predict internal multiples uses the inverse scattering series (Weglein et al., 1997). The method predicts internal multiples where the only required inputs for the algorithm are the data itself and a search limiting parameter epsilon. It has been displayed that reformulating the calculation domain such that the input and output domains are equivalent allows for the use of a nonstationary epsilon (Innanen, 2015). The version of the algorithm in offset-time is outlined where epsilon can vary in both spatial and temporal dimensions. With the domain of calculation in offset-time this allows for the testing and determining of an epsilon schedule based on the input seismic dataset. For some geologic models in this domain a single epsilon value is insufficient for the prediction of multiples while also minimizing artifacts. Displayed is a nonstationary epsilon implementation that assists in artifact minimization.

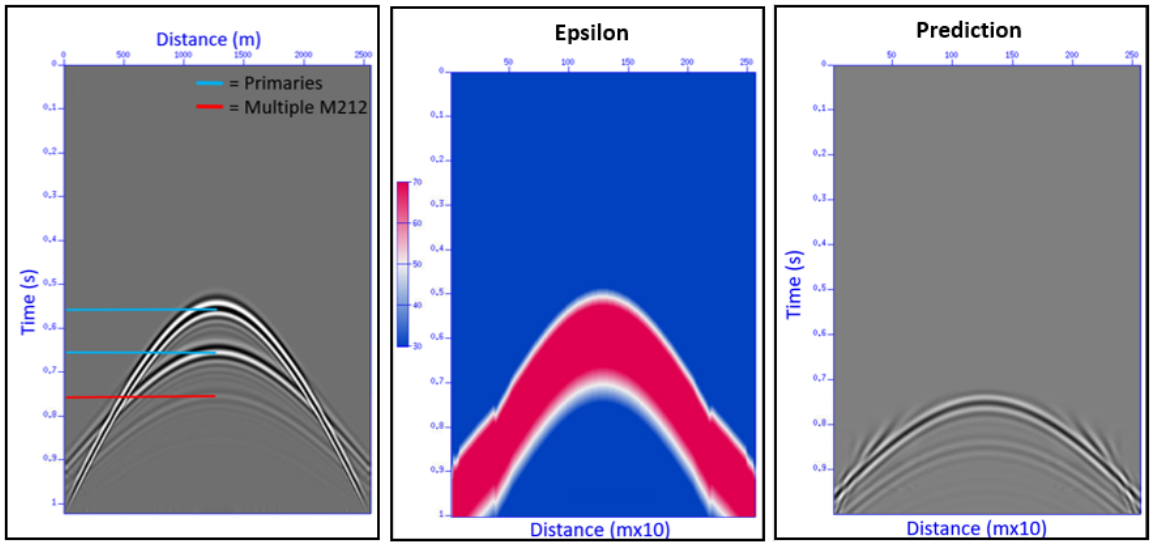

FIG. 1. (Left) Shot record with two primaries and first order internal multiple defined (Middle) epsilon schedule used for prediction varying in both offset and time (Right) offset-time internal multiple prediction with nonstationary epsilon.

Inverse scattering series internal multiple prediction with depth dependent scalars

Andrew Iverson and Kris Innanen

ABSTRACT

Interbed multiples continue to be detrimental to the processing and interpretation of seismic data. One prospective method to attenuate interbed multiples uses the inverse scattering series developed by Weglein et al in the 1990's. The method predicts internal multiples from the recorded data with no additional subsurface information requirements. The issue addressed in this report involves the amplitudes of the predicted internal multiples. This report displays how a depth dependent scalar can be added to the algorithm to account for errors in the prediction amplitude and improve accuracy for specific cases. The location of the scalar application in the inverse scattering series is outlined.

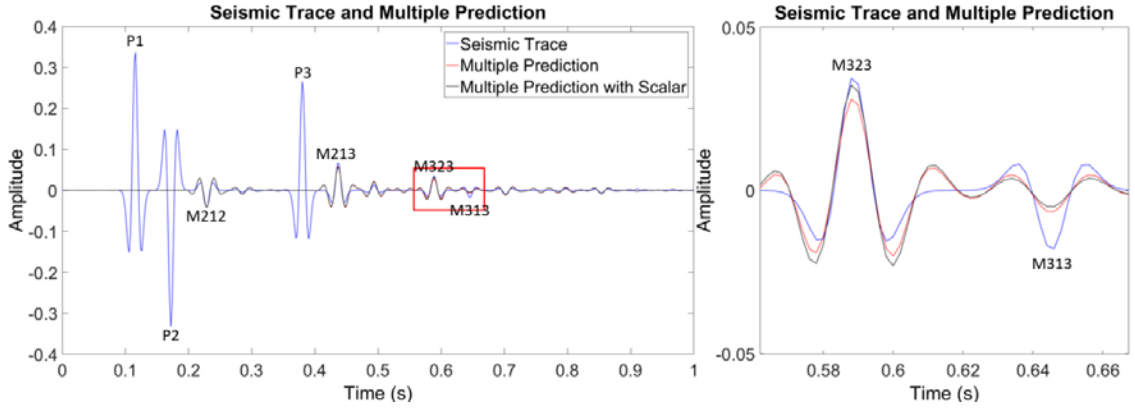

FIG. 1. (Left) Trace with scaled and unscaled predictions (Right) Two multiples M323 and M313.

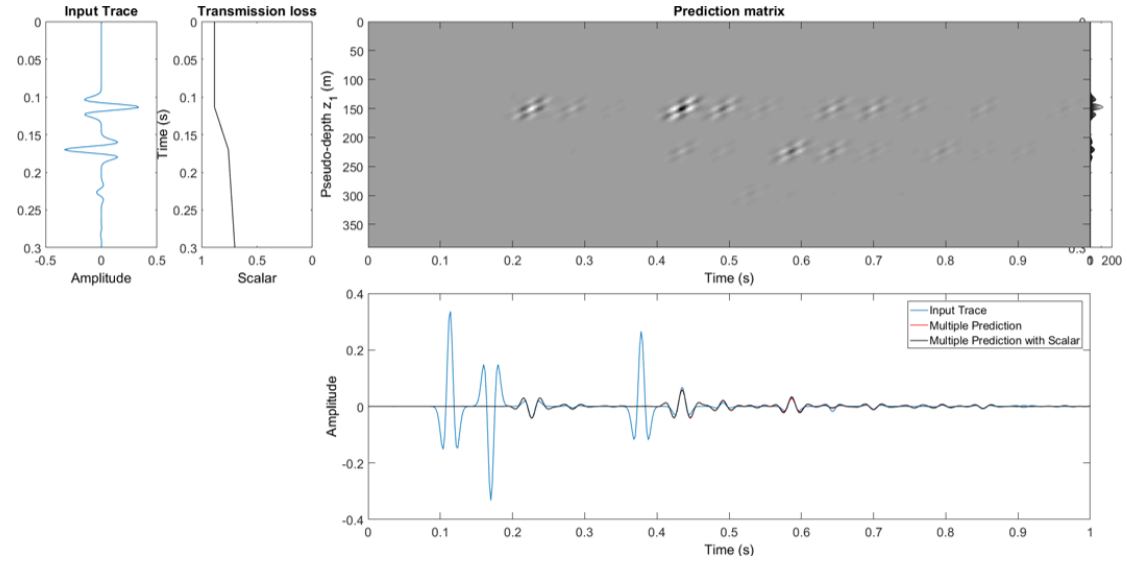

FIG. 2. (Top Left) Trace and transmission loss (Top Right) pseudo-depth and time plot with scalar applied (Bottom Right) Trace and internal multiple prediction.

FWI with DFP optimization using an approximate low-resolution Hessian

Scott Keating and Kris Innanen

ABSTRACT

Quasi-Newton optimization methods have been shown to provide considerable improvements in the convergence rate of full waveform inversion (FWI). These methods use approximate Hessian matrices to generate an update direction. The DFP method uses an approximate Hessian which predicts observed changes in the gradient, while remaining nearest in a least-squares sense to the previous approximate Hessian. By using a low-resolution approximation to the Hessian to initialize the method, we attempt to increase the rate of convergence. This work is ongoing, currently there are significant challenges in using the inverse of the Hessian on the low-resolution scale to provide a meaningful inverse on the high-resolution scale.

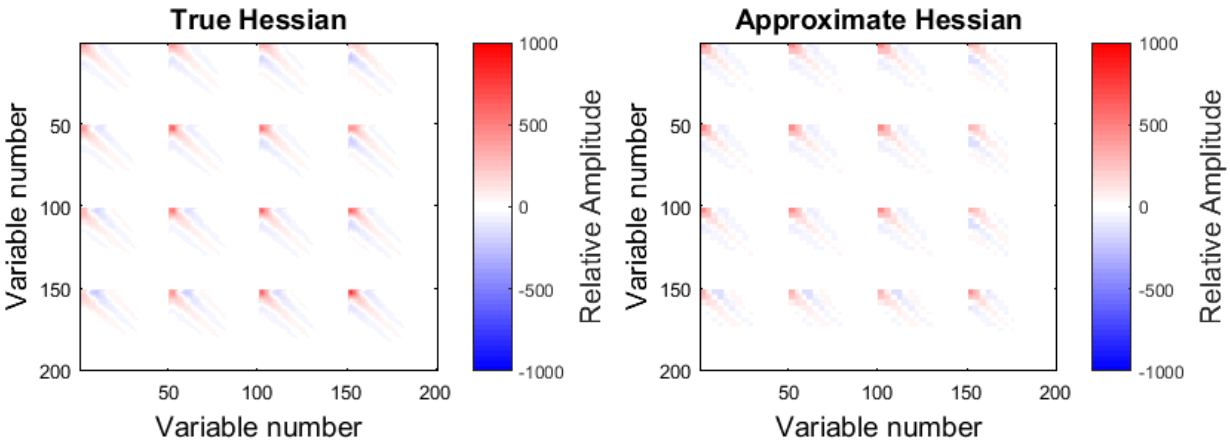

FIG. 1. LEFT: Section of the exact Gauss-Newton Hessian matrix for an example FWI problem, defined on a 10m grid. RIGHT: Section of an approximate Gauss-Newton Hessian matrix, calculated at considerably lower cost, on a 33.3m grid. The approximate Hessian is very close to the true Hessian in a least-squares sense, making it an appealing starting approximation for the DFP approach.

Multi-resolution Newton optimization in full waveform inversion

Scott Keating* and Kris Innanen

ABSTRACT

Full waveform inversion typically defines many more variables in the inversion than can be expected to be independently recovered. This prevents usage of more powerful optimization techniques where large numbers of variables become very expensive. Here, FWI is performed with a model resolution defined based on the data frequencies considered at each iteration. This allows for Newton optimization to be employed in the recovery of the low frequency part of the model, considerably reducing cross-talk on long wavelength scales.

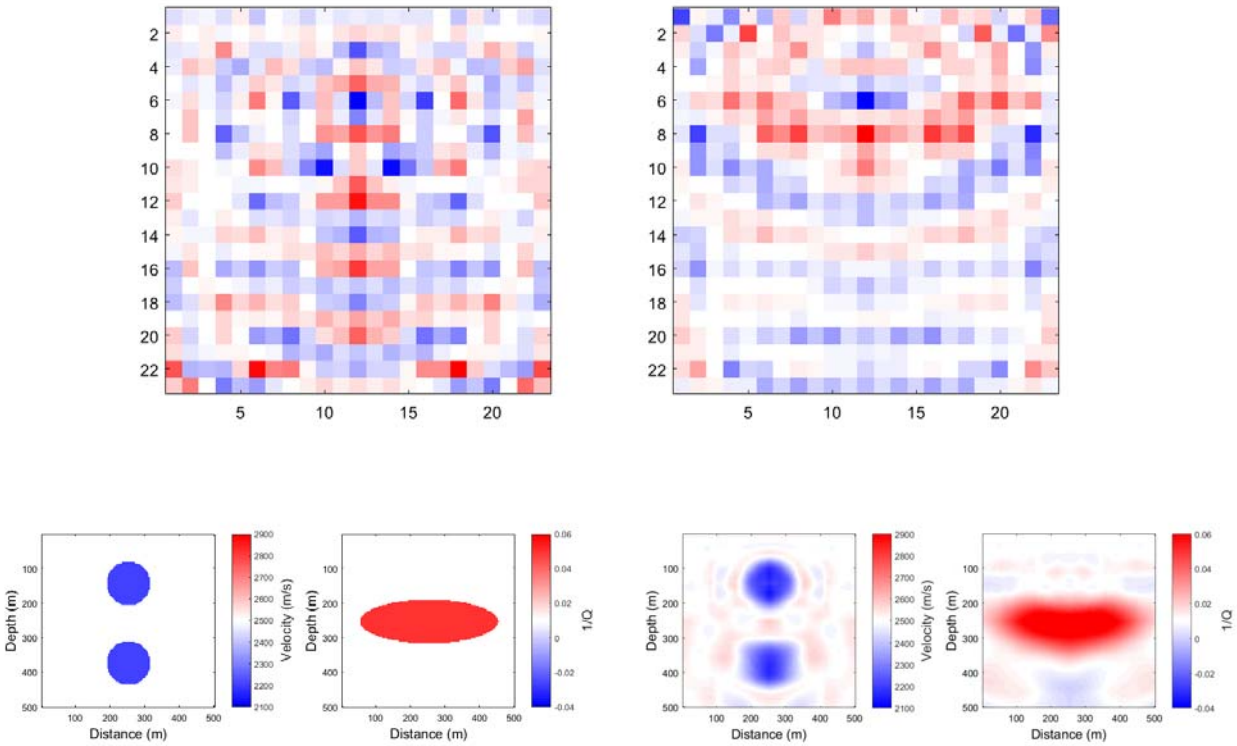

FIG. 1. TOP: Unscaled calculated update for square slowness (left) and reciprocal Q (right) before smoothing for the 1-14Hz data band. BOTTOM LEFT: True velocity (left) and reciprocal Q (right) BOTTOM RIGHT: Recovered velocity (left) and reciprocal Q (right) after considering data up to 14 Hz. Note that the update is calculated on a considerably coarser grid, but the recovered model is accurate on large wavelength scales.

Using the parallel MUMPS solver for frequency domain full waveform

Scott Keating and Kris Innanen

ABSTRACT

Frequency domain finite difference (FDFD) wave propagation is often used in full waveform inversion (FWI) research. The major cost in FDFD is the factorization of a large, sparse matrix. This means that solving the problem for an additional source term is inexpensive, but also raises challenging problems for parallelization. Parallelization over source terms offers negligible benefits as no refactorization of the matrix is required. Parallelization over different frequencies is possible, but limited by the number of frequencies considered, which may be small. This work focusses on using the MUMPS solver, which allows for massive parallelization of the factorization itself.

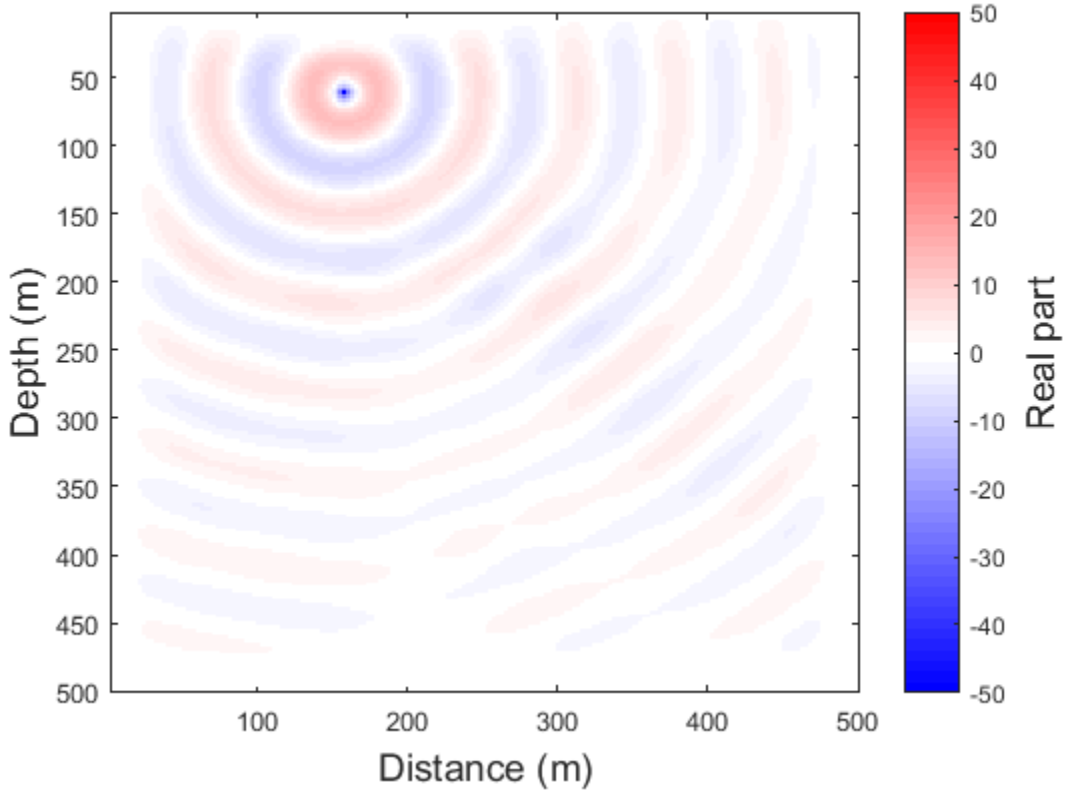

FIG. 1. Example wavefield for a single frequency component, and a single shot. Parallelization over shots is not efficient in a frequency domain approach, and parallelization over frequencies may be limited, so more effective parallelization approaches are needed.

A (full) waveform inversion based on P- and S- wave separation

Hassan Khaniani*, Shahpoor Moradi and Daniel Trad

ABSTRACT

The use of fully elastic wave equation in seismic Reverse Time Migration (RTM) and Full Waveform Inversion (FWI) has the artifact of collocation of P- and S- wave. We show that collocation of the P- and S- waves produces crosstalk errors which produce uncertainty in migration and FWI result. We develop a waveform migration and inversion algorithm using separation of P- and S- wave and the gradient function of FWI. A multicomponent RTM is developed that is based on the propagation of pure P- and S- waves. With the multicomponent forward propagation of sources and the backward propagation of receivers, we apply the formulation of FWI for multiparameter extraction with less uncertainty as compared to the use of the fully elastic propagation.

We demonstrate the performance of P-to-P and P-to-S wave separation using the flat-layered model in Figure (1a) with the perturbation in V_P and V_S . The density is set to be constant and equal to 2000 kg⁄m3. We generate 112 elastic shots with shot spacing of 8 m on the surface. Here, 251 receivers are evenly distributed at 4 m intervals on the surface. Figure (1b and 1c) compare the P-to-P and P-to-S migration and inversion results. As seen, the perturbations in V_P and V_S are consistent with the amplitude recovered in the inversion result of P-to-P and P-to-S data respectively.

The combination of the acquisition fold on the reflectors as a result of number of shots, offset range of source and receiver spread, their position and complexity of the structures with the AVO effects play the main role in quality of true amplitude P- and S-waves imaging/inversion results. In this study, we illustrate the advantage of P- and S- wave separation in Marmousi elastic model where, the image of reflected P- and S- waves experience different illumination in complex medium.

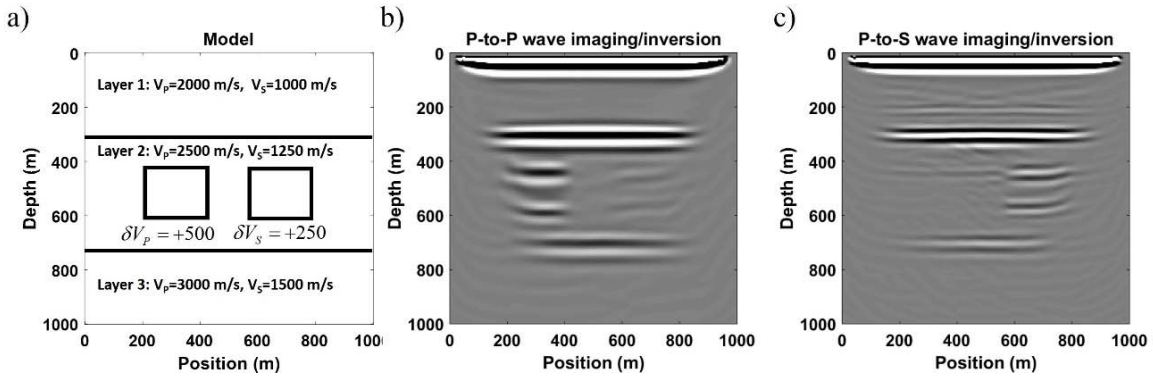

FIG. 1. The waveform separation using migration and inversion. a) Three layers model with perturbation in P- and S- wave velocities, V_P and V_S . b) Migration and inversion for bulk modulus κ from P-to-P wave. c) Migration and inversion for shear modulus μ from P-to-S wave.

Inclusion of spatial sampling and migration artefacts in AVO/Az analysis using Kirchhoff approximation

Hassan Khaniani and Daniel Trad

ABSTRACT

We quantify the uncertainty of linearized Amplitude Variation with Offset/Azimuth (AVO/Az) analysis of seismic P-P wave in a Horizontal Transverse Isotropic (HTI) model. We use Kirchhoff scattering and imaging operators to modify analytical values of AVO/Az based on the numerical artefacts produced by poor sampling and deficiencies of the operators to reproduce true amplitude migration. To compensate for errors due to numerical artefacts of sampling and migration, we present a multiparameter inversion for azimuthal parameters based on the reconstruction of total waveforms by representation on numerical dictionaries obtained by optimization. The computational operator for modeling the dictionaries is based on a 3D Kirchhoff scattering formulation, while the migration operator is based on Prestack Time Migration (PSTM). All operators consider the footprints of acquisition and migration operator in the estimation of AVO/Az characteristics of dictionaries. The amplitude and traveltime kernels during modeling are based on the linearized reflection coefficients of the HTI medium and the Double Square Root (DSR) equation of PSTM respectively. We show that the inclusion of the artifacts of acquisition and processing in the numerical estimation of AVO/Az values improves the accuracy of conventional analytical curve fitting. The Kirchhoff operator is a target oriented algorithm, which reduces the computation time of modeling and migration at specific target layers.

In Figure 1, we perform the AVO/Az analysis on a field data set. A Common Image Gather (CIG) obtained from the acquisition fold of 221 shot is provided by an oil operating company. In Figure 1a, we show a time slice of a formation at the depth of 3200 m, then used interpolation to map trace amplitudes into x-y coordinates. In Figure 1b, we tried the Basis Dictionary Fitting (BDF) algorithm with initial anisotropic values of $\varepsilon = -.05$, $\delta = -0.01$ and $\gamma = 0.1$ for the upper layer. In this experiment, the AVO/Az pattern obtained from developed BDF algorithm is consistent with radiation patterns of the field data CIG gather.

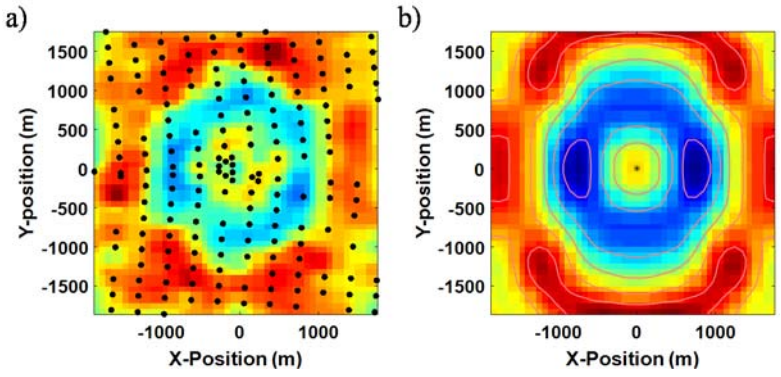

FIG. 1. AVO/Az least squares fitting of true data shown in (a) is compared to resultant dictionaries obtained from numerical evaluation as shown in (b). The dots in (a) represents the position of the sources.

Particle swarms for numerical wave equation

Michael P. Lamoureux* and Heather K. Hardeman

ABSTRACT

Motivated by the possibility of computation speed-ups using massive parallelization on fast graphical processing units, we investigate the use of particle swarms to produce a numerical simulation of seismic wave motion in heterogeneous media in 2D and 3D.

It is well known that Brownian motion of particles bouncing about at random forms a useful model for diffusion of heat. In the limit as particle numbers going to infinity, the Brownian motion leads to the diffusion equation: a second order, linear, parabolic partial differential equation. A similar model with correlated, but still random, particle motion leads to the acoustic wave equation in dimensions one, two and three.

Focusing on the Green's function for individual source and receiver pairs in a seismic experiment, we aim to compute the numerical simulation of wave motion using large numbers of independently acting particles to recover the source/receiver response without modelling the entire seismic waveform in the experiment. We present the mathematics behind the theory of the particle simulation as well as a few numerical studies.

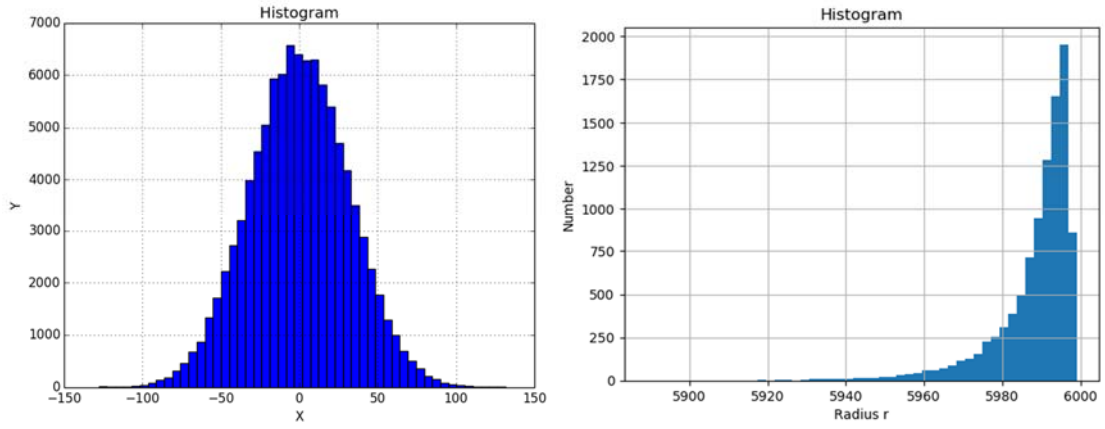

FIG. 1. (Left) Green's function for 1D diffusion equation, via a particle simulation. (Right) Green's function for a 2D wave equation, via a particle simulation.

Comparison of refraction inversion methods

Bernard Law* and Daniel Trad

ABSTRACT

Near surface weathering statics correction are traditionally done using first arrival times. Generalized Linear Inversion (GLI) and refraction tomography are two commonly used methods. Both methods can include model weight and data weight in the cost function to incorporate reflection residual statics measurements. The modified GLI and refraction tomography cost functions can improve the stability of the solution. Full waveform inversion (FWI) updates the velocity model by minimizing the misfit between the recorded field data and the modeled wavefield. FWI can provide higher resolution model than ray theory based methods. We compare Both GLI and refraction tomography methods using synthetic model and field data. We also review the full wave form inversion method and use synthetic model to demonstrate its potential and limitations for refraction inversion.

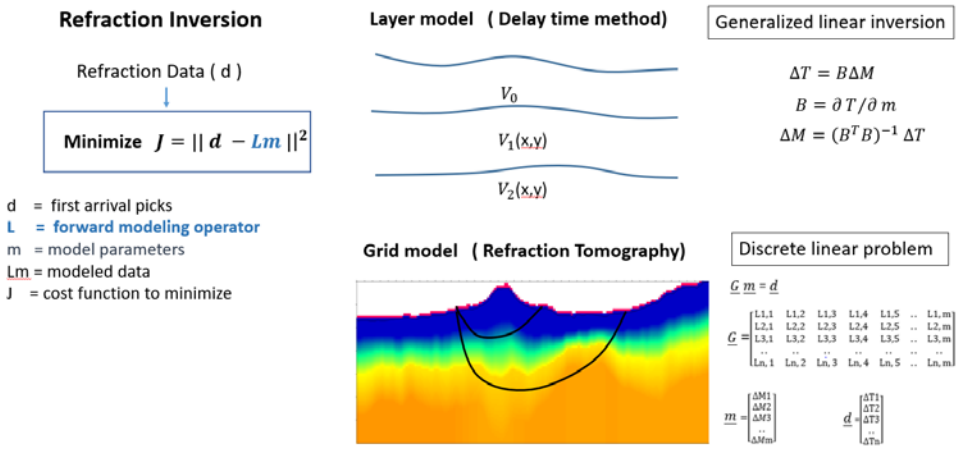

FIG. 1. GLI and refraction tomography methods.

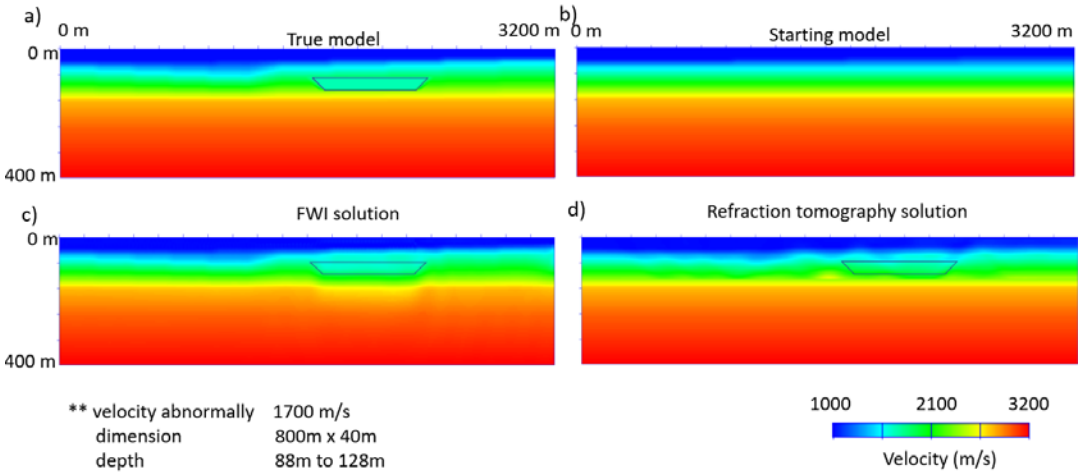

FIG. 2. a) True model for FWI refraction test. b) Starting model with linear velocity gradients. c) FWI solution. d) Travel time refraction tomography solution.

Comparison of traveltime computation and ray tracing methods

Bernard Law and Daniel Trad

ABSTRACT

Travel times and ray paths of the propagation of seismic body wave in heterogenous media are used in seismic tomography, imaging and inversion processes. In this study, we review the seismic ray theory, basic principles of the fast marching, wavefront construction and paraxial method. We analyze their differences and similarities to investigate the effectiveness of these methods in refraction tomography and seismic imaging. We compare the travel times from these method to a finite difference synthetic shot record of the Marmousi model and find travel time from all three methods are accurate except at area where rays diverge. We also used the travel time from the fast marching method in the refraction tomography processing of the Hussar 2D dataset. The CDP stack from the refraction tomography processing is more coherent and better resolved than the CDP stack with datum static correction only.

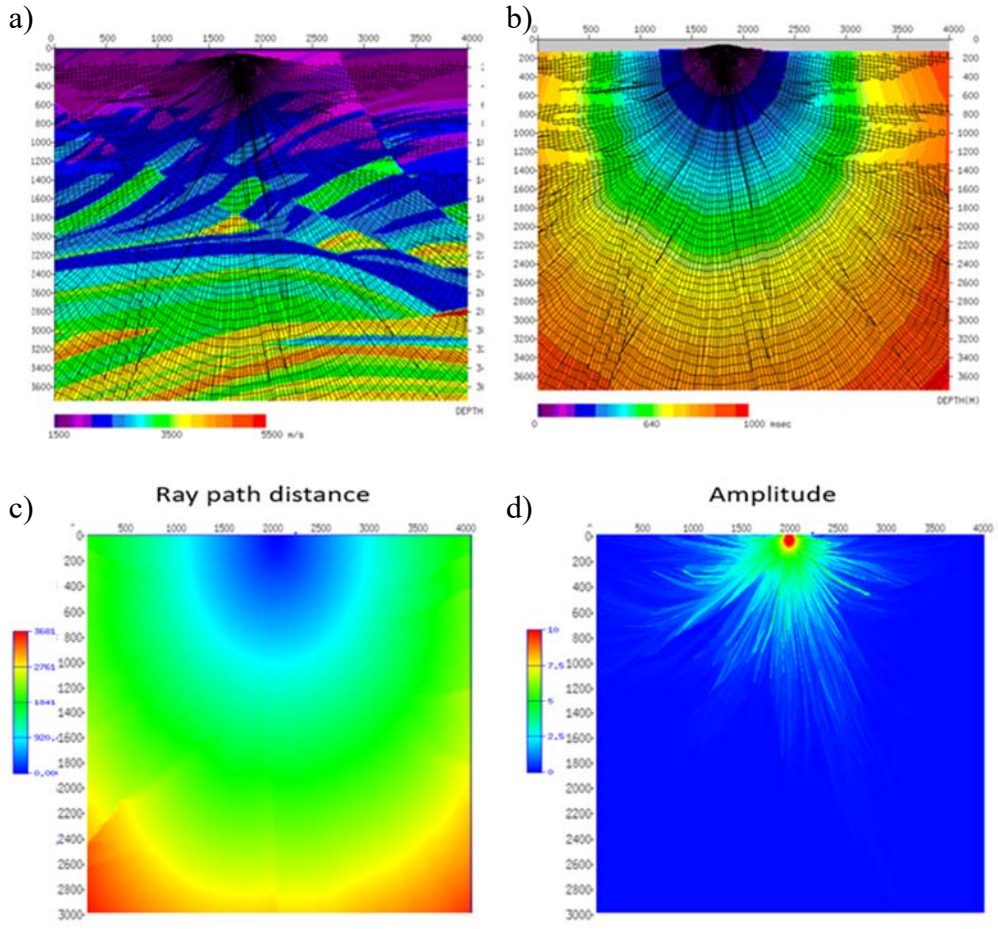

FIG. 1. a) Wavefronts from Wavefront construction method. b) Travel time c) Ray path distance. d) Amplitude.

DAS and seismic installations at the CaMI Field Research Station, Newell County, Alberta

Don Lawton*, Malcolm Bertram, Amin Saeedfar and Marie Macquet

ABSTRACT

Distributed Acoustic Sensing (DAS) optical fiber was installed at the Containment and Monitoring Institute Field Research Station (FRS) in Newell County, Alberta. Straight and helical optical fibers have been installed in two 350 m deep wells and in a 1.1 km long trench, to assess DAS recording for VSP and surface seismic surveys. The installation schematic is shown in Figure 1a. One of the wells had both straight and helical fibres cemented on the outside of fiberglass casing. Zero-offset vertical seismic profile (VSP) data and walkaway VSP data have been collected along multiple azimuths from this well, using an envirovibe source over a 10-160 Hz sweep over 16 s. Two different interrogators were used to record the data over separate surveys, with both yielding excellent data quality. A comparison of DAS to geophone data was enabled through having 24 3C geophones also cemented on the outside of the casing. Some envirovibe shots have been recorded into the trench fiber with an output trace spacing of 0.25 m. The shot records are dominated by unaliased surface waves.

In addition to the DAS fiber, 100 3C geophones were buried on a 10 m x 10 m grid centered in a CO_2 injection well at the FRS (Figure 1b). These geophones were cemented into PVC tubing and drilled to a depth of 1 m below surface. This array will be used for not only microseismic recording by CaMI at the site, but also for some limited imaging around the injection well. Some results from recent data collection will be shown in this and other presentations at this year's meeting.

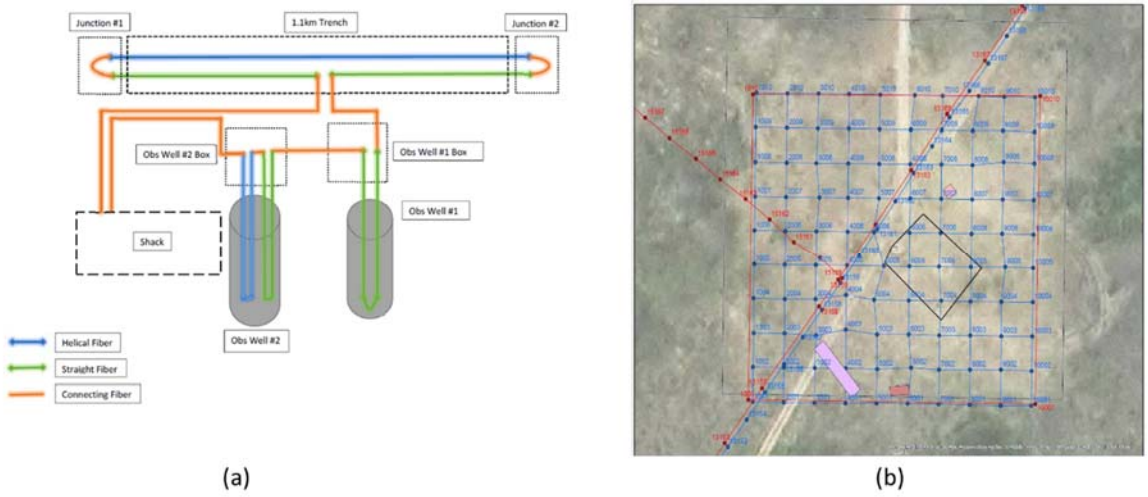

FIG. 1. (a) DAS layout at the CaMI Field Research Station in Newell County, Alberta; (b) layout of buried geophone array.

Frequency domain FWI in VTI medium

Junxiao Li*, Kris Innanen, Wenyong Pan and Geng Yu

ABSTRACT

In this study, a frequency-domain elastic full waveform inversion algorithm for 2-D VTI media has been developed. The forward problem used in this inversion algorithm is simulated by applying frequency domain finite difference method, which is a fast approach for multi-source and multi-receiver acquisition. For the anisotropic inversion of VTI media, five elastic constants (C_{11}, C_{13}, C_{33}, C_{44} and density) have to be dealt with. In this paper, the gradients of four elastic constants are calculated in matrix forms. To accelerate the convergence rate of inversion, the pseudo-Hessian is also implemented in the objective function. The inversion results in the paper show that parameters C_{11}, C_{13} and C_{33} can be inverted properly, yet the inversion result of C_{44} is not satisfying.

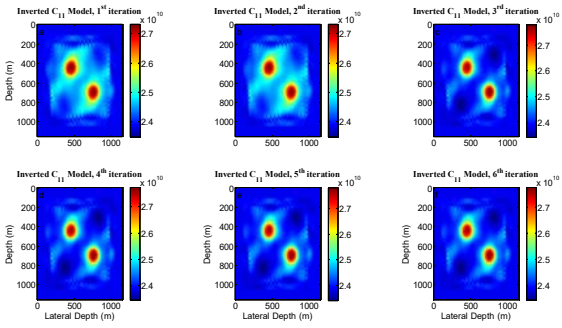

FIG. 1. Inversion results of C_{11} with the increase of iteration steps.

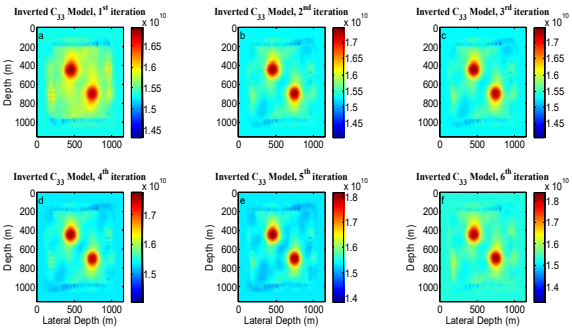

FIG. 2. Inversion results of C_{33} with the increase of iteration steps.

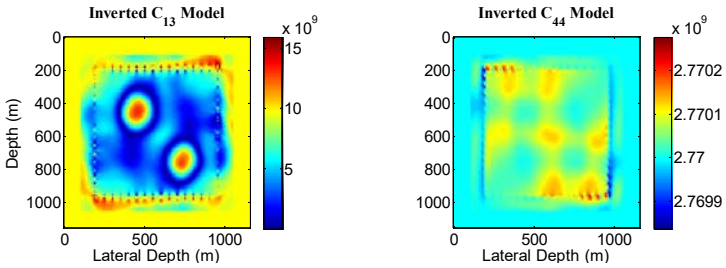

FIG. 3. Inversion results of C_{13} and C_{44}.

Second order H-PML for anisotropic forward wavefield simulation

Junxiao Li, Kris Innanen and Bing Wang

ABSTRACT

As the classical PML methods are primarily designed for first-order wave equation system, they cannot be applied to the second-order wave system directly. However, the first-order wave equations are based on the iterations of velocity and stress components. This implies when the first-order based wave equations are used into full waveform inversion (FWI), the velocity components should be transformed into displacement components to calculate the misfit function. It is necessary to develop a PML for the second order wave equations. In this paper, The Hybrid perfectly matched layer (H-PML) is extended to simulate second order displacement-stress elastic wave equations. In this research report, the simulation results with both H-PML and C-PML in isotropic and anisotropic media are compared. H-PML is capable of absorbing boundary reflections in both isotropic and anisotropic media, but the C-PML only works perfectly in isotropic media. The simulation results with H-PML for both first order and second order elastic wave equations show its efficiency in boundary reflections suppression.

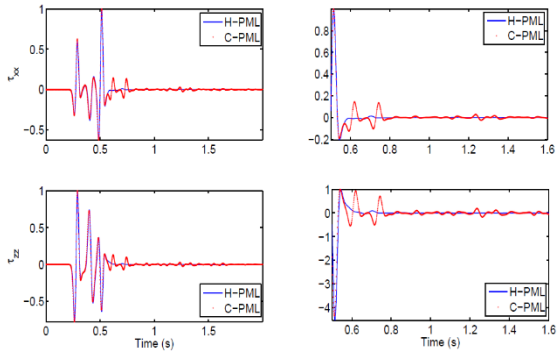

FIG. 1. (Left) Waveform comparison between second order H-PML and C-PML in anisotropic medium. (Right) Start from 0.6 s, reflections from boundaries are detected in C-PML.

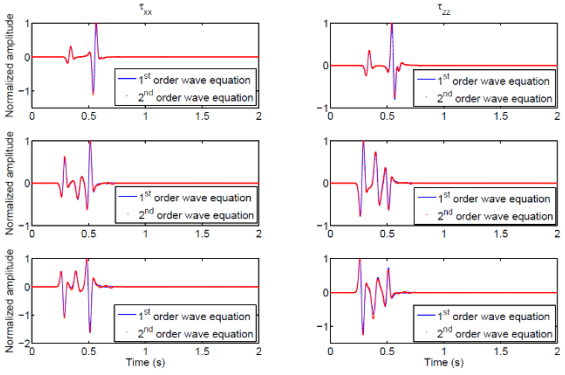

FIG. 2. (Left) Waveform comparison between second order H-PML and first-order H-PML in anisotropic medium.

Cascaded Deconvolution Filters

Laurence R. Lines* and Sven Treitel

ABSTRACT

There are few seismic wavelets that have an exact deconvolution filter, but one of these is an exponentially damped sinusoid. As shown by Lines and Treitel (1983, Geophysics) this wavelet has an exact 3-term inverse. Unlike most seismic wavelets, a Wiener deconvolution filter can be designed that shapes this wavelet to an output that is a nearly perfect spike. Let the exponentially damped sinusoid be defined by:

$$w(t) = e^{-\alpha t} \sin \omega_0 t, \;\; \alpha > 0, \; t \geq 0$$

It can be shown that its deconvolution filter is given by:

$$f(t) = (f_0, f_1, f_2) = \frac{e^{\alpha}}{\sin \omega_0} \left[1, \; -2e^{-\alpha} \cos \omega_0, \; e^{-2\alpha} \right]$$

For the majority of seismic wavelets where a perfect spike is not achievable, one can shape the actual wavelet to an exponentially damped sinusoid prior to deconvolution and then apply a Wiener filter that will spike the exponentially damped wavelet. This cascaded deconvolution appears to hold some promise, as shown by the resolving kernel in a computational example in Figure 1.

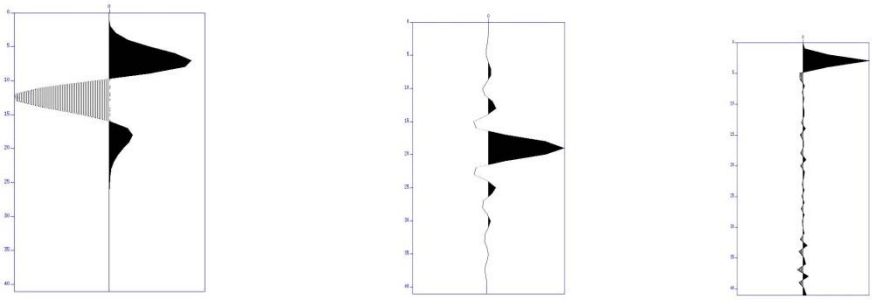

FIG. 1. (left) A seismic wavelet used by Dey (1999 M.Sc. thesis); (centre) the output of convolving a Wiener deconvolution filter with the wavelet (resolving kernel); (right) the resolving kernel obtained by a cascaded deconvolution. The resolving kernel is much closer to the desired spike with the cascaded deconvolution.

Characterizing intrinsic and stratigraphic Q in VSP data with information measures, Part II

Siming Lv and Kris Innanen

ABSTRACT

In an earlier report that has the same title as this, an information measure was devised and conducted on the synthetic vertical seismic profiling (VSP) data sets, with the ability to amplify small differences produced by the processes of intrinsic amplitude attenuation and stratigraphic filtering, aiming at discriminating between the two. The information measure was adapted to seismic records like this: for a discrete zero-offset VSP data set, each of its time snapshots was regarded as a "message"; we used Shannon entropy to measure the amount of information carried by the "messages", which represents the degree of disorder of the wave field at the instants of time, and investigated the entropy variation with time. It was observed that the intrinsic Q and stratigraphic Q always tend to affect the measured entropy result in the opposite way. For the first-order entropy, wave fields including intrinsic Q tend to contribute to small entropy values while wave fields including stratigraphic Q tend to contribute to big entropy values. Making use of this attribute of entropy, this research investigates the relationship between: (a) the entropy peak increase from the wave field that associates with neither intrinsic Q nor stratigraphic Q to the wave field under simultaneous effects of intrinsic and stratigraphic Q, and (b) the strength of stratigraphic Q relative to total Q measured by the spectral ratio method. A seemingly positive relationship between them is found, implying that the entropy behavior may be used as an indicator of the relative strength of intrinsic Q and stratigraphic Q when they are both active. The speculation is supported by the result of an information measure on a field VSP data.

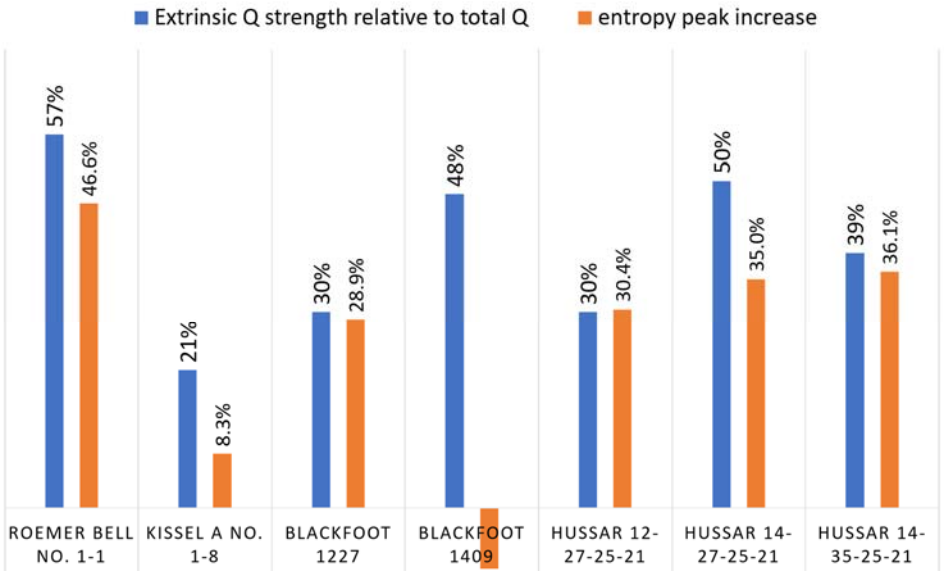

FIG. 1. Comparison between stratigraphic (extrinsic) Q strength relative to total Q and the entropy peak increase from the synthetic wave field including neither intrinsic Q nor stratigraphic Q to the synthetic wave field including both intrinsic Q and stratigraphic Q, built from seven wells.

Reservoir simulations and feasibility study for seismic monitoring at CaMI.FRS

Marie Macquet* and Don Lawton

ABSTRACT

The Containment and Monitoring Institute (CaMI) of CMC Research Institutes Inc., in collaboration with the University of Calgary, has developed a comprehensive Field Research Station (FRS) in southern Alberta, Canada. The purpose of CaMI.FRS is to develop new technologies to prevent and monitor early leakages of a deepest, large-scale CO_2 reservoir. To simulate a leakage, a small amount of CO_2 (< 1000 t/year over 5 years) will be inject a shallow surface (300m depth). In this study, we focus the feasibility study of seismic time-lapse monitoring using surface seismic instruments. A part of the feasibility work is also the determination of threshold of CO_2 gas-phase detection at shallow depth.

The first step of the feasibility study is the reservoir simulation. We test here the influence of the maximum bottom-hole pressure (and reservoir temperature) and of the ratio vertical permeability over horizontal permeability on the amount of CO_2 you can inject and on the gas plume shape. The next step is the fluid simulation, necessitated to estimate the variation in elastic parameters induced by the gas injection. We test different methods to compute the bulk modulus of the fluid (Reuss, Voigt, HRV and Brie) and compare their results. We also test the influence of several parameters (matrix bulk modulus, porosity and initial saturated bulk modulus) on the results of the fluid substitution. We finally use a 3D finite difference modelling to simulate the seismic response in the elastic models generated for the baseline, for 1 year of injection and for 5 years of injection.

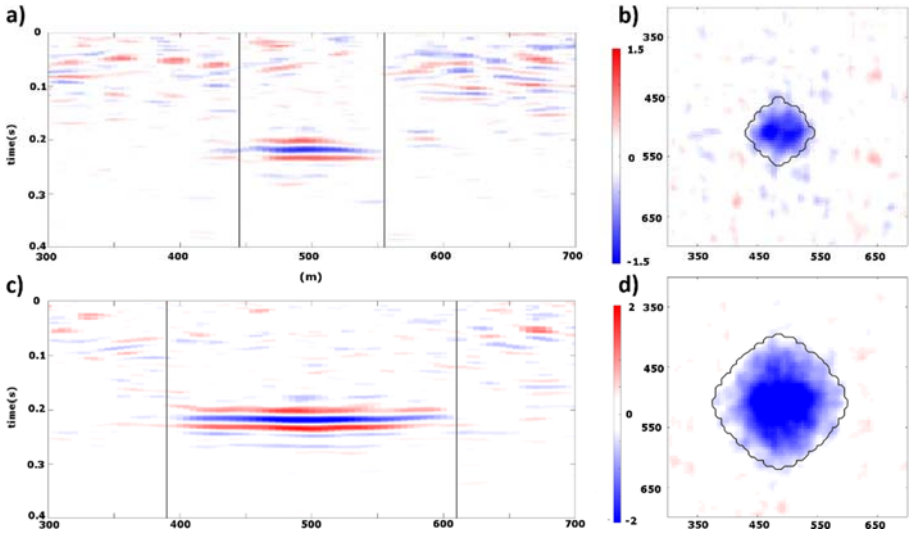

FIG. 1. Results of the difference between the simulated time lapse periods and the baseline seismic volumes, using a SNR of 20. a) Vertical section along the injector well, for 1 year of injection. b) Horizontal section at the top of the reservoir, for 1 year of injection. c) Vertical section along the injector well, for 5 years of injection. d) Horizontal section at the top of the reservoir, for 5 years of injection. Black lines show the lateral expansion of the CO_2 plume.

A model-based AVAZ inversion for azimuthal anisotropy

Faranak Mahmoudian, Josh Curtis, HuShun Zhou and Kristof De Meersman

ABSTRACT

AVAZ inversion can extract natural fracture network properties from 3D pre-stack seismic amplitudes, hence providing important information for unconventional reservoir characterization and hydraulic fracturing stimulation. The commonly used AVAZ inversion is a time sample-by-sample procedure to invert for the HTI symmetry axis direction, analog to dominant fracture orientation, and the anisotropic gradient B_{ani}, analog to fracture density. The technique is based on the Rüger equation for PP reflection-coefficients from a boundary of two HTI media. The near angle Rüger approximation results in a 90° ambiguity on the orientation estimate and relative, band-limited, B_{ani} values. We present a model-based AVAZ inversion to invert for interval B_{ani}. The method is coded using the Earth Signal Ltd processing system. Our method is, an extension of the isotropic model-based inversion by Hampson and Russell (2013) and simultaneously invert for isotropic elastic properties and B_{ani}. The orientation direction is input to our model-based AVAZ, estimated by a sample-by-sample procedure in which the 90° ambiguity is removed by constraining the results to the stress information provided by the major stress direction or well control. We have tested the proposed model-based AVAZ inversion on synthetic azimuthal gathers, and the inversion for interval B_{ani} was successful. This facilitates a meaningful interpretation of azimuthal anisotropy values, extracted from pre-stack seismic amplitudes.

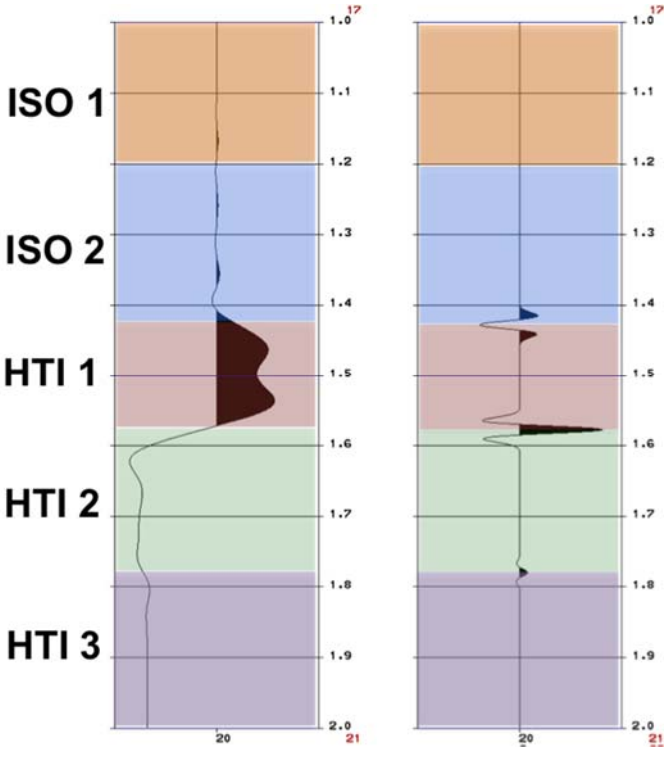

FIG. 1: AVAZ inversion results from synthetic data, generated over a five layer model. (left) B_{ani} estimate (interval property) from the proposed model-based AVAZ inversion. (right) B_{ani} estimate (relative property) from conventional AVAZ inversion.

Quantifying Footprint

Gary F. Margrave*

ABSTRACT

A method is presented to numerically estimate the degree of seismic acquisition footprint in a 3D seismic volume. Operating on time (or depth) slices, the method first constructs digital representations of the source and receiver grids and then these grids are crosscorrrelated with a chosen time slice. For orthogonal source and receiver grids, the procedure is especially simple since only correlation lags orthogonal to the source or receiver lines need be examined. Footprint causes a periodicity in the crosscorrelations whose period is the ratio between the line spacing and the image bin dimension. In a series of examples using real data, it is observed that the grid correlation measurement is much more sensitive than mere visual assessment to detect footprint. This is especially useful for comparing the effectiveness of alternative methods of footprint suppression.

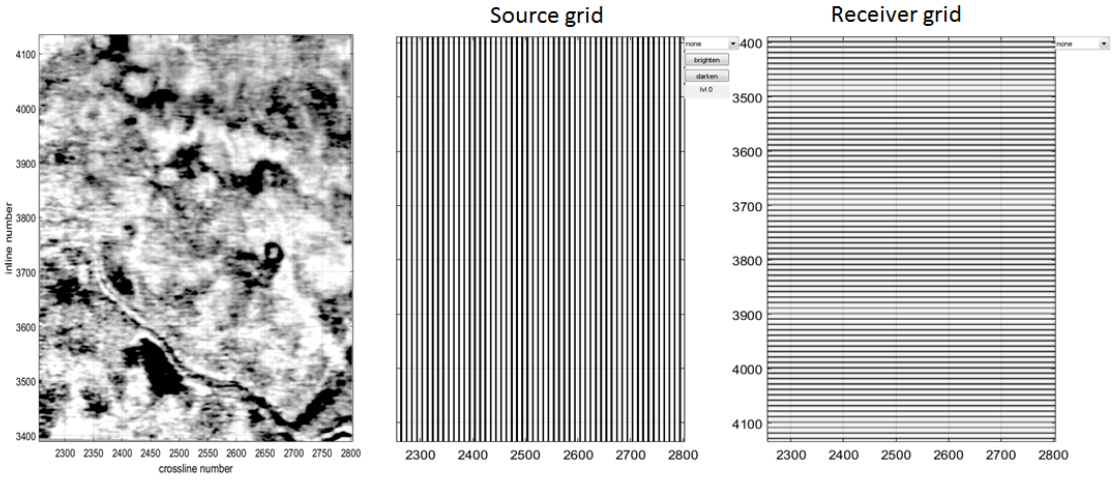

A time slice showing apparent receiver footprint (east-west) and less obvious source footprint. The time slice has an image bin size of 82.5 ft. (square) while the source and receiver line separations are 825 ft.

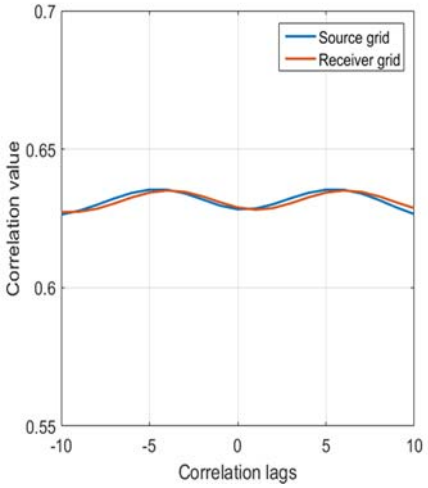

At left is the result of crosscorrelating the source and receiver grids with the time slice. For the source grid, only lags in the lateral direction are needed while for the receiver grid the necessary lags are vertical. As can be seen, there is a periodicity of 10 in the correlations which is the ratio of the acquisition line spacing to the image bin size. This is a direct indicator of footprint.

Simultaneous estimation and correction of nonstationary time-shifts and phase rotations

Gary F. Margrave

ABSTRACT

Constant phase rotations and constant time shifts are the constant and slope of a polynomial approximation to the seismic wavelet phase. Errors in the estimation of either one cause a bias in the subsequent estimation of the other. It follows that estimations of time-shifts followed by subsequent phase estimates, as is commonly done in well tying, is subject to this bias meaning that alignment errors cause compensating phase errors and a very questionable solution. A strategy is presented to overcome this bias whereby the alignment is estimated though correlation of trace envelopes and it is demonstrate that this is much more accurate. This strategy is then extended to the nonstationary case where, in a series of numerical experiments, it is demonstrated that nonstationary phase rotations and time delays can be reliably measured with good quality data.

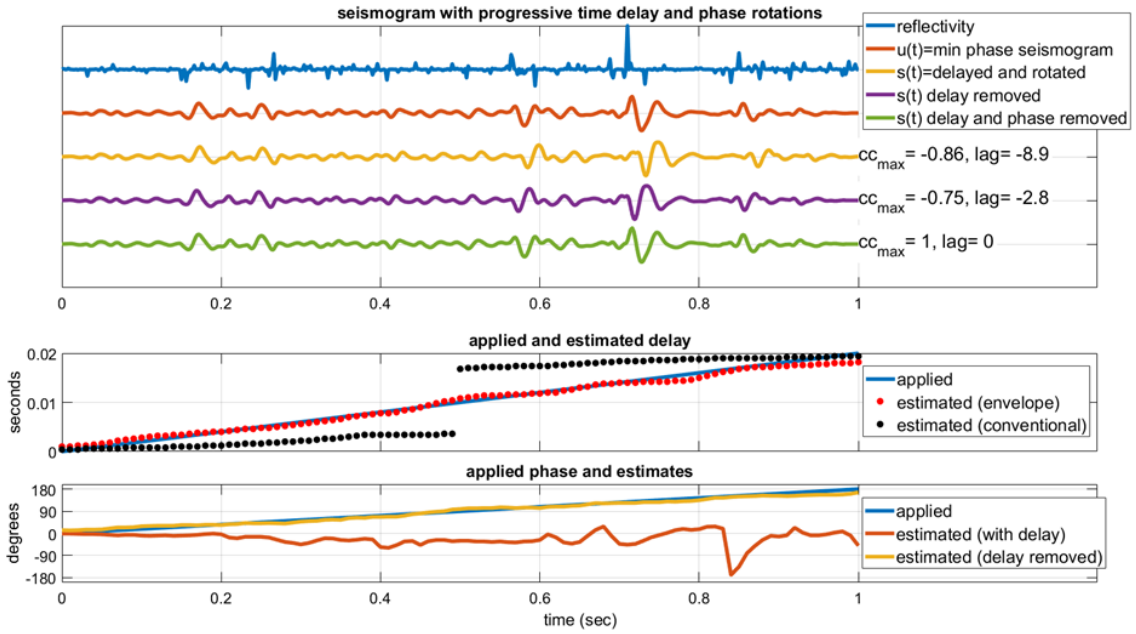

In the above, both a time-variant delay and a time-variant phase have been applied to the reference trace, $u(t)$, to give the seismic trace $s(t)$. The envelope correlation method has successfully estimated the delay while conventional correlation has not. When this delay is removed, the phase is estimated with good accuracy. When the phase is estimated without first removing the delay, the result is nearly zero which is clearly wrong. This is because the applied phase and time delays had tended to compensate for each other (in this case only).

Near-surface seismic characterization from sparsely sampled data sets

Andrew Mills and Kris Innanen

ABSTRACT

Multichannel analysis of surface waves (MASW) is a near-surface characterization technique used to estimate shear wave velocities and layer geometries of the shallow subsurface. Typically, MASW uses closely spaced geophones to adequately sample surface waves. In this study, a field data set acquired with greater than ideal receiver separation is used for near-surface velocity inversion.

The least-squares velocity inversion algorithm is developed, for application to shot records containing dispersive ground roll arrivals. The Priddis Thumper Experiment data set, consisting of a 200 m receiver line with 5 m geophone spacing, is used for this study. Individual shot records are stacked, interpolated, and filtered, to reduce spatial aliasing and isolate surface waves. The inversion is then applied to the dispersion curves generated from these processed shot records, producing 1D shear wave velocity profiles. 1D velocity profiles are generated for various source points and combined to produce a 2D velocity profile over the survey line. Bedrock depth is estimated at approximately 20 m, consistent with shallow borehole drill cuttings.

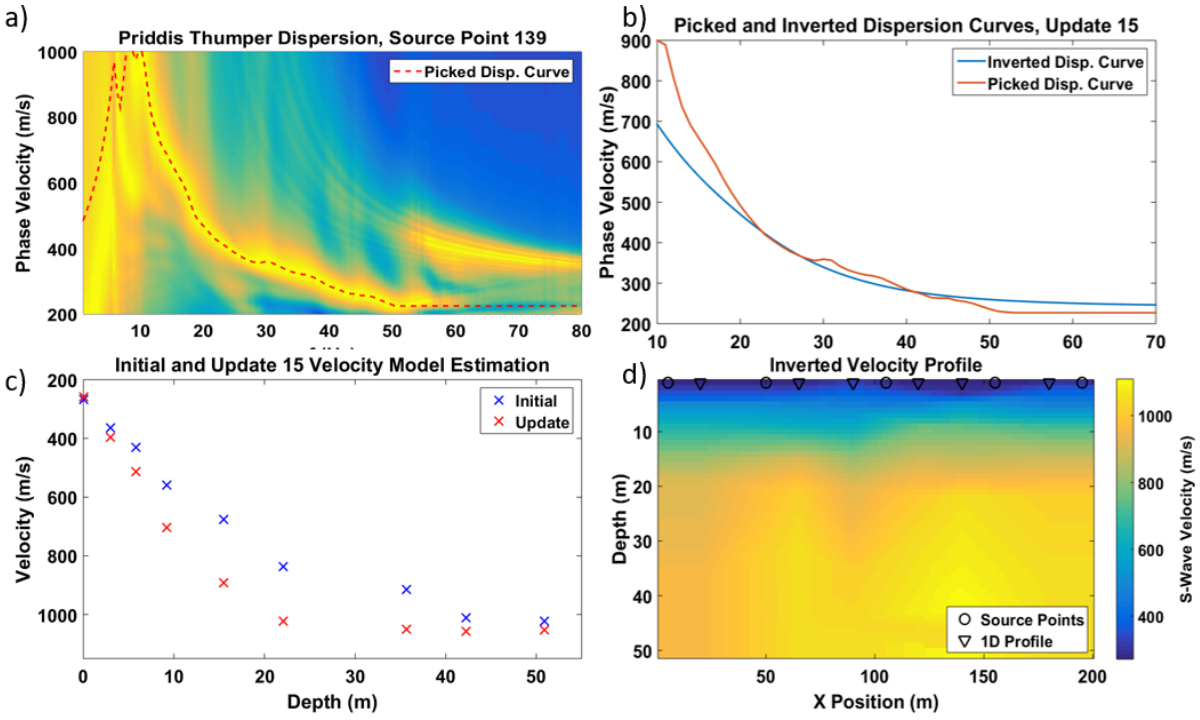

FIG. 1. a) Dispersion spectra and picked dispersion curve generated from processed sparsely sampled data. b) Dispersion curve inversion results. c) Initial estimate (blue) and inverted 1D Vs profile (red). d) Inverted 2D Vs profile, built from bilinear interpolation of individual 1D Vs profiles.

Bi-objective optimization for seismic survey design

Jorge Monsegny

ABSTRACT

I apply a bi-objective optimization strategy to search the best seismic survey design in illumination and cost senses. Due to the conflicting goals of obtaining a good subsurface illumination at the lowest possible cost it is not possible to obtain an optimum survey in both senses simultaneously, but instead it is possible to get a set of surveys, called Pareto front, that shows the trade-off between the conflicting objectives. As a result, the Pareto front could be used as a decision tool to tune quality versus cost. I use the mixed-integer, free-derivative, nonlinear optimization algorithm called Particle Swarm Optimization and Mesh Adaptive Direct Search. The Particle Swarm Optimization part is used to escape local minima while the mixed-integer part is used to deal with integer aspects of a seismic survey design like the number of receivers and sources, to name but a few.

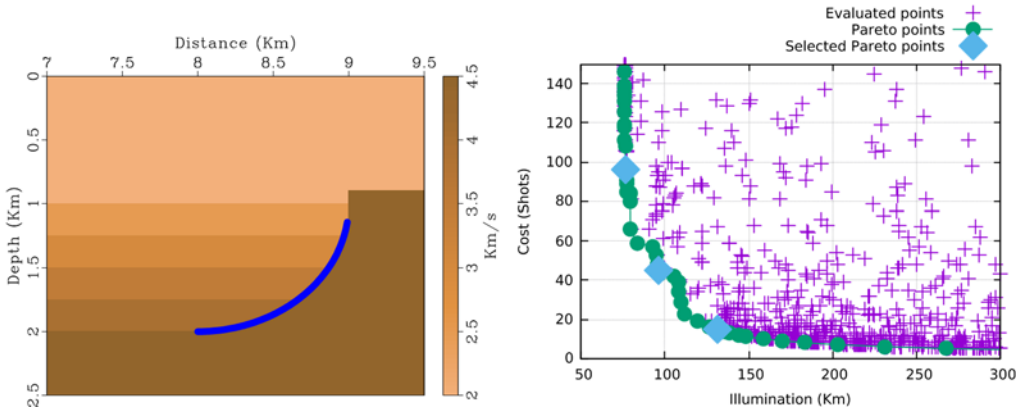

FIG. 1. Left: Velocity model with region of interest highlighted. Right: Pareto front obtained from the bi-objective optimization that shows the trade-off between survey illumination and cost.

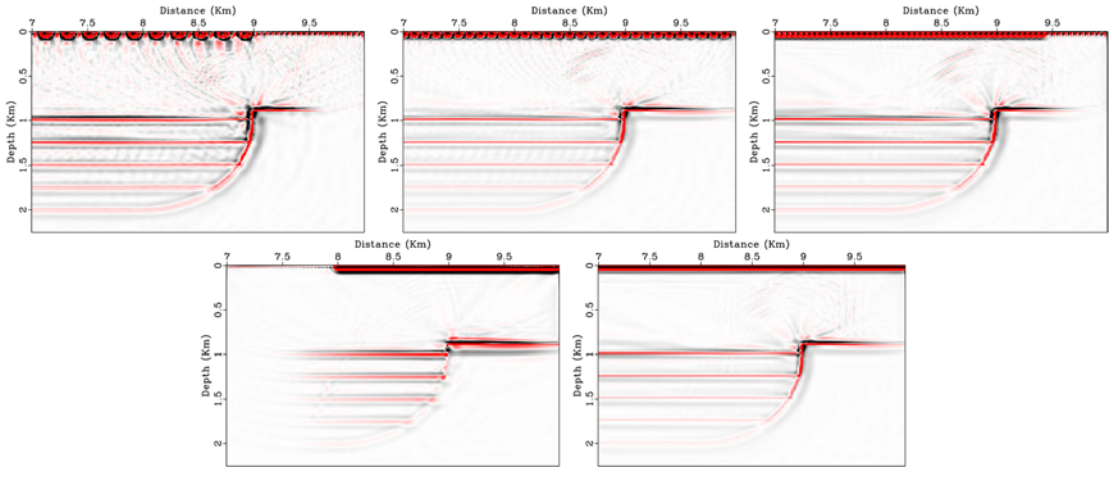

FIG. 2. Comparison of RTM migrations. Above: With data generated using selected surveys from the Pareto front of FIG 1(15, 45 and 96 shots, respectively). Below: Generated from a usual survey above target with 100 shots and a complete survey with 1000 shots. The usual survey shows less definition in the region of interest than the surveys obtained from the optimization process.

Quantum computing impact on exploration seismology

Shahpoor Moradi* and Daniel Trad

ABSTRACT

Quantum Computation (QC) is manipulation and processing the information utilizing the laws of Quantum Mechanics (QM). The building block of QC is a quantum bit (qubit). QM allows qubit to exist in an arbitrary superposition of zero and one, unlike the classical bit that can admit only zero or one. This astonishing feature allows the quantum computer to perform parallel computations with only one processor to solve some certain problems exponentially faster than the most existing supercomputers. Our goal, as summarized in Figure 1, is to design the quantum algorithms to solve the expensive computational problems in exploration seismology, such as 3D wave modeling, Reverse Time Migration, and elastic Full Waveform Inversion. Utilizing the qubits substantially reduces the memory required to store the data and speeds up the computational time of the algorithms by quantum parallelism.

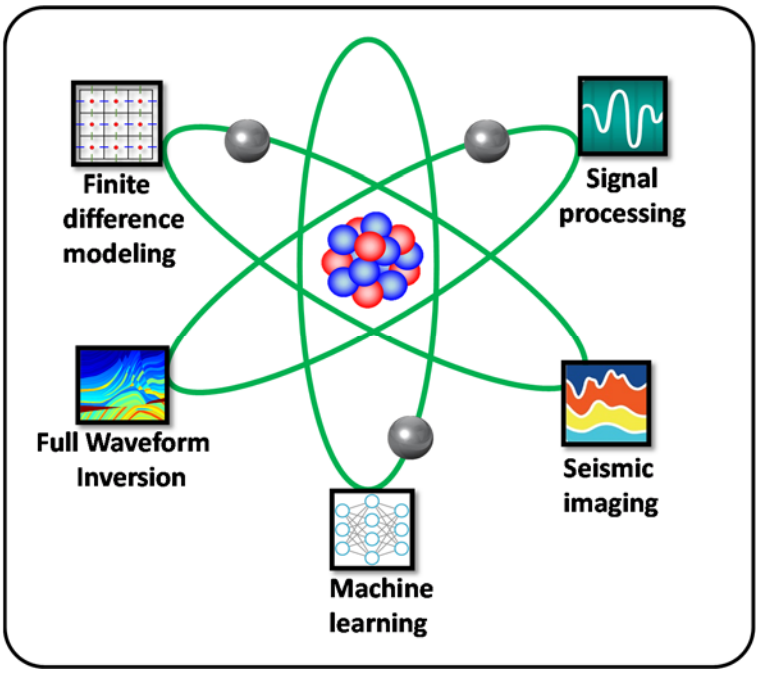

FIG. 1. Potential applications of quantum computation in seismic problems.

Characterizing heavy oil reservoirs using isotropic-elastic FWI with walk-away VSP data

Wenyong Pan, Kristopher Innanen and Yu Geng

ABSTRACT

Seismic full-waveform inversion (FWI) methods hold strong, though still largely untapped, potential to recover multiple subsurface elastic properties for reservoir characterization and monitoring. Simultaneously updating multiple physical parameters introduces the problem of interparameter tradeoff. The three-parameter isotropic-elastic FWI problem can be posed using any one of a wide range of possible parameterizations. Choice of model parameterization is critical to successful field data applications of multiparameter FWI. Monitoring of production or injection in reservoirs, while challenging, admits data acquisition modes that support simultaneous multiparameter FWI. Walk-away vertical seismic profile (W-VSP) represents one key example. A multicomponent W-VSP dataset within a shallow unconventional (Heavy oil) reservoir provides an ideal environment for both clear demonstration of the potential of multiparameter FWI, and for analysis of the influence of model parameterization. Six model parameterizations are considered for isotropic-elastic FWIs. We begin analyzing interparameter tradeoff with scattering radiation patterns for each of these parameterizations, supplementing them with the recently-introduced *interparameter contamination kernels*. Synthetic W-VSP isotropic-elastic FWI experiments indicate that density profiles are most strongly influenced by the interparameter contaminations; depending on model parameterization, the inverted density profile can be over-estimated, under-estimated or spatially distorted. The model parameterization, velocity-density, appears amongst the six cases to provide stable and informative density features not included in the starting model. These conclusions are confirmed on the multicomponent field W-VSP dataset, in which Heavy oil zone of interest features in density, P-wave / S-wave velocity ratio and Poisson's ratio matching well data appear clearly.

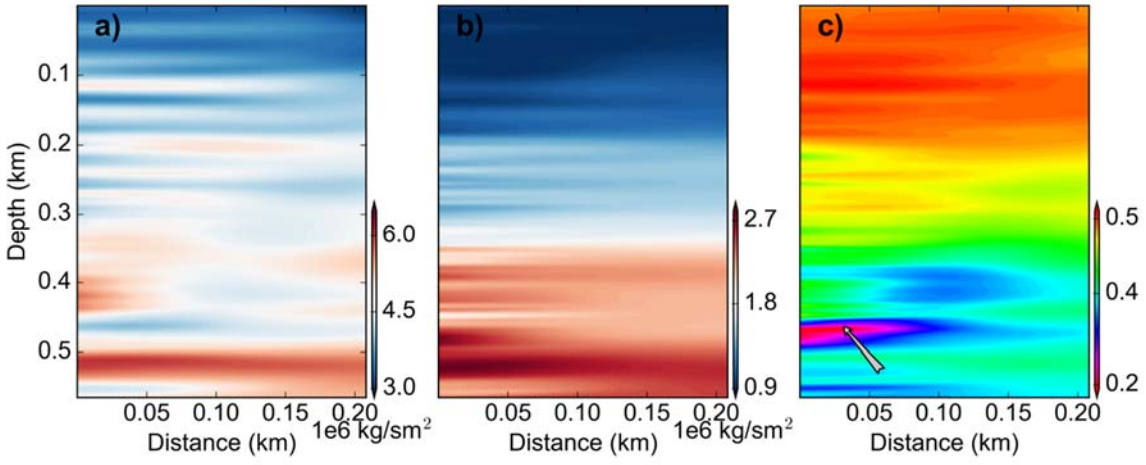

FIG. 1. (a), (b) and (c) show the inverted P-wave impedance, S-wave impedance and Poisson's ratio models using isotropic-elastic FWI with velocity-density parameterization.

Interparameter tradeoffs quantification and reduction in isotropic-elastic FWI: synthetic experiments and real dataset application

Wenyong Pan, Yu Geng and Kristopher Innanen*

ABSTRACT

The problem of inverting for multiple physical parameters in the subsurface using seismic FWI is complicated by interparameter tradeoff arising from inherent ambiguities between different physical parameters. Parameter resolution is often characterized using scattering radiation patterns, but these neglect some important aspects of interparameter tradeoff. More general analysis and mitigation of interparameter tradeoff in isotropic-elastic FWI is possible through judiciously chosen multiparameter Hessian matrix-vector products. We show that products of multiparameter Hessian off-diagonal blocks with model perturbation vectors, referred to as *interparameter contamination kernels*, are central to the approach. We apply the multiparameter Hessian to various vectors designed to provide information regarding the strengths and characteristics of interparameter contamination. With numerical experiments, we observe that S-wave velocity perturbations introduce strong contaminations into density and phase-reversed contaminations into P-wave velocity, but themselves experience only limited contaminations. Based on these findings, we examine a novel strategy to mitigate the influence of interparameter tradeoff with approximate contamination kernels. Furthermore, we recommend that the local spatial and interparameter tradeoff of the inverted models be quantified using extended multiparameter point spread functions (EMPSFs). With a synthetic Marmousi model example and a land seismic field data example, we confirm that the new inversion strategy suppresses the interparameter contamination effectively and provides more reliable density estimations in isotropic-elastic FWI as compared to standard simultaneous inversion approach.

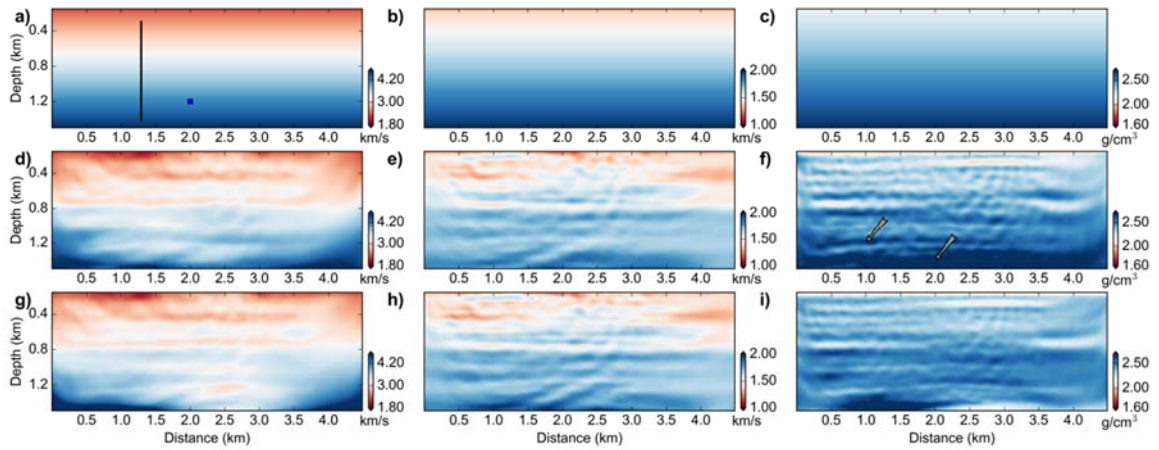

FIG. 1. (a), (b) and (c) show the initial P-wave velocity, S-wave velocity and density models; (d), (e) and (f) show the inverted P-wave velocity, S-wave velocity and density models using standard simultaneous inversion strategy; (g), (h) and (i) show the inverted models using new method.

Comparison between RTM gradient and PSPI gradient in the process of FWI

Sergio Romahn, Marcelo Guarido and Kristopher Innanen

ABSTRACT

Full waveform inversion (FWI) can be described as an iterative cycle of four steps. Firstly, we generate synthetic seismic data (modelled shots) from a smoothed initial model and obtain the difference among observed and modelled shots (data residuals). Secondly, we migrate the data residual (using the current velocity model) and stack. This step produces the gradient. Thirdly, we scale the gradient in order to create a velocity update. And finally, we obtain a new velocity model by adding the velocity update to the current velocity model. We start another cycle by using the new velocity model. This report is focused in the second step of the cycle. Standard FWI uses reverse time migration (RTM) to obtain the gradient. On the other hand, iterative modeling, migration and inversion (IMMI) opens the door to use any type of migration method to produce the gradient. In this report, we compare the performance of the phase shift plus interpolation (PSPI) migration and RTM to obtain the gradient. We start pointing out the fundamental difference between these two methods: the fact that the first one is a one-way and the second one is a two-way wave operator. Then, we analyze the migration response and highlight the consequences of the previous point. Finally, we compare the inversion result that we obtained by applying both methods. The PSPI and RTM gradients were scaled by applying the well calibration technique. We used synthetic data in an acoustic frame in this experiment. We found that both methods are suitable for producing the FWI gradient. However, the PSPI gradient is more sensitive to the initial velocity model than RTM, because its one-way wave operator does not recover long wavelengths as the RTM's two-way wave operator does. This characteristic allows RTM producing a better inversion specially, in the deeper part of the model.

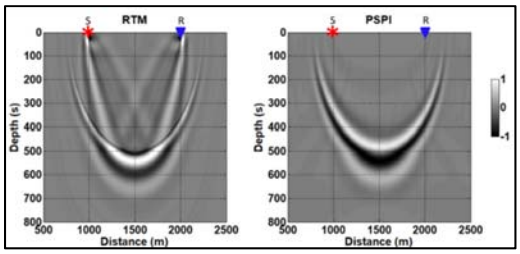

FIG. 1. Migration response of RTM and PSPI.

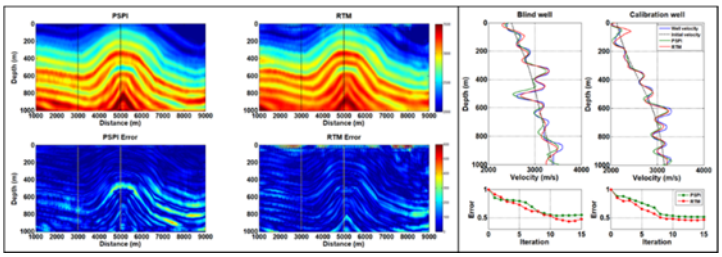

FIG. 2. FWI result for a RTM gradient and a PSPI gradient.

The seismic physical modelling laboratory as a tool for design and appraisal of FWI methods

Sergio Romahn* and Kristopher Innanen

ABSTRACT

We applied full waveform inversion of PP seismic data recorded through the CREWES seismic physical modelling laboratory facility. Although physical modelling introduces certain challenges that must be addressed, it represents a potentially unique way of validating and appraising complex methods involving real measurements of seismic waveforms. One key advantage is that we know the subsurface model that we want to solve; therefore, we can monitor model errors almost exactly. Another advantage is that we can control and vary many acquisition parameters. In several respects, we deal with physical modelling data in a similar way we do with real seismic surface data. For example, the wavelet has to be estimated and we must take noise, attenuation, amplitude variations from shot to shot, etc., into account. However, physical modelling data have particularities that need to be addressed, such as source-receiver directivity and changing waveform with offset. We present an early stage, robust workflow for preparation of raw physical modelling data to use as input to FWI; ultimately this will make the CREWES physical modelling lab an almost unique tool for validating and appraising FWI. We show in detail all processing required to make physical modelling data suitable for being inverted. As an important example of practical FWI algorithm, we used iterative modelling, migration and inversion (IMMI) which aims to incorporate standard processing techniques into the full waveform inversion process. This involves several approximations and internal calibration steps. The gradient is approximated for applying on pre-critical reflections using the phase shift plus interpolation (PSPI) migration. We derived non-stationary matched filters from well information to calibrate the gradient. We also iteratively applied Gaussian smoothers to frequency-band fixed migrated data residuals as an alternative form of the frequency multi-scale FWI. The overall recovery of P-wave velocity variations is quite dramatic, though comparison of blind and calibration well information shows that FWI must work hard in order to generate long-wavelength updates which differ significantly from the geology near the calibration wells.

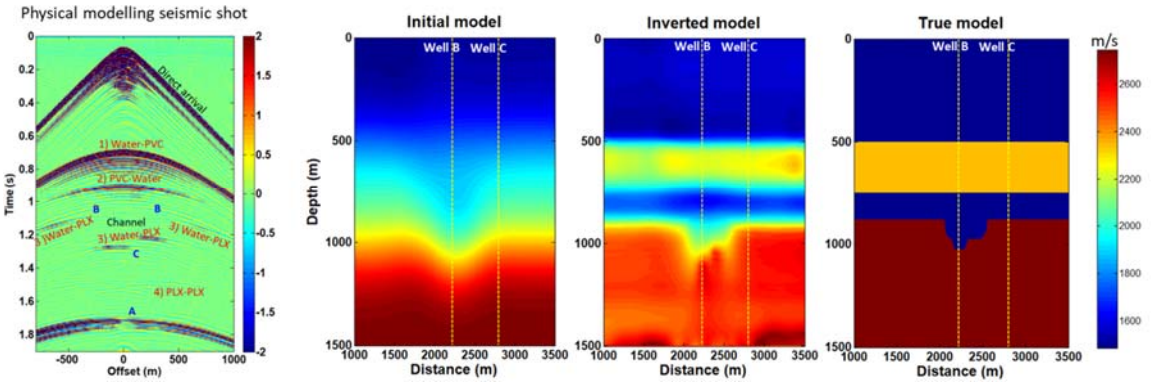

FIG. 1. FWI applied to physical modelling seismic shots. Well C was used to calibrate the gradient.

The Least-Mean-Square (LMS) algorithm and its geophysical applications

Brian Russell[1]*

ABSTRACT

In geophysical analysis, we are familiar with the least-squares or Wiener-Levinson algorithm since is the basis for solving many of our most common processing problems. The least-squares method is applied to problems in which a set of unknown weights are extracted which transform a measured signal into a desired signal. To apply the least-squares algorithm the signal must first be fully acquired, which is standard practice in seismic acquisition. The least-mean-square (LMS) algorithm, on the other hand, is an adaptive filter that does not require knowledge of the full signal, but determines the weights adaptively on a sample by sample basis. The LMS algorithm lead to the development of the first feedforward neural networks, which were only able to solve linearly separable problems. It was then was extended to feedforward networks that could solve nonlinearly separable problems. Thus, an understanding of the LMS algorithm is the first step in understanding neural networks and machine learning.

In this talk, I will use a simple example to explain the LMS algorithm, and will compare it to the least-squares method as well as the gradient descent and conjugate gradient algorithms. The example used is the prediction of the weights that will be applied to two phase shifted sinusoids to predict a third sinusoid. This problem has a deterministic solution, and therefore each method can be judged on its ability to converge to the known solution. Figure 1 shows the performance of the (a) gradient descent, (b) conjugate gradient, and (c) LMS algorithms in this task. Note that the LMS algorithm starts chaotically but quickly converges to the correct result.

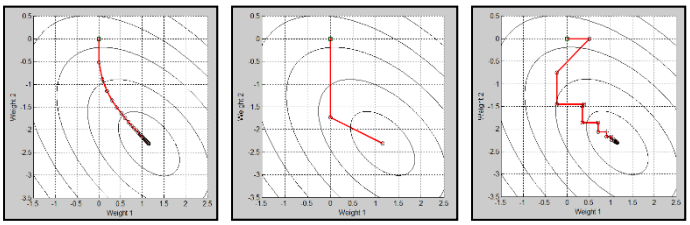

(a) (b) (c)

FIG 1: In the above figures, three algorithms are used to iterate from an initial guess pair of weights (shown by the square at 0,0) to the correct answer (a circle at 1.15,-2.3), where (a) shows the path of the gradient descent algorithm, (b) shows the path of the conjugate gradient algorithm, and (c) shows the path of the LMS algorithm.

After the discussion of the theory behind the LMS algorithm using this simple problem I will apply the method to several geophysical examples, including both deconvolution and the multi-attribute prediction of reservoir parameters.

[1] HampsonRussell, A CGG GeoSoftware Company, Calgary, Alberta, brian.russell@cgg.com

Seismic monitoring with continuous seismic sources

Tyler W. Spackman* and Don C. Lawton

ABSTRACT

The Containment and Monitoring Institute has established a Field Research Station (FRS) in Newell County, Alberta which will be used to study how injected carbon dioxide behaves in the subsurface, as well as to test various measurement, monitoring and verification technologies to determine their applicability for use in monitoring subsurface fluid injection projects. One technology of interest that will be tested is the use of permanent, or continuous, seismic sources. A synthetic source function representing the sweep of a continuous seismic source was created and used to generate synthetic shot records. Additionally, a correlation routine was developed to handle multiple shot records, each originating from an individual sweep, and then remove the sweep overprint and suppress noise. To serve as a baseline dataset against which to compare data acquired using a continuous seismic source, a 2D seismic line, acquired in May 2017, was processed. A similar processing flow will be developed and semi-automated for use with continuous source data. Field work is ongoing at the FRS, and includes the installation and testing of permanent seismic sources. Based on raytracing and analysis of offset-dependent synthetic seismograms, an offset of 110 m between the continuous seismic source and the VSP recording well will give an optimal combination of spatial coverage and incident angle content in recorded seismic data.

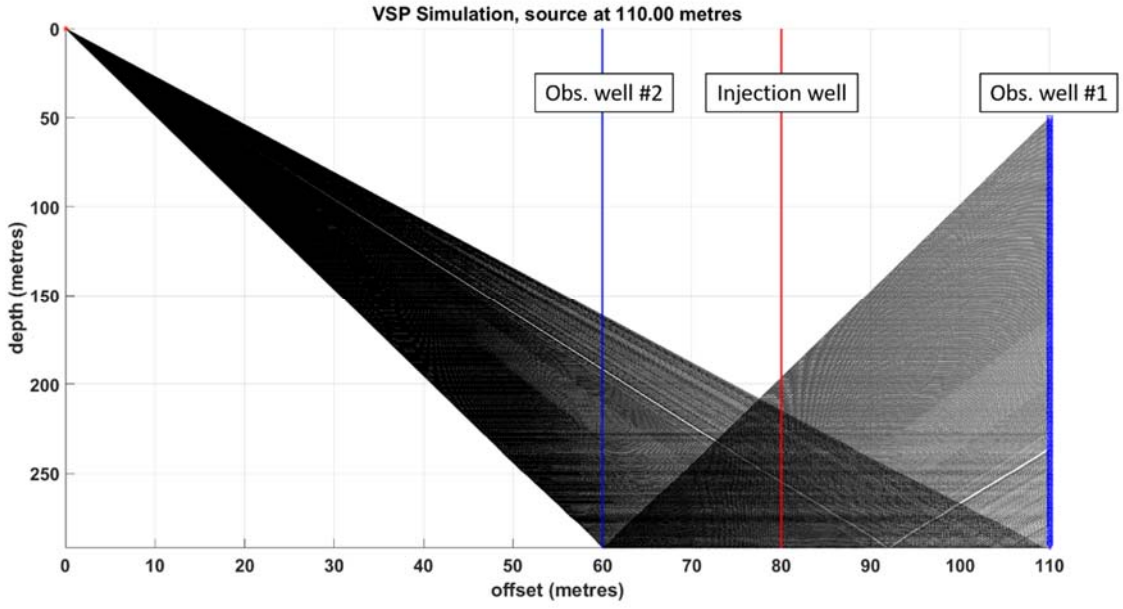

FIG. 1. VSP raytracing through the FRS velocity model using a source-receiver offset of 110 m.

Multicomponent inverse scattering series internal multiple prediction Part I: Analytical analysis of input preparation

Jian Sun*, Kristopher A.H. Innanen, Daniel Trad and Yu Geng

ABSTRACT

The input preparation is the essential step for the ISS-IMP prediction. Since the wave-mode conversion can only be handled in the top layer, an inappropriate will misleads the conversion in lower layers which disorders lower-higher-lower relationship of events reflected by the same layer but with different wave mode conversions. In this paper, we analyze the possible input preparation methods for the algorithm implementing in different domains using wavenumber related elastic stolt migration, slowness related elastic stolt migration, time-stretching method in plane wave domain, and the best-fitting method with high resolution hyperbolic radon transform. The advantages and weaknesses of each approach are discussed.

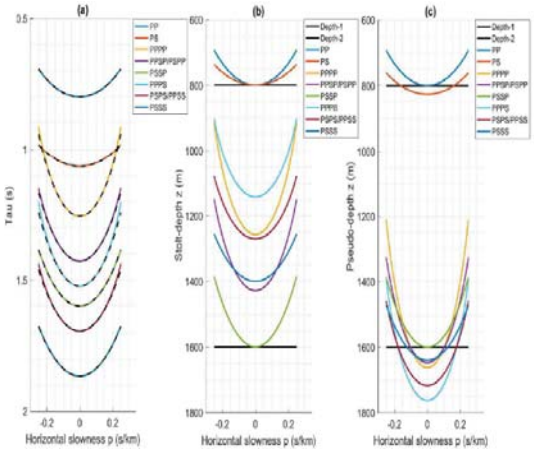

FIG. 1. Comparison between stolt-migration, time-stretching, and best-fitting in pseudo-depth.

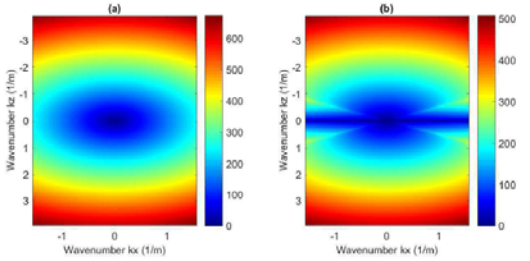

FIG. 2. The angular frequency in function of wavenumber. (a) $\omega(k_z^P)$. (b) $\omega(k_z^{SV})$.

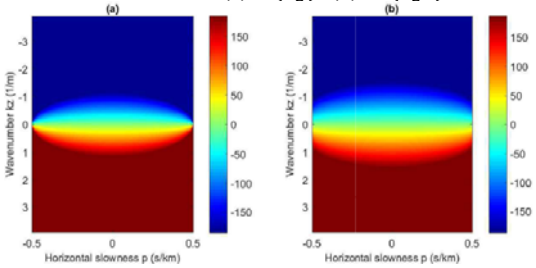

FIG. 3. The angular frequency in function of horizontal slowness. (a) $\omega(p_z^P)$. (b) $\omega(p_z^{SV})$.

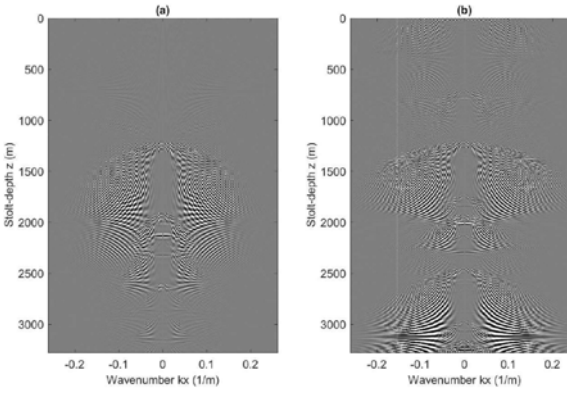

FIG. 4. Elastic stolt-migration with two constant velocities in wavenumber pseudo-depth domain.

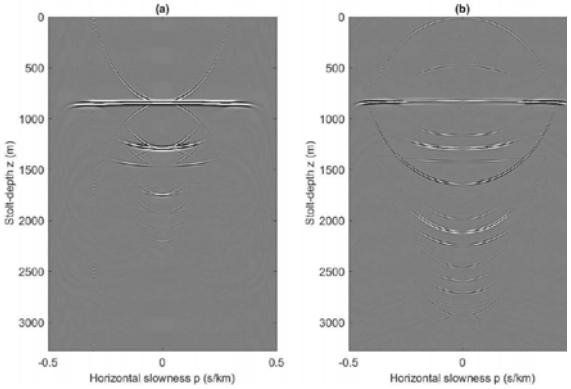

FIG. 5. Elastic stolt-migration with two constant velocities in horizontal-slowness pseudo-depth domain.

Multicomponent inverse scattering series internal multiple prediction Part II: Synthetic application

Jian Sun, Kristopher A.H. Innanen, Daniel Trad and Yu Geng

ABSTRACT

Identifying lower-higher-lower relationship is essential to inverse scattering series internal multiple prediction, which is more difficult for multicomponent predictions due to the wave-mode conversion of P- and S-waves. Since only conversions happened in the top layer can be handled by the algorithm, the input preparation for elastic internal multiple prediction becomes to an intractable problem. In paper of part I, we analytically analyzed the advantages and defects of input preparation using different methods, elastic stolt-migration, vertical traveltime stretching, and best-fitting velocity obtained by high resolution radon transform. In this paper, to examine the conclusions indicated previously, a synthetic model is utilized to implemented the multicomponent internal multiple prediction with different inputs generated by these approaches.

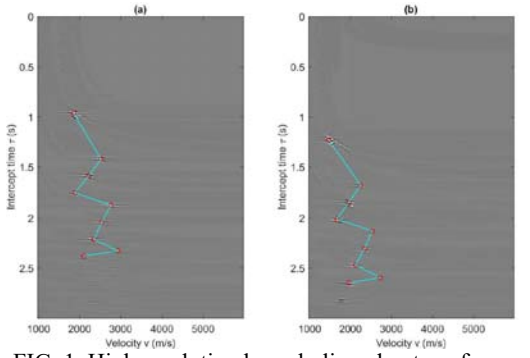

FIG. 1. High resolution hyperbolic radon transform.

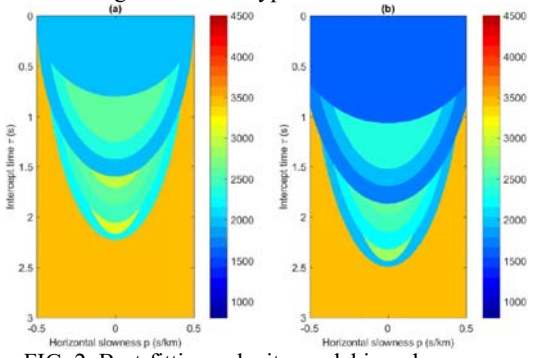

FIG. 2. Best-fitting velocity model in radon space.

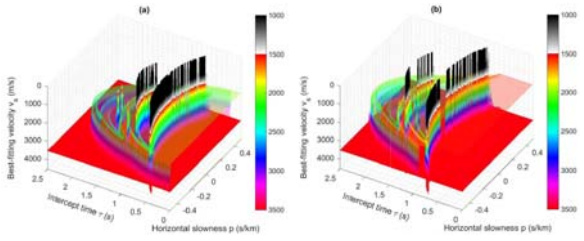

FIG. 3. Best-fitting velocity matching for P-P and P-SV.

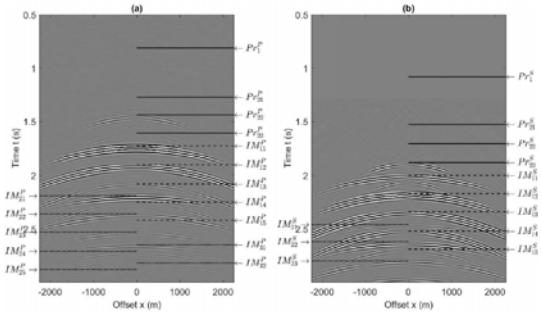

FIG. 4. Prediction with time-stretching, $\epsilon = 96$ms.

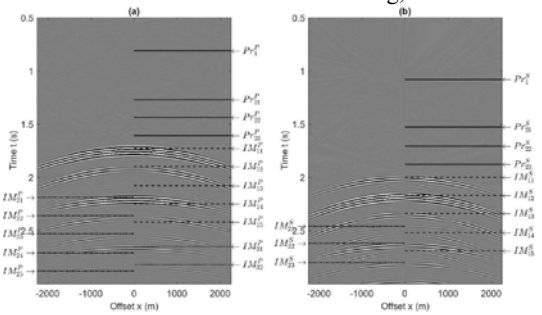

FIG. 5. Prediction with best-fit velocity, $\epsilon = 200$ms.

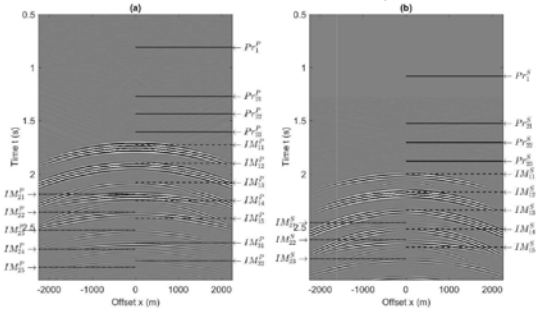

FIG. 6. Prediction with cross-validating of time-stretching and best-fitting velocity, $\epsilon = 96$ms.

Mismatches between physics and operators for least squares migration: a comparison between Kirchhoff and RTM

Daniel Trad*

ABSTRACT

Least squares migration is designed to calculate the reflectivity model that can best predict the data under the Born approximation assumption. This is achieved by iteratively modifying the reflectivity model with updates obtained by mapping the prediction errors from data to model space. This approach assumes that every error in prediction is due to an error in reflectivity. This assumption is wrong, except for the very special case of synthetic data and a matching modeling operator in LSMIG (wave equation instead of Born). Because LSMIG always assumes Born modeling, even for synthetic data the prediction error is due to mismatches between "physics" and data. Therefore, each update to the reflectivity contains wrong components. The larger the mismatch, the larger the contribution of these wrong components. Usually, this noise is attenuated by model regularization, but not always effectively. Often the model regularization can be the dominant effect in the inversion, so instead of seeing the effect of inverting the Hessian, we may see the effects of filtering the noise. In this work, I compare several situations for LSMIG using both Kirchhoff and RTM operators. Also, I show the effect of residual adaptive filtering instead of model filtering as a possible way to remove the inversion noise.

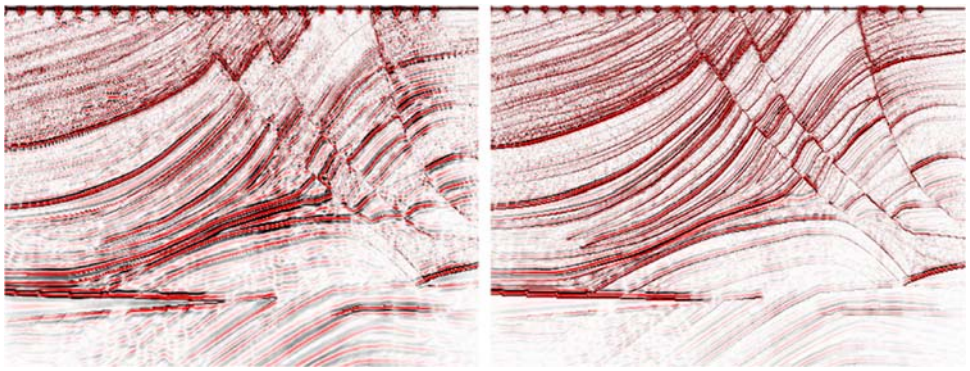

FIG 1. RTM (left) vs LSRTM (right) with 9 iterations and 25 shots. Ideal conditions for LSMIG (no mismatches).

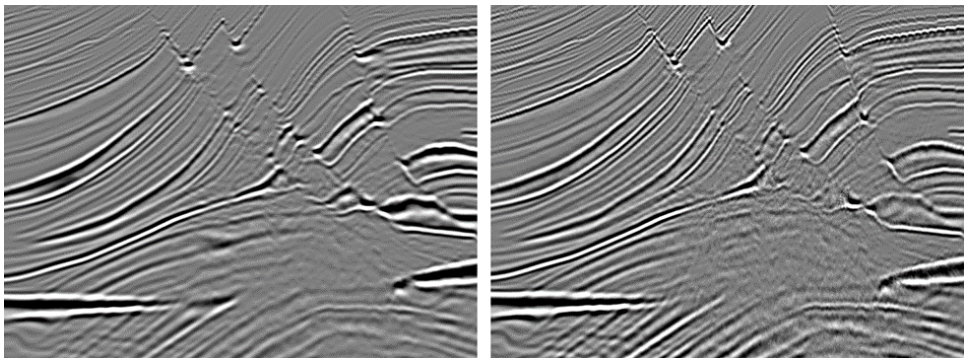

FIG. 2. Kirchhoff migration and LSKirchhoff. Noise controlled by residual filtering.

The Duvernay Formation-the application of structure and simultaneous inversion for reservoir characterization

Ronald Weir*, L. Lines and D. Lawton

ABSTRACT

This paper describes the analysis of multi-component inversion data integrated with structural interpretation. This workflow is used for characterizing a low permeability unconventional reservoir, both in a structural and lithologic sense. This includes the determination of a time-depth relationship using synthetic seismograms, generation of seismic derived structural maps, and the determination of inversion based parameters of density, shear wave, and p wave velocity. The model based procedure includes poststack (acoustic) inversion, AVO prestack inversion, and joint PP-PS inversion. With these rock properties determined, calculations are made to determine Young's Modulus, Poisson's Ratio and brittleness. Faults are mapped based on time slices, isochrons and observing correlatable vertical displacements. The seismic attribute analysis has identified significant variability in Duvernay Formation within the 3-D volume; highlighting areas which may have reservoir characteristics suitable for fracture stimulation, as well as areas exhibiting poor brittleness characteristics, arguably less suitable for development. The fault mapping has identified a system of N-S Duvernay-to-Precambrian faults, in the proximity of nearby well completion activity. These faults appear to be linked to the induced seismicity triggered by hydraulic fracture completion activity in this area.

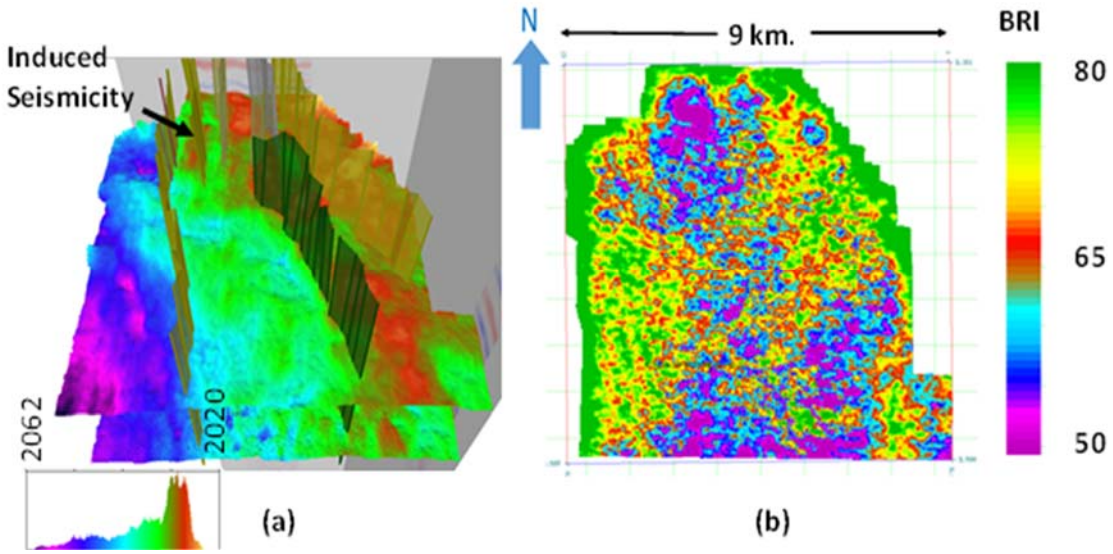

FIG. 1. Perspective view showing interpreted basement-rooted, steeply dipping faults (a) as well as Gilwood and Precambrian horizons extracted from the PP data volume. b) Stratal slice showing brittleness index (BI, units percentage) calculated from Young's modulus (E) and Poisson's Ratio (PR) within the Duvernay interval. The interpreted north-south (N-S) faults are marked. The arrow in 17 (a) indicates where induced seismicity has occurred.

Comparison between least-squares reverse time migration and full-waveform inversion

Lei Yang, Daniel O. Trad and Wenyong Pan

ABSTRACT

The inverse problem in exploration geophysics usually consists of two parts: seismic imaging and velocity model constructing. In this paper, we compare the algorithms for least-squares reverse time migration (LSRTM) and full-waveform inversion (FWI) and use numerical examples to understand the differences. LSRTM uses Born approximation as the modelling method because it requires the adjoint of migration (linear inversion), while FWI uses finite-difference modelling because it does not require an adjoint-pair operator (non-linear inversion). Linearized Born modelling can update model perturbations by a linear conjugate gradient method, but may have severe inaccuracies and inversion noise if the initial model is poor. Both, FWI and LSRTM depend on the initial model largely, but FWI has a mechanism to improve the velocities and LSRTM does not. Conversely, FWI suffers from cycle skipping while LSRTM does not. For LSRTM, the long wavelength components of the gradient are considered to be noise, while for FWI they are considered to be signal. In this work we try to use a FWI algorithm to solve for reflectivity instead of using standard LSRTM.

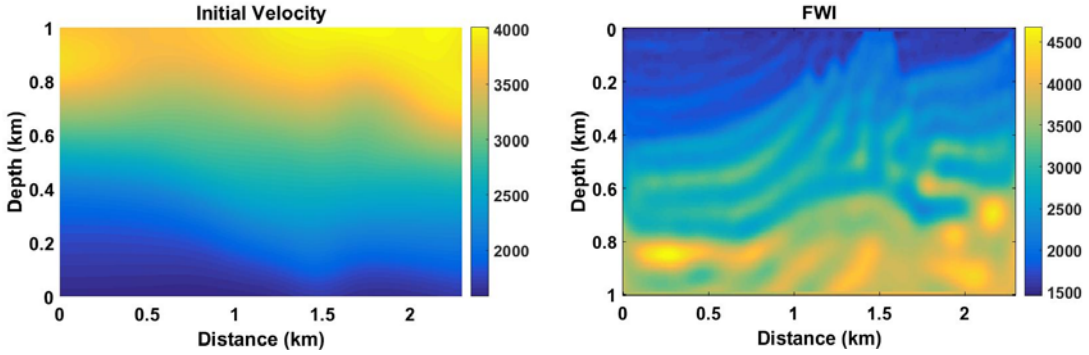

FIG. 1. The initial smoothed model and FWI result from the smoothed model.

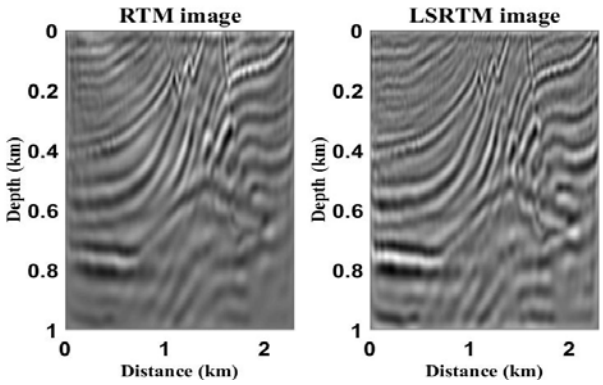

FIG. 2. RTM calculated as the gradient of the residuals, and LSRTM image using FWI algorithm.